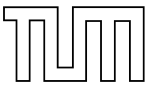

Technische Universität München

Pilot Contamination Reduction in Massive MIMO Systems

Master Thesis

Sergi Liesegang Maria

Fakultät für Elektrotechnik und Informationstechnik
Professur für Methoden der Signalverarbeitung
Univ.-Prof. Dr.-Ing. Wolfgang Utschick

Professur für Methoden der Signalverarbeitung
Technische Universität München
D-80290 München
Germany

http://www.msv.ei.tum.de

Pilot Contamination Reduction in Massive MIMO Systems

Master Thesis

Sergi Liesegang Maria

Fakultät für Elektrotechnik und Informationstechnik
Professur für Methoden der Signalverarbeitung
Univ.-Prof. Dr.-Ing. Wolfgang Utschick

Abstract

Massive MIMO systems have been pointed out as one of the possible strategies to enhance system performance and reach the high data rates modern wireless communications demand. It represents a breakthrough in modern investigations given the new degrees of freedom and the extra dimensional space it provides. However, given the lack of channel knowledge, estimation must be employed. After this process, some interference due to the fast variation of the channel, which implies users sharing training sequences, is left. This is commonly referred to as pilot contamination and heavily compromises the throughput, specially in the large scale antennas regime. In this thesis, we will first study in detail this dramatic effect for later introducing different proposals that attempt to reduce its impact. In particular, we will start with the use of two main filters as basic processing. Next, allocation schemes to properly distribute users are discussed. Then, we will suggest projection based methods that transform the estimates with the purpose of canceling the undesired portions and strengthen the user destined signals. At the end of this analysis, it is shown numerically that the approaches presented behave well in these scenarios and help mitigate the interference created. This allows a faster and more robust transmission of information to take place in environments where pilot contamination is present.

Contents

Chapter 1

Introduction

There has been a huge increase in the demand of higher data rates for wireless communications during the past decades [1]. Large improvements have been achieved throughout the last mobile generation systems by means of exploiting different degrees of freedom. e.g. time and frequency. Nevertheless, to meet the current service requirements of the market, imposed by companies and their clients, the tendency is now to employ multiple antennas at both ends [2] so that spatial dimensions can also be explored and the channel properties can be further leveraged. This approach is commonly referred to as Multiple-Input-Multiple-Output (MIMO). In some sense, it allows the parties involved in the communication, transmitter and receiver, to distinguish between different directions and exploit them for rate enhancement.

1.1 Motivation

The potential of such technology has drawn interest among both, academical and industrial community, given the promising improvements these new degrees of freedom can offer [3] when properly extended. In particular, the usage of large antenna arrays at the Base Station (BS), known as massive MIMO [4], has revealed even more notorious achievements in throughput, energy and spectral efficiency [5] with very simple linear processing techniques. Thus, a relatively low complexity is required. We will see that data rate can grow unbounded with the number of antennas. That is why it is at the forefront of the today's research

in the broadband area. In fact, it allows the usage of cheap User Terminals (UTs) as the multiantenna technology, unfeasible there, is implemented at the BS exclusively [6][7]. This reduces the overall cost of the system and only minor changes are needed in current devices. Additionally, researchers still seek for other solutions to keep in pace with the high current mobile communication usage. For instance, the use of milimiter waves also enables rates to improve enormously and has gained special relevance in this area, e.g. see [8]. However, we will not consider these bands in our project but restrict to microwaves.

1.2 Problem Statement

To take full benefit of the massive MIMO characteristics, the channel has to be known at the transmitter and receiver [5][6]. However, in real communication systems, this quantity has to be estimated given the lack of information [9]. To do so, a set of training sequences are used but, due to the fast variation of the channel, the amount of different ones is limited. Therefore, some users have to share the same pilot, leading to interference in the estimate which cannot be removed easily. This fact is commonly known as pilot contamination [10] and it results in a bottle-neck for massive MIMO systems since data rate is highly dependent on the quality of those estimates [3] [11]. In other words, poor values lead to dramatic effects on performance and limit our communication.

In this project, we aim to analyze the impact of this contamination. We will focus on the data rate as magnitude to measure how this effect deteriorates data communication. In fact, the main quantity studied here will be the sum rate, although a fairer approach will be also contemplated that will make use of the throughput variance. Notwithstanding, the principal goal of this work is to find methods that reduce this interference and filter out pilot contamination. Then, two processing schemes, based on imperfect channel knowledge, will serve as starting point to overcome the problem. In addition, suitable power allocation schemes are also included. Later, given the special properties of channels and covariance matrices, which apply in the large scale regime, pilots will be assigned to users accordingly, not randomly. Finally, following a similar line of research, we will design some projection operators that will be applied to the channel estimates. This way, signals will be transformed into interference-free. Overall, we are interested in mitigating this contamination so that the potential of massive MIMO can be totally released.

1.3 Thesis Outline

This project is organized as follows. First, in Chapter 2, we introduce the necessary concepts and mathematical tools to develop the entire work, such as massive MIMO technology and linear processing. The preliminary assumptions, like the channel model and its asymptotic properties depending on our knowledge, will be also included in that part. Later, in Chapter 3, the need for channel estimation is presented, together with some methods to perform it. At that point, pilot contamination appears and is analyzed in detail. The dramatic effects it has on performance are then highlighted. Next, in Chapter 4, the set of possible approaches to combat this interference are discussed. We will start with the use of filters, then the user allocation and finally the projection of the estimates. Chapter 5 is reserved for simulations, where numerical results, used to corroborate the previous findings, are properly shown. Conclusions are given in Chapter 6, together with a brief summary and futures lines of research.

Chapter 2

Preliminaries

In this chapter, we will announce some of the preliminary knowledge and concepts necessary to understand and go on with the thesis. In addition, the main assumptions used in this project will also be presented.

First we make an overview of the system used in the whole project, both for forward and reverse links. Then, the concept of massive MIMO is introduced, together with some important properties and facts that apply in this regime. Finally, the channel model employed in the simulations is described.

2.1 System Overview

Throughout all this work, we will be dealing with a Multiuser Multiple-Input-Single-Output (MU-MISO) system with M antennas at the BS serving K single antenna UTs. It can be shown that this scenario is analogous to the MIMO system with K inputs and M outputs [12]. In addition, thanks to usage of orthogonal frequency division multiplex (OFDM) symbols as transmission scheme [13], flat frequency fading can be assumed, like in [14], and channels become multiplicative. Therefore, to represent our communication links, either Uplink (UL) or Downlink (DL), the following linear model with additive noise, depicted in Fig. 2.1, is considered

$$\boldsymbol{y} = \boldsymbol{H}\boldsymbol{x} + \frac{1}{\sqrt{\rho}}\boldsymbol{n} \tag{2.1}$$

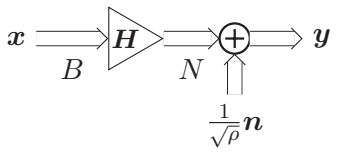

Figure 2.1: Linear MIMO Channel Model with Additive Noise

where, in virtue of the central limit theorem (CLT), the noise vector $\boldsymbol{n} \in \mathbb{C}^N$ can be assumed to be an Independent Identically Distributed (i.i.d.) complex Gaussian Random Variable (RV), i.e. $\boldsymbol{n} \sim \mathcal{N}_{\mathbb{C}}(\mathbf{0}, \mathbf{I}_N)$. Note that for the sake of simplicity, we assume all signal-to-noise ratios (SNRs) to be equal, which means noise quality is the same in all directions as well as transmit power. This fact is represented by the term ρ, further discussed in the upcoming section, where we distinguish between the UL and DL cases. In particular, thanks to the normalization factor, UTs can transmit with unit power in the UL. Likewise, BS is assumed to perform a uniform allocation in the DL with the same overall transmit power as that of the UL.

The channel matrix $\boldsymbol{H} \in \mathbb{C}^{N \times B}$ is defined so that its elements represent the gain of the channel between the BS antenna and each user. This magnitude can also be written as $\boldsymbol{H} = [\boldsymbol{h}_1, \ldots, \boldsymbol{h}_B]$, where $\boldsymbol{h}_i \in \mathbb{C}^N$ denote the individual user channels between BS and UTs. They are assumed mutually independent and constant within a coherence time of T channel accesses. Besides, when considering the worst case scenario, the channel matrix can be represented by a Rayleigh distribution [15]. Hence, the individual channels are also complex Gaussian RVs with covariance $\boldsymbol{C}_{\boldsymbol{h}_i} = \mathrm{E}[\boldsymbol{h}_k \boldsymbol{h}_k^{\mathrm{H}}] \in \mathbb{C}^{N \times N}$, i.e. $\boldsymbol{h}_i \sim \mathcal{N}_{\mathbb{C}}(\mathbf{0}, \boldsymbol{C}_{\boldsymbol{h}_i})$. This matrix will play an important role in our project and it is first introduced in Section 2.3. Furthermore, it can be shown that to achieve capacity, the input signal $\boldsymbol{x} \in \mathbb{C}^B$ has to be complex Gaussian distributed [16], i.e. $\boldsymbol{x} \sim \mathcal{N}_{\mathbb{C}}(\mathbf{0}, \mathbf{I}_B)$. Note that for simplicity, we assume its entries are i.i.d. with unit variance. As a result, the received signal $\boldsymbol{y} \in \mathbb{C}^N$ is also complex Gaussian distributed with zero-mean and covariance matrix

$$\boldsymbol{C}_{\mathrm{y}} = \mathrm{E}[\boldsymbol{y}\boldsymbol{y}^{\mathrm{H}}] = \sum_{i=1}^{N} \boldsymbol{C}_{\boldsymbol{h}_i} + \frac{1}{\rho}\mathbf{I}_N \tag{2.2}$$

In general, it is assumed that channel, noise and transmitted signal are independent. Therefore, we can write the following statements

$$\mathrm{E}[\boldsymbol{x}\boldsymbol{n}^{\mathrm{H}}] = \mathrm{E}[\boldsymbol{x}]\mathrm{E}[\boldsymbol{n}^{\mathrm{H}}] = \mathbf{0} \quad \text{and} \quad \mathrm{E}[\boldsymbol{H}\boldsymbol{x}] = \mathrm{E}[\boldsymbol{H}]\mathrm{E}[\boldsymbol{x}] \tag{2.3}$$

On the other hand, regarding the data rate, we will consider separate decoding [16] to allow the usage of linear filters and simplify their design, as seen in Section 4.1. Then, the corresponding sum rate R_{sum} is given by

$$R_{\text{sum}} = \sum_{k=1}^{K} R_k \tag{2.4}$$

where the individual rates R_k are computed assuming scenarios with high mobility [15], where fast fading instead of slow fading is contemplated. This means that the channel coherence time τ_c is very small compared to the codewords lengths, fact that results into channels with rapid variability and thus, the use of an ergodic expression for the user rates

$$R_k = \mathrm{E}[\log_2(1 + \gamma_k)] \tag{2.5}$$

where γ_k is the is the Signal-to-Interference-plus-Noise Ratio (SINR) of user k, which changes depending on the direction of the channel, UL or DL, and will be defined accordingly in Section 2.2.2. Note that the magnitude in (2.5) is just the expectation of the instantaneous rates, averaged over several channel coherence intervals. Moreover, to obtain a more reliable result, we will average also over several covariance coherence intervals T_c, where the covariance matrix changes and which are assumed to be quite larger than τ_c since second-order statistics do not change as fast as channel realizations or accesses. To this end, as we will mention in Chapter 5, Monte-Carlo simulations will be used to compute these expectations and obtain the resulting numerical values.

Moreover, note that, for the sake of simplicity, since our work does not rely on actual symbol values, we assume that the number of channel accesses is equal to the coherence time of the channel. We further consider that both are one, i.e. $\tau_c = T = 1$, which means the channel is constant over a single symbol. That is why from now on, we refer to both, access and realization, indistinctly. We average then over a certain number of these intervals within different cases of their corresponding statistics, as defined in Chapter 5.

2.1.1 Reverse Link

In the case of the reverse link (also known as UL), the K users are transmitting towards the M antennas of the BS. Then, it is straightforward that B will be the number of UTs K while N the number of antennas at the BS M. This way, the channel matrix, here denoted as $\boldsymbol{H}_{\text{ul}}$, has size $M \times K$ whereas the transmitted signal $\boldsymbol{x}_{\text{ul}}$ is a K dimensional vector and both, the noise $\boldsymbol{n}_{\text{ul}}$ and received signal $\boldsymbol{y}_{\text{ul}}$, have length M. In addition, we now use a certain ρ_{ul}, equal for all users, to designate the SNR of this link. Overall, the expression in (2.1) yields

$$\boldsymbol{y}_{\text{ul}} = \boldsymbol{H}_{\text{ul}}\boldsymbol{x}_{\text{ul}} + \frac{1}{\sqrt{\rho_{\text{ul}}}}\boldsymbol{n}_{\text{ul}} \tag{2.6}$$

2.1.2 Forward Link

In the forward link (or DL), users become the receivers. Thereby, now we must assign $B = M$ and $N = K$ to be consistent with the previous notation and maintain the physical sense. Consequently, we can define the received signal in a similar way as before

$$\boldsymbol{y}_{\text{dl}} = \boldsymbol{H}_{\text{dl}}\boldsymbol{x}_{\text{dl}} + \frac{1}{\sqrt{\rho_{\text{dl}}}}\boldsymbol{n}_{\text{dl}} \tag{2.7}$$

with $\boldsymbol{H}_{\text{dl}} \in \mathbb{C}^{K\times M}$, $\boldsymbol{x}_{\text{dl}} \in \mathbb{C}^{M}$, $\boldsymbol{n}_{\text{dl}} \in \mathbb{C}^{K}$ and $\boldsymbol{y}_{\text{dl}} \in \mathbb{C}^{K}$. It is important to highlight also that $\rho_{\text{ul}} \neq \rho_{\text{dl}}$ given that to allow a fair comparison between both links, the same amount of total transmit power has to be used in both cases. As we will see in Section 4.1, for simplicity ρ_{dl} must be equal to one and the total power constraint, K times ρ_{ul}, to ensure the aforementioned condition, i.e. BS transmitting with the same energy as all users together.

2.1.3 Channel Reciprocity

Real systems use either Time Division Duplex (TDD) or Frequency Division Duplex (FDD) for the two-way communication [11]. However, as seen in Chapter 3, we will employ a TDD approach given the fast variability of the channel. In that case, it is widely assumed that channels in both directions are reciprocal, i.e. $\boldsymbol{H}_{\text{dl}}^{\text{H}} = \boldsymbol{H}_{\text{ul}} = \boldsymbol{H}$, since gains remain the same and the only thing changing is the physical direction of the channel [17]. This way, the notation in the previous expressions can be simplified as well as the channel estimation process, as discussed in Section 3.1.

2.2 Massive MIMO

Massive MIMO is the term used to define the extension of the previously introduced MU-MISO (or its equivalent MIMO) technology, where a large number of antennas M is used in comparison with the number of users K. This fact enables simple filtering techniques to achieve capacity since special properties of the channel apply when $M \gg K$ and M grows without bound.

An important aspect to point out is that, as well as in other communication schemes, channel knowledge is essential here. Nonetheless, as we will see in Section 3.1, only covariance matrices are assumed to be known, whereas channels must be estimated. Consequently, the quality of this process limits the performance of the entire system. Obtaining a suitable and reliable outcome becomes indeed, one of the major problems in massive MIMO and the one we want to address and solve in this thesis.

2.2.1 Law of Large Numbers

In order to understand the potential of massive MIMO, in this section we will explain briefly the Law of Large Numbers (LLN), since the usage of a large number of BS antennas enables the communication rate to boost in an unlimited way. This will be clearly seen in Section 2.2.2, where we analyze the impact and properties of the channel in such conditions.

The main idea behind this theorem is that, given a RV defining a set of experiments, the sample measurements tend to the real moments for a large number of realizations. For instance, when looking at the average of those samples (or just sample mean), it can be shown that it becomes closer to statistical mean the more observations used.

Nevertheless, given the nature of our system, we are more interested in this behavior for second order moments, which can be formulated in a similar way. Specifically, according to the LLN, for any couple of random vectors $\boldsymbol{x} \in \mathbb{C}^M$ and $\boldsymbol{y} \in \mathbb{C}^M$ with i.i.d. entries, the following statements apply

$$\lim_{M\to\infty} \frac{1}{M}\boldsymbol{x}^{\mathrm{H}}\boldsymbol{x} \overset{\text{a.s.}}{=} \mathrm{E}[|x_i|^2] \tag{2.8}$$

$$\lim_{M\to\infty} \frac{1}{M}\boldsymbol{x}^{\mathrm{H}}\boldsymbol{y} \overset{\text{a.s.}}{=} \mathrm{E}[x_i^* y_i] \tag{2.9}$$

where $\boldsymbol{x}^{\mathrm{H}}\boldsymbol{x} = \|\boldsymbol{x}\|_2^2$. Furthermore, in the case of zero-mean and independent variables, the previous magnitudes can be further simplified

$$\lim_{M\to\infty} \frac{1}{M}\boldsymbol{x}^{\mathrm{H}}\boldsymbol{x} \overset{\text{a.s.}}{=} \text{var}\{x_i\} \tag{2.10}$$

$$\lim_{M\to\infty} \frac{1}{M}\boldsymbol{x}^{\mathrm{H}}\boldsymbol{y} \overset{\text{a.s.}}{=} 0 \tag{2.11}$$

As we will see in the following sections, these two variables will refer to the channels of two different users, which are assumed to fulfill the previous conditions at first. Thereby, it will be revealed how these convergences become one of the key aspects in massive MIMO and that represent a clear advantage with respect to (w.r.t.) ordinary multi-antenna technologies [17].

2.2.2 Linear Processing

At this point, we need to introduce two additional magnitudes to continue with our analysis. In particular, an equalizer matrix $\boldsymbol{G} = [\boldsymbol{g}_1, \ldots, \boldsymbol{g}_K] \in \mathbb{C}^{M\times K}$, which transforms the received signal $\boldsymbol{y}_{\text{ul}}$, and a precoder $\boldsymbol{P} = [\boldsymbol{p}_1, \ldots, \boldsymbol{p}_K] \in \mathbb{C}^{M\times K}$, which processes the input data stream $\boldsymbol{s} \in \mathbb{C}^K$ so that $\boldsymbol{x}_{\text{dl}} = \boldsymbol{P}\boldsymbol{s}$, will be used to represent the linear processing applied. Note that since $\boldsymbol{s}$ plays the role of the user information, like $\boldsymbol{x}_{\text{ul}}$, we will consider it to be i.i.d., i.e. $\boldsymbol{s} \sim \mathcal{N}_{\mathbb{C}}(\boldsymbol{0}, \mathbf{I}_K)$, which means $\boldsymbol{x}_{\text{dl}}$ has now covariance matrix $\boldsymbol{P}\boldsymbol{P}^{\mathrm{H}}$. This way, we can formulate the expressions in (2.6) and (2.7) in their processed form

$$\bar{\boldsymbol{y}}_{\text{ul}} = \boldsymbol{G}^{\mathrm{H}}\boldsymbol{y}_{\text{ul}} = \boldsymbol{G}^{\mathrm{H}}\boldsymbol{H}\boldsymbol{x}_{\text{ul}} + \frac{1}{\sqrt{\rho_{\text{ul}}}}\boldsymbol{G}^{\mathrm{H}}\boldsymbol{n}_{\text{ul}} \tag{2.12}$$

$$\bar{\boldsymbol{y}}_{\text{dl}} = \boldsymbol{H}^{\mathrm{H}}\boldsymbol{P}\boldsymbol{s} + \frac{1}{\sqrt{\rho_{\text{dl}}}}\boldsymbol{n}_{\text{dl}} \tag{2.13}$$

These tools will help us define the SINRs in both directions, which can vary depending on the channel knowledge assumptions we make and that are described in Sections 2.2.3 and 2.2.4 accordingly.

Regarding the asymptotic properties introduced before, we now focus on the channels $\boldsymbol{h}_k$ as object of study. To ease the analysis, let us first consider a set of i.i.d. channels, i.e. $\boldsymbol{C}_{\boldsymbol{h}_k} = \sigma_k^2\mathbf{I}_M$, although covariances are usually not scaled identities but matrices with a certain structure.

In that case, considering two channels $\boldsymbol{h}_i$ and $\boldsymbol{h}_j$, $i \neq j$, it is straightforward to translate the statements from Section 2.2.1 with these other variables

$$\lim_{M\to\infty} \frac{1}{M} \boldsymbol{h}_i^{\mathrm{H}} \boldsymbol{h}_i \overset{\text{a.s.}}{=} \sigma_i^2 \tag{2.14}$$

$$\lim_{M\to\infty} \frac{1}{M} \boldsymbol{h}_i^{\mathrm{H}} \boldsymbol{h}_j \overset{\text{a.s.}}{=} 0 \tag{2.15}$$

These facts are commonly known as *channel hardening* and *asymptotic orthogonality* respectively, and they clearly justify the usage of a ordinary Matched Filter (MF) as filtering technique. It can be easily inferred that, with this simple approach, all interference coming from other users can be removed for $M \to \infty$ (2.15) whereas the channel of the main user is strengthened (2.14)

$$\frac{1}{M} \boldsymbol{H}^{\mathrm{H}} \boldsymbol{H} \to \mathrm{diag}(\sigma_1^2, \ldots, \sigma_K^2) \tag{2.16}$$

This way, as we will see in the upcoming sections, the SINR converges to the SNR, which in turn increases with M without limit. As a result, we can obtain infinite rates with a very simple and low-complexity processing scheme. That is why massive MIMO has caught the attention of the scientific community and represents a huge breakthrough in the wireless communications field.

On the other hand, a similar analysis is still valid in the case of non i.i.d. channels, although it is a more tough to proof. It relies on the fact that those RVs can be simply expressed as $\boldsymbol{h}_k = \boldsymbol{C}_{\boldsymbol{h}_k}^{1/2} \boldsymbol{h}'_k$ where $\boldsymbol{h}'_k$ corresponds to the previous i.i.d. channels. Consequently, when looking at the inner product between different channels, one can see that, according to random matrix theory results [7] and under certain circumstances, we have

$$\lim_{M\to\infty} \frac{1}{M} \boldsymbol{h}_i^{\mathrm{H}} \boldsymbol{h}_j = \lim_{M\to\infty} \frac{1}{M} \boldsymbol{h}_i'^{\mathrm{H}} \boldsymbol{C}_{\boldsymbol{h}_i}^{\mathrm{H}/2} \boldsymbol{C}_{\boldsymbol{h}_j}^{1/2} \boldsymbol{h}'_j = \begin{cases} \text{cnst} & \text{if} \quad i = j \\ 0 & \text{if} \quad i \neq j \end{cases} \tag{2.17}$$

which is also introduced in [18]. Somehow, this is a special version of the LLN and can be also demonstrated in the case of the mean. Thereby, the asymptotic properties of the channel are maintained both, hardening and orthogonality. Consequently, a similar diagonalisation of the channel to the one in (2.16), takes place when using the MF. Besides, this enables us to fully exploit massive MIMO advantages while focusing on more realistic channels with a certain covariance matrix $\boldsymbol{C}_{\boldsymbol{h}_k} \neq \mathbf{I}_M$. From now on, we will restrict ourselves then to this model, first described in Section 2.1 and later in 2.3.

2.2.3 Perfect Channel Knowledge

To determine the SINRs in the UL and the DL, we first need to define their corresponding transmit symbol estimate, which we represent by $\hat{x}_k = \boldsymbol{g}_k^{\mathrm{H}} \boldsymbol{y}_{\mathrm{ul}}$ and $\hat{s}_k = \boldsymbol{e}_k^{\mathrm{H}} \bar{\boldsymbol{y}}_{\mathrm{dl}}$ respectively. Note that notation has been slightly changed w.r.t. equations (2.12) and (2.13) to avoid any possible future confusion, i.e. $\hat{\boldsymbol{x}} = \bar{\boldsymbol{y}}_{\mathrm{ul}}$ and $\hat{\boldsymbol{s}} = \bar{\boldsymbol{y}}_{\mathrm{dl}}$ are now the processed received signals. Then, $\hat{x}_k$ and $\hat{s}_k$ are the respective portions of information destined to user k. Hence, assuming first that we have perfect channel knowledge at the transmitter and receiver, we can express the individual SINR γ_k of each link as follows

$$\gamma_{k,\mathrm{ul}} = \frac{|\boldsymbol{g}_k^{\mathrm{H}} \boldsymbol{h}_k|^2}{\frac{1}{\rho_{\mathrm{ul}}} + \sum_{n \neq k} |\boldsymbol{g}_k^{\mathrm{H}} \boldsymbol{h}_n|^2} \tag{2.18}$$

$$\gamma_{k,\mathrm{dl}} = \frac{|\boldsymbol{h}_k^{\mathrm{H}} \boldsymbol{p}_k|^2}{\frac{1}{\rho_{\mathrm{dl}}} + \sum_{n \neq k} |\boldsymbol{h}_k^{\mathrm{H}} \boldsymbol{p}_n|^2} \tag{2.19}$$

where it is assumed that the equalizer has norm one and the noise has unit power (2.1). Besides, considering the use of MF for precoding and equalizing, i.e. $\boldsymbol{p}_k = \beta \boldsymbol{h}_k$ and $\boldsymbol{g}_k = \frac{1}{\|\boldsymbol{h}_k\|_2} \boldsymbol{h}_k$ respectively, both terms yield

$$\gamma_{k,\mathrm{ul}} = \frac{|\boldsymbol{h}_k^{\mathrm{H}} \boldsymbol{h}_k|^2}{\frac{\|\boldsymbol{h}_k\|_2^2}{\rho_{\mathrm{ul}}} + \sum_{n \neq k} |\boldsymbol{h}_k^{\mathrm{H}} \boldsymbol{h}_n|^2} \tag{2.20}$$

$$\gamma_{k,\mathrm{dl}} = \frac{|\boldsymbol{h}_k^{\mathrm{H}} \boldsymbol{h}_k|^2}{\frac{1}{\beta^2 \rho_{\mathrm{dl}}} + \sum_{n \neq k} |\boldsymbol{h}_k^{\mathrm{H}} \boldsymbol{h}_n|^2} \tag{2.21}$$

where β is the scaling factor that ensures the power constraint is fulfilled in the transmission, as discussed in Section 4.1. Therefore, in the large-scale regime ($M \to \infty$), this maximum-ratio combining leads to the following SINRs

$$\gamma_{k,\mathrm{ul}} = \frac{\frac{1}{M} |\boldsymbol{h}_k^{\mathrm{H}} \boldsymbol{h}_k|^2}{\frac{1}{M} \left(\frac{\|\boldsymbol{h}_k\|_2^2}{\rho_{\mathrm{ul}}} + \sum_{n \neq k} |\boldsymbol{h}_k^{\mathrm{H}} \boldsymbol{h}_n|^2 \right)} \approx M \rho_{\mathrm{ul}} \|\boldsymbol{h}_k\|_2^2 \tag{2.22}$$

$$\gamma_{k,\mathrm{dl}} = \frac{\frac{1}{M} |\boldsymbol{h}_k^{\mathrm{H}} \boldsymbol{h}_k|^2}{\frac{1}{M} \left(\frac{1}{\beta^2 \rho_{\mathrm{dl}}} + \sum_{n \neq k} |\boldsymbol{h}_k^{\mathrm{H}} \boldsymbol{h}_n|^2 \right)} \approx M \beta^2 \rho_{\mathrm{dl}} \|\boldsymbol{h}_k\|_2^2 \tag{2.23}$$

where we used the fact that channels of different users become orthogonal for large M. Note that in the i.i.d. case, according to (2.14) we could write

$\|\boldsymbol{h}_k\|_2^2 \to \sigma_k^2$. Overall, it is proved that the SINR converges to the SNR, which is proportional to M and thus, grows without bound. As a result, when substituting these terms into the rate expression of (2.5), we can see that it also increases endlessly with the number of BS antennas as $\gamma_k \propto M$. This parameter is then known as the gain of the antenna array or simply *array gain*.

Moreover, note that any filter with the shape of a matched filter will end in the previous results. For instance, in the case of the equalizer, any front-end of the form $\boldsymbol{G} = \boldsymbol{H}\boldsymbol{A}^{-1}$, with $\boldsymbol{A}$ depending on the channel realizations and statistics (see Section 4.1), will allow the asymptotic characteristics to take place and thus, lead the SINR to be proportional to the number of BS antennas M as well as the user rate to grow without bound.

2.2.4 Imperfect Channel Knowledge

In real systems, channel knowledge is far from perfect since estimation is needed and there is always some randomness left after the process. Then, we cannot assume that this information is given and that estimates are available error-free.

To take this into account, e.g. see [19], two different perspectives are presented, each of which defines a lower bound on the achievable rate. Both represent the deterioration of the performance whenever the channel information is not perfect.

2.2.4.1 CDI Lower Bound

The first approach that considers erroneous channel knowledge is given by the author in [20]. It relies on the fact that the channel is constituted by its statistical mean, known at the receiver, plus some random part

$$\boldsymbol{h}_k = \mathrm{E}[\boldsymbol{h}_k] + (\boldsymbol{h}_k - \mathrm{E}[\boldsymbol{h}_k]) = \mathrm{E}[\boldsymbol{h}_k] + \tilde{\boldsymbol{h}}_k \tag{2.24}$$

where $\mathrm{E}[\boldsymbol{h}_k]$ is the known mean and $\tilde{\boldsymbol{h}}_k = \boldsymbol{h}_k - \mathrm{E}[\boldsymbol{h}_k]$ is denoted as the unknown part. Then, the author assumes the worst case scenario where $\tilde{\boldsymbol{h}}_k$ is considered to be additional Gaussian noise. In that case, it can be shown that the user rates can be lower bounded in the following manner

$$R_k = \mathrm{E}[\log_2(1+\gamma_k)] \geq \log_2(1+\underline{\gamma}_k^{\mathrm{CDI}}) = \underline{R}_k^{\mathrm{CDI}} \tag{2.25}$$

where $\underline{R}_k^{\mathrm{CDI}}$ is the lower bound achievable rate and $\underline{\gamma}_k^{\mathrm{CDI}}$ the equivalent SINR, different for the UL and DL scenarios

$$\underline{\gamma}_{k,\text{ul}}^{\text{CDI}} = \frac{|\text{E}[\boldsymbol{g}_k^{\text{H}}\boldsymbol{h}_k]|^2}{\frac{\text{E}[\|\boldsymbol{g}_k\|_2^2]}{\rho_{\text{ul}}} + \text{var}\{\boldsymbol{g}_k^{\text{H}}\boldsymbol{h}_k\} + \sum_{n\neq k}\text{E}[|\boldsymbol{g}_k^{\text{H}}\boldsymbol{h}_n|^2]} \tag{2.26}$$

$$\underline{\gamma}_{k,\text{dl}}^{\text{CDI}} = \frac{|\text{E}[\boldsymbol{h}_k^{\text{H}}\boldsymbol{p}_k]|^2}{\frac{1}{\rho_{\text{dl}}} + \text{var}\{\boldsymbol{h}_k^{\text{H}}\boldsymbol{p}_k\} + \sum_{n\neq k}\text{E}[|\boldsymbol{h}_k^{\text{H}}\boldsymbol{p}_n|^2]} \tag{2.27}$$

where now expected values instead of realizations are employed. Note then, that the variance terms, included also in $\text{E}[|\bullet|^2] = \text{var}\{\bullet\} + |\text{E}[\bullet]|^2$, are introduced as a new source of noise coming from both, main and interfering users, and they represent the randomness in (2.24). As a result, we can get rid of the expectation in (2.25) as now, $\underline{\gamma}_k^{\text{CDI}}$ is no longer a RV, like γ_k, but constant and dependent on the channel statistics only. That is why this approach is commonly referred to as Channel Distribution Information (CDI) lower bound on the achievable rate. It establishes a more realistic and reliable measure for the system performance and has been widely accepted [21][22].

To further understand how this erroneous information affects the rate, we can reformulate the previous terms using again the MF as processing technique

$$\underline{\gamma}_{k,\text{ul}}^{\text{CDI}} = \frac{|\text{E}[\boldsymbol{h}_k^{\text{H}}\boldsymbol{h}_k]|^2}{\frac{\text{E}[\|\boldsymbol{h}_k\|_2^2]}{\rho_{\text{ul}}} + \text{var}\{\boldsymbol{h}_k^{\text{H}}\boldsymbol{h}_k\} + \sum_{n\neq k}\text{E}[|\boldsymbol{h}_k^{\text{H}}\boldsymbol{h}_n|^2]} \tag{2.28}$$

$$\underline{\gamma}_{k,\text{dl}}^{\text{CDI}} = \frac{|\text{E}[\boldsymbol{h}_k^{\text{H}}\boldsymbol{h}_k]|^2}{\frac{1}{\beta^2\rho_{\text{dl}}} + \text{var}\{\boldsymbol{h}_k^{\text{H}}\boldsymbol{h}_k\} + \sum_{n\neq k}\text{E}[|\boldsymbol{h}_k^{\text{H}}\boldsymbol{h}_n|^2]} \tag{2.29}$$

Note that for simplicity, we only consider the randomness coming from the channel itself and not from the estimate. That is why, to illustrate the main point here, we use $\boldsymbol{h}_k$ for the filters instead of what we really have, $\hat{\boldsymbol{h}}_k \neq \boldsymbol{h}_k$, as we will explain in the next section first, and later in Chapter 3. Also, it is important to highlight that to simplify derivations, now we have considered the equalizer not to be normalized, i.e. $\boldsymbol{g}_k = \boldsymbol{h}_k$, and thus, we need to introduce the scaling factor $\text{E}[\|\boldsymbol{g_k}\|_{\boldsymbol{2}}^{\boldsymbol{2}}]$ in (2.26). It represents the power of the equalized noise and can be easily found in the following

$$\begin{aligned}\text{E}[|\boldsymbol{g}_k^{\text{H}}\boldsymbol{n}|^2] &= \text{E}[\boldsymbol{g}_k^{\text{H}}\boldsymbol{n}\boldsymbol{n}^{\text{H}}\boldsymbol{g}_k] = \text{E}[\boldsymbol{g}_k^{\text{H}}\text{E}[\boldsymbol{n}\boldsymbol{n}^{\text{H}}]\boldsymbol{g}_k] = \text{E}[\boldsymbol{g}_k^{\text{H}}\mathbf{I}\,\boldsymbol{g}_k] \\ &= \text{E}[\boldsymbol{g}_k^{\text{H}}\boldsymbol{g}_k] = \text{E}[\|\boldsymbol{g}_k\|_2^2] = \text{E}[\|\boldsymbol{h}_k\|_2^2] = \text{tr}(\boldsymbol{C}_{\boldsymbol{h}_k})\end{aligned} \tag{2.30}$$

which is clearly different from the instantaneous normalization factor given by $\|\boldsymbol{g}_k\|_2^2 = \|\boldsymbol{h}_k\|_2^2$, which in turn is assumed to be one in (2.19).

Moreover, concerning the expectation of the inner product, we know that given two zero-mean and jointly Gaussian distributed RV $\boldsymbol{x}$ and $\boldsymbol{y}$, we can express the expectation $\mathrm{E}[|\boldsymbol{x}^{\mathrm{H}}\boldsymbol{y}|^2]$ as follows

$$\mathrm{E}[|\boldsymbol{x}^{\mathrm{H}}\boldsymbol{y}|^2] = \mathrm{tr}(\mathrm{E}[\boldsymbol{x}\boldsymbol{x}^{\mathrm{H}}]\mathrm{E}[\boldsymbol{y}\boldsymbol{y}^{\mathrm{H}}]) + |\mathrm{tr}(\mathrm{E}[\boldsymbol{y}\boldsymbol{x}^{\mathrm{H}}])|^2 \tag{2.31}$$

Then, by setting $\boldsymbol{x} = \boldsymbol{h}_i$ and $\boldsymbol{y} = \boldsymbol{h}_j$, it can be shown that $\underline{\gamma}_k$ becomes

$$\underline{\gamma}_{k,\mathrm{ul}}^{\mathrm{CDI}} = \frac{|\mathrm{tr}(\boldsymbol{C}_{\boldsymbol{h}_k})|^2}{\frac{\mathrm{tr}(\boldsymbol{C}_{\boldsymbol{h}_k})}{\rho_{\mathrm{ul}}} + \sum_n \|\boldsymbol{C}_{\boldsymbol{h}_k}\|_{\mathrm{F}}^2 + \sum_{n\neq k} |\mathrm{tr}(\boldsymbol{C}_{\boldsymbol{h}_n})|^2} \tag{2.32}$$

$$\underline{\gamma}_{k,\mathrm{dl}}^{\mathrm{CDI}} = \frac{|\mathrm{tr}(\boldsymbol{C}_{\boldsymbol{h}_k})|^2}{\frac{1}{\beta^2\rho_{\mathrm{dl}}} + + \sum_n \|\boldsymbol{C}_{\boldsymbol{h}_k}\|_{\mathrm{F}}^2 + \sum_{n\neq k} |\mathrm{tr}(\boldsymbol{C}_{\boldsymbol{h}_n})|^2} \tag{2.33}$$

where $\| \bullet \|_{\mathrm{F}}$ is the matrix Frobenius norm. For a general M, it can be seen that $\underline{\gamma}_k^{\mathrm{CDI}} \leq \gamma_k$ since more noise is included, which clearly worsens the performance. However, authors in [23] demonstrate that in the large-scale regime, $\underline{\gamma}_k^{\mathrm{CDI}} \approx \gamma_k$. Thus, incorrect channel knowledge does not affect rate when $M \to \infty$, yet this condition cannot be fulfilled in reality given obvious physical reasons and limitations. As a result, erroneous information must be taken into consideration once designing our system, as we will see in Chapter 4.

2.2.4.2 CSI Lower Bound

Another approach which considers this fact is exposed in [24]. There, authors believe that the true channel remains unknown and must be estimated, as exposed in Section 3.1, leading to an error during that process that can be expressed in the following manner

$$\tilde{\boldsymbol{h}}_k = \boldsymbol{h}_k - \hat{\boldsymbol{h}}_k \tag{2.34}$$

with $\hat{\boldsymbol{h}}_k$ being the estimate, or known part, and $\tilde{\boldsymbol{h}}_k$ the corresponding estimation error of the k-th channel $\boldsymbol{h}_k$. To take into account this incorrect knowledge, we introduce extra noise in the received signal, considered again to be Gaussian to face the worst case scenario. Then, it can be shown that the SINRs in (2.18) and (2.19) can be equivalently written as

$$\underline{\gamma}_{k,\text{ul}}^{\text{CSI}} = \frac{|\boldsymbol{g}_k^{\text{H}}\hat{\boldsymbol{h}}_k|^2}{\frac{1}{\rho_{\text{ul}}} + \sum_n \boldsymbol{g}_k^{\text{H}}\boldsymbol{C}_{\tilde{\boldsymbol{h}}_n}\boldsymbol{g}_k + \sum_{n\neq k}|\boldsymbol{g}_k^{\text{H}}\hat{\boldsymbol{h}}_n|^2} \tag{2.35}$$

$$\underline{\gamma}_{k,\text{dl}}^{\text{CSI}} = \frac{|\hat{\boldsymbol{h}}_k^{\text{H}}\boldsymbol{p}_k|^2}{\frac{1}{\rho_{\text{dl}}} + \sum_n \boldsymbol{p}_n^{\text{H}}\boldsymbol{C}_{\tilde{\boldsymbol{h}}_k}\boldsymbol{p}_n + \sum_{n\neq k}|\hat{\boldsymbol{h}}_k^{\text{H}}\boldsymbol{p}_n|^2} \tag{2.36}$$

where $\boldsymbol{C}_{\tilde{\boldsymbol{h}}_k}$ is the covariance matrix of the error and represents the worsening of the performance in this situation. In the case of the linear MMSE estimate, Section 3.1.2, this magnitude can be easily defined. Overall, here the effective noise is the result of the original Additive White Gaussian Noise (AWGN), present in all communication links, and the estimation error.

Furthermore, when comparing with the previous point of view, we first see that here we rely on channel realizations and not on statistics. That is why this approach can be named as Channel State Information (CSI) lower bound on the achievable rate. Similarly to before, it establishes a feasible and more faithful value for the user. In addition, note that now the equalizer in (2.35) is assumed to be normalized as no controversy in the expression is generated. Nevertheless, regarding the rate, the expectation in (2.5) cannot be removed since we have instantaneous magnitudes. Hence, now $\underline{\gamma}_k^{\text{CSI}}$ is again a RV, just like γ_k, but with smaller values for finite M. This results in the following user rate

$$R_k = \text{E}[\log_2(1+\gamma_k)] \geq \text{E}[\log_2(1+\underline{\gamma}_k^{\text{CSI}})] = \underline{R}_k^{\text{CSI}} \tag{2.37}$$

Finally, similar conclusions can be drawn from this perspective. First, when using MF as filtering scheme, it can be shown that the SINRs are smaller than in the case of perfect channel knowledge. And second, that in the case of large M, this effects are removed and the converge towards the SNR is achieved.

2.3 Channel Model

Throughout the whole project, specially in the simulations chapter, a spatial channel model will be used for the system analysis and data results. It is a particular case defined by the 3GPP community, which we will introduce in the first part of this section. Note that this standard will define the channel and a way to obtain its covariance. Also, under certain circumstances, special properties hold and an approximation of these matrices can be applied. We will discuss later, in the second part, that they can be transformed into diagonals,

fact that leads to a substantial improvement of complexity. This assumption will be mentioned and employed in the remainder of the thesis.

2.3.1 3GPP Standard

As mentioned in Section 2.1, we will not assume i.i.d. channels but channels with a certain covariance matrix. This magnitude will be defined in the following. Note that in the whole project we will consider a single cell scenario where the BS, equipped with M antennas, serves the K users. A similar analysis can be done for the multi-cell case [11][25].

Thereby, let us start by assuming the BS can be described as a Uniform Linear Array (ULA). Then, following the reasoning from [26], it can be shown that the channel $\boldsymbol{h}_k$ for a multi-path environment results

$$\boldsymbol{h}_k = \sqrt{\beta_k} \sum_{n=1}^{N_P} \boldsymbol{a}(\theta_{k,n}) \alpha_{k,n} = \sqrt{\beta_k} \boldsymbol{A}_k \boldsymbol{\alpha}_k \tag{2.38}$$

where β_k models the slow fading, e.g. shadowing (equal for all signal paths), N_P is the number of paths and $\alpha_{k,n} \sim \mathcal{N}_{\mathbb{C}}(0, \sigma^2_{k,n})$ are the coefficients representing the fast fading and time variation of the channel. The steering vector $\boldsymbol{a}(\theta_{k,n})$, with constant angles of arrival $\theta_{k,n}$, can be expressed as

$$\boldsymbol{a}(\theta_{k,n}) = \begin{bmatrix} 1 \\ e^{-j2\pi \frac{D}{\lambda} \sin(\theta_{k,n})} \\ \vdots \\ e^{-j2\pi(M-1) \frac{D}{\lambda} \sin(\theta_{k,n})} \end{bmatrix} \tag{2.39}$$

where D is the antenna spacing, set to $\lambda/2$, and $\lambda = c/f$, with carrier frequency f and c the light speed, the wavelength employed. Therefore, the corresponding covariance matrix is given by

$$\boldsymbol{C}_{\boldsymbol{h}_k} = \beta_k \boldsymbol{A}_k \text{diag}(\sigma^2_{k,1}, \ldots, \sigma^2_{k,N_P}) \boldsymbol{A}_k^{\text{H}} \tag{2.40}$$

which can be seen to have a Toeplitz structure [27]. In addition, all the required parameters to build this matrices can be found in [28], where a reliable method to find them is proposed. In our case, we will use the urban macro scenario with 8 degrees of angle spread and a central frequency of 1.9 GHz. Note that, as we will use later in Chapter 5, the path loss, plus other correction factors, will be multiplied at the end of the computations to each covariance

matrix. Its expression can be found in Table 5.1 from [28]

$$\mathrm{PL}_k = 34.5 + 35\log_{10}(d) \tag{2.41}$$

where d is the distance between UT and BS. For our simulations, we will further assume that users are distributed uniformly in the cell with hexagonal layout of radius 1000 m and with a minimum distance to the BS of 35 m.

Overall, we will compute the matrix according to expression in (2.40) and the model from [28] and afterwards, generate the channels with these covariances according to Section 2.1, i.e. $\boldsymbol{h}_k \sim \mathcal{N}_{\mathbb{C}}(\mathbf{0}, \boldsymbol{C}_{\boldsymbol{h}_k})$.

2.3.2 DFT Approximation

As already mentioned, here we will present an approximation of the covariances by means of the unitary DFT matrix $\boldsymbol{F} \in \mathbb{C}^{M\times M}$ defined below

$$\boldsymbol{F} = \frac{1}{\sqrt{M}}\begin{bmatrix} 1 & 1 & \cdots & 1 \\ 1 & e^{-j2\pi/M} & \cdots & e^{-j2\pi(M-1)/M} \\ \vdots & \vdots & \ddots & \vdots \\ 1 & e^{-j2\pi(M-1)/M} & \cdots & e^{-j2\pi(M-1)^2/M} \end{bmatrix} \tag{2.42}$$

Note that, as discussed above, covariance matrices have a Toeplitz structure given the spatial model we are using (ULA). Then, according to [27], it can be approximated by a circulant matrix and thus, we can write

$$\boldsymbol{C}_{\boldsymbol{h}_k} \approx \boldsymbol{F}^{\mathrm{H}}\boldsymbol{D}_{\boldsymbol{h}_k}\boldsymbol{F} \tag{2.43}$$

where $\boldsymbol{D} = \mathrm{diag}(\boldsymbol{F}\boldsymbol{C}_{\boldsymbol{h}_k}\boldsymbol{F}^{\mathrm{H}})$. As shown in [29], this approximation converges to the true value in the large-scale regime ($M \to \infty$), which makes it perfect for massive MIMO systems. It can be understood in the sense that this DFT matrix diagonalizes the covariance given the particular structure of channels in this model, which leads it become the eigenvector basis.

Finally, to apply this transformation, we just need to multiply the channel vector by $\boldsymbol{F}$. From (2.43), it follows that $\boldsymbol{C}_{\boldsymbol{h}_k}^{1/2} \approx \boldsymbol{F}^{\mathrm{H}}\boldsymbol{D}_{\boldsymbol{h}_k}^{1/2}$. Then, taking into account that $\boldsymbol{h}_k = \boldsymbol{C}_{\boldsymbol{h}_k}^{1/2}\boldsymbol{h}'_k$ (see Section 2.2.2), we have

$$\boldsymbol{F}\boldsymbol{h}_k \approx \boldsymbol{F}\boldsymbol{F}^{\mathrm{H}}\boldsymbol{D}_{\boldsymbol{h}_k}^{1/2}\boldsymbol{h}'_k = \boldsymbol{D}_{\boldsymbol{h}_k}^{1/2}\boldsymbol{h}'_k \tag{2.44}$$

Chapter 3

Pilot Contamination

In this chapter we will introduce the concept of pilot contamination, principal subject matter in this thesis and main problem we aim to solve. Thereby, its causes and consequences are explained to clearly understand this issue.

First, we expose the process of channel estimation, essential in any real and modern communication system. In particular, we will discuss and compare two methods to do this task. Second, we present the pilot contamination effect, together with the impact it has on the system performance and specially, in the user rate. We will make special emphasis on the properties and behavior of the two estimates whenever this interference is present.

3.1 Channel Estimation

In the past, it was widely assumed that transmitter and receiver knew the channel perfectly [30]. In fact, some authors still dedicate some of their research to study scenarios where full and error-free channel knowledge is available. However, this leads to unattainable results since in real systems, this information is not given away for free. Therefore, as mentioned before, channels must be estimated and the quality of this procedure conditions highly the overall performance. This is why current investigations focus on this assumption and try to give suitable and feasible solutions, e.g. see [11][19][23].

The most common method for channel estimation is the use of training sequences [21]. In particular, it can be shown that only one symbol per user is

necessary to estimate the channel in the reverse link, whereas a codewords of length M are required in the case of the DL [31]. Therefore, when M increases without bound, it becomes quickly unfeasible to estimate the channel in that direction given its fast variation ($\tau_c \ll M$). That is why TDD systems are preferred over FDD, since channel reciprocity does not apply in the frequency domain, specially when the gap between simultaneous transmissions is large. In other words, propagation for both directions in the case of FDD is not the same and thus, estimation must be done for each of them. This clearly discards FDD approaches when M starts to increase and reinforces the use of TDD when it comes to estimation. This decision is in fact, supported by many authors, e.g. [11][25], since it provides a reliable and conceivable duplex communication.

Thereby, the whole procedure goes as follows. First, training sequences, known to both ends, transmitter and receiver, are send by each user in the UL to estimate the channel in that direction. Then, this information is used for two purposes. On the one hand, it will be employed at the BS for data processing at reception, i.e. equalization in the reverse-link transmission. On the other hand, these estimates are converted by means of the Hermitian operator, $\hat{\boldsymbol{h}}_{k,\text{dl}} = \hat{\boldsymbol{h}}_{k,\text{ul}}^{\text{H}}$ (see Section 2.1.3), and used as filtering technique in the case of the DL, i.e. input signals are precoded using these estimates in the forward-link . Diverse options for these schemes will be seen in detail in Section 4.1.

Furthermore, in this project we will assume that covariance matrices are known at both ends, since their estimation represents another challenge [32] and is far beyond the scope of our work. Then, with regard to estimation, we will focus only on the channel itself and concentrate on the approach via UL training sequences. In particular, we distinguish between the Least Squares and Linear Minimum Mean Square Error estimates.

Finally, it is important to see that, given that training is only done in the UL, channel knowledge is kept at the BS exclusively. We assume no feedback is used throughout the project. Therefore, any usage of this information is restricted to the BS, while users remain blind as they are not aware of the estimation.

3.1.1 Least Squares

The first and easiest estimator is the so-called Least Squares (LS). It tries to minimize the absolute squared value of the difference between true and estimated value. However, in the next section, we will see that this strategy is not the best way to go due to its high sensitivity to pilot contamination.

To begin with, let us define the set of pilot sequences $\boldsymbol{\psi}_k$ that each user employs for channel estimation and a certain training time T_{tr}, which determines their corresponding length, i.e. $\boldsymbol{\psi}_k \in \mathbb{C}^{T_{\text{tr}}} \, \forall k$. We can gather together all of them and use the matrix form $\boldsymbol{\Psi} = [\boldsymbol{\psi}_1, \ldots, \boldsymbol{\psi}_K]^{\text{H}} \in \mathbb{C}^{K \times T_{\text{tr}}}$. Note that, as already mentioned above, the estimation of the reverse-link only requires one symbol, i.e. $T_{\text{tr}} = 1$. Also, it is obvious that this value cannot exceed the coherence time of the channel τ_c because estimation would not have sense otherwise, i.e. inconsistent result would be obtained if channel changes during estimation. Nevertheless, it can be inferred that the more time used, the better the outcome becomes, specially when we deal with interference during the process. In fact, authors in [11] argue that, in presence of pilot contamination, the optimal approach is to use half the available time of the communication for estimation and the other half for data transmission, i.e. $T_{\text{tr}} = \tau_c/2$.

Furthermore, as we will see later, for a good quality, it is crucial that training sequences are orthogonal and unique to each user, meaning the product between two sequences of different users must be zero. Also, to ease notation, we impose them to be unit length, i.e. their inner product must result one. In other words, for the moment we assume that $T_{\text{tr}} \geq K$, meaning each user has a unique pilot, and all of them form an orthonormal basis, i.e. $\boldsymbol{\Psi}\boldsymbol{\Psi}^{\text{H}} = \mathbf{I}_K$.

Overall, we can express the received signal in this UL estimation as

$$\boldsymbol{Y}_{\text{tr}} = \boldsymbol{H}\boldsymbol{\Psi} + \frac{1}{\sqrt{\rho_{\text{tr}}}}\boldsymbol{N}_{\text{tr}} \tag{3.1}$$

with $\boldsymbol{Y}_{\text{tr}}$, $\boldsymbol{N}_{\text{tr}} \in \mathbb{C}^{M \times T_{\text{tr}}}$ being the output and noise respectively. They can be understood as the set of M dimensional vectors from (2.1) over T_{tr} channel accesses. It is assumed that the SNR of the UL is observed here, i.e. $\rho_{\text{tr}} = \rho_{\text{ul}}$, as we have the same power and channel quality. Therefore, our goal is to obtain the best approximation of the channel $\boldsymbol{H}$ from the expression in (3.1). In particular, according to the definition introduced at the beginning of this section, the LS estimate of this matrix would be given by

$$\hat{\boldsymbol{H}}^{\text{LS}} = \underset{\boldsymbol{H}}{\text{argmin}} \|\boldsymbol{Y}_{\text{tr}} - \boldsymbol{H}\boldsymbol{\Psi}\|_2^2 = \boldsymbol{Y}_{\text{tr}}\boldsymbol{\Psi}^{\text{H}}(\boldsymbol{\Psi}\boldsymbol{\Psi}^{\text{H}})^{-1} = \boldsymbol{Y}_{\text{tr}}\boldsymbol{\Psi}^{\text{H}} \tag{3.2}$$

where $\hat{\boldsymbol{H}}^{\text{LS}} = [\hat{\boldsymbol{h}}_1^{\text{LS}}, \ldots, \hat{\boldsymbol{h}}_K^{\text{LS}}] \in \mathbb{C}^{M \times K}$ is the aforementioned magnitude. Notwithstanding, we will use the notation from authors in [18], since it is the starting point of all our project. Hence, we define $\boldsymbol{\Phi} = [\boldsymbol{\phi}_1, \ldots, \boldsymbol{\phi}_K]$ as the set

of new LS estimates of the channel matrix, i.e. $\boldsymbol{\Phi} = \hat{\boldsymbol{H}}^{\text{LS}}$ and $\boldsymbol{\phi} = \hat{\boldsymbol{h}}_k^{\text{LS}}$.

Moreover, focusing on the k-th estimate $\boldsymbol{\phi}_k$, we can find its expression as

$$\boldsymbol{\phi}_k = \boldsymbol{Y}_{\text{tr}}\boldsymbol{\psi}_k = \boldsymbol{h}_k + \frac{1}{\rho'_{\text{tr}}}\boldsymbol{n}' \tag{3.3}$$

where $\boldsymbol{n}' = \boldsymbol{N}_{\text{tr}}\boldsymbol{\psi}_k \in \mathbb{C}^M$ is the transformed version of the noise and ρ'_{tr} the SNR associated. As we can see, after correlation with the orthogonal pilot sequence, the resulting estimate contains the desired channel $\boldsymbol{h}_k$ plus some error term. Besides, since in reality we are estimating only one symbol over T_{tr} channel accesses, it is straightforward to see that $\rho'_{\text{tr}} = T_{\text{tr}}\rho_{\text{tr}}$. This is due to the fact that the channel for each user has duration one, i.e. $\boldsymbol{h}_k \in \mathbb{C}^{M\times 1}$. This justifies the statement announced before: the more time we dedicate for estimation, the better this process will result. For instance, in the extreme case of having an infinite T_{tr}, the noise portion would be completely removed and the estimate would be the true channel, error-free.

All this analysis holds for the case of having unique pilots exclusively and does not really show how this estimate behaves in unfavorable conditions, where interference is included. This will be precisely revealed in Section 3.2.

3.1.2 Linear Minimum Square Error

The other approach to cope with channel estimation is the Linear Minimum Mean Square Error (LMMSE). In this case and unlike before, statistical information is now exploited. This strategy tries then to minimize the mean square error between estimate and true value by means of a linear form. From the results in [18], we can express the k-th estimator as follows

$$\hat{\boldsymbol{h}}_k^{\text{LMMSE}} = \underset{\boldsymbol{h}_k}{\operatorname{argmin}}\, \text{E}[\|\boldsymbol{h}_k - \hat{\boldsymbol{h}}_k\|_2^2|\boldsymbol{\phi}_k] = \text{E}[\boldsymbol{h}_k|\boldsymbol{\phi}_k] = \boldsymbol{C}_{\boldsymbol{h}_k}\boldsymbol{C}_{\boldsymbol{\phi}_k}^{-1}\boldsymbol{\phi}_k \tag{3.4}$$

where $\boldsymbol{C}_{\boldsymbol{\phi}_k} = \text{E}[\boldsymbol{\phi}_k\boldsymbol{\phi}_k^{\text{H}}] \in \mathbb{C}^{M\times M}$ is the covariance matrix of the zero-mean LS estimate and that can be expressed as

$$\boldsymbol{C}_{\boldsymbol{\phi}_k} = \boldsymbol{C}_{\boldsymbol{h}_k} + \frac{1}{T_{\text{tr}}\rho_{\text{tr}}}\mathbf{I}_M \tag{3.5}$$

which can be seen to have always full-rank, regardless of $\boldsymbol{C}_{\boldsymbol{h}_k}$, given the presence of AWGN. Furthermore, as we will see in Section 4.1, we need to define the corresponding estimation error covariance matrix $\tilde{\boldsymbol{C}}_k \in \mathbb{C}^{M\times M}$

$$\tilde{\boldsymbol{C}}_k = \mathrm{E}[(\boldsymbol{h}_k - \boldsymbol{\theta}_k)(\boldsymbol{h}_k - \boldsymbol{\theta}_k)^{\mathrm{H}} | \boldsymbol{\phi}_k] = \boldsymbol{C}_{\boldsymbol{h}_k} - \boldsymbol{C}_{\boldsymbol{h}_k} \boldsymbol{C}_{\boldsymbol{\phi}_k}^{-1} \boldsymbol{C}_{\boldsymbol{h}_k} \tag{3.6}$$

Note also that this method is far more sophisticated than the previous one as it relies on a certain observation, here $\boldsymbol{\phi}_k$ too, and channel statistics to determine outcome. Its performance is highly conditioned by this term then. Additionally, it can be shown that it coincides with the Bayesian estimate with Maximum A Posteriori (MAP) decision rule [33], sharing all its interesting characteristics. Besides, we will use here the notation from [18] as well and thus, we introduce $\boldsymbol{\theta}_k = \hat{\boldsymbol{h}}_k^{\mathrm{LMMSE}}$. We can express all of them in a more compact notation by setting $\boldsymbol{\Theta} = [\boldsymbol{\theta}_1, \ldots, \boldsymbol{\theta}_K]$, later used in Chapter 4.

On the other hand, an important property of this estimator must be pointed out. It is related to the covariance matrix of the channel, defined in Section 2.3, although it can be applied to any channel fulfilling the following condition. We require the number of multipaths in the scenario to be sufficiently small compared to the number of antennas at the BS. Then, it is evident that covariances will be rank deficient as we can distinguish more paths than the existent.

This fact has special importance when dealing with massive MIMO systems, as M tends to infinity, fact that leads the previous situation to occur. Thereby, whenever this happens, it can be shown that covariance create a null-space, containing the channel directions that are far away from its own [references]. As a result, this matrix will remove all the components from a vector that are lying on that subspace, e.g. channels with very different angle of arrivals.

In our case, this can be translated to the covariance matrix $\boldsymbol{C}_{\boldsymbol{h}_k}$, present in the estimate $\boldsymbol{\theta}_k$, and that will filter out the parts of the observation (or estimate) $\boldsymbol{\phi}_k$ not belonging to $\boldsymbol{h}_k$. Somehow, we will obtain a purer estimate of the channel as only similar components are kept, contaminated ones are discarded and thus, a better system performance is achieved. We will see this later on.

3.2 Pilot Contamination

At this point, we are able to introduce the concept of pilot contamination. It can be defined as an interference affecting channel estimation, caused during the first phase of the process, and that it cannot be, in principle, canceled. As already said, it implies a tremendous deterioration of the data rate results and must be taken into account while investigating upon future communications.

The main problem of channel estimation in massive MIMO systems with scenarios of high mobility is the fast variation of the channel. As a result, we cannot dispose of as many orthogonal pilots as users we have, which means some of them have to share training sequences. This can be reflected in the fact that normally we have $T_{\text{tr}} < K$ as τ_c is very small. Even in the case of $\tau_c = K$, we cannot assign the entire interval τ_c to T_{tr} as we would not leave any time for data transmission and no useful communication would be possible. Note that the number of orthogonal sequences of length U is, by definition, U.

In the following. we will see in detail the impact of not having enough pilots over the LS estimate, which suffers from it first. Later, we will go back to the SINR expressions from (2.18) and (2.19), which we will see exhibit a saturation along with increasing values of M. Consequently, user rates will no longer grow without bound given that now $\gamma_k \not\propto M$.

3.2.1 Estimate Deterioration

During the process of channel estimation through the LS approach, the outcome will not only be a function of the desired channel plus some random noise, but it will also include channels belonging to users that share the same pilot sequence. Therefore, the resulting estimate is contaminated and that is why this effect is usually named pilot contamination, e.g. see [10]. All this can be observed in the expression of the estimate from (3.3), which now reads as

$$\boldsymbol{\phi}_k = \mathbf{Y}_{\text{tr}}\boldsymbol{\psi}_k = \boldsymbol{h}_k + \sum_{n \in \mathcal{I}_k} \boldsymbol{h}_n + \frac{1}{\rho'_{\text{tr}}}\boldsymbol{n}' \tag{3.7}$$

where $\mathcal{I}_k$ is the set of all user sharing the same training sequence as the main user k. Hence, extra terms are now added in the estimation of $\boldsymbol{h}_k$ and they suppose a large decrease of its quality, specially for large M. In that regime, noise power is usually small compared to the main signals given the large array gains, i.e. number of BS antennas, and the SNR tends to be large. As a result, this interference prevails in front of noise and must be taken into account in massive MIMO and measures to combat it must be sought.

Moreover, note that pilot contamination has been present in all kinds of communication systems. However, its impact can be ignored in scenarios with a low SNR, e.g. SISO systems, since power of the interfering portions is smaller than the noise energy. Thus, contamination does not really degrade the estimation nor the transmission and it is not generally considered there.

On the other hand, a different behavior is experienced in the case of the LMMSE estimator. In particular, given the properties of the covariance matrices explained in Section 3.1.2, which apply for large M, the effect of pilot contamination can be completely removed as long as users sharing the same pilots do not have a lot of structure in common. This is due to the fact that the interfering terms in $\boldsymbol{\phi}_k$, namely $\sum_{n\in\mathcal{I}_k}\boldsymbol{h}_n$, are filtered by $\boldsymbol{C}_{\boldsymbol{h}_k}$ in $\boldsymbol{\theta}_k$. This is proven in detail in [33], where it is seen that interference mitigation is enhanced when going from the LS strategy to the LMMSE. That is why we opt for this second approach when it comes to channel estimation.

A more advanced arguing of this decision will be provided in Section 4.2, where the LMMSE properties are optimally exploited.

3.2.2 SINR Ultimate Bounds

Despite the previous analysis, the main impact of pilot contamination is observed in the SINR expression, which saturates for large values of M. Thereby, now we have that processing techniques rely on the contaminated estimates as perfect knowledge is no longer valid, i.e. $\boldsymbol{g}_k = f(\hat{\boldsymbol{h}}_k)$ and $\boldsymbol{p}_k = f(\hat{\boldsymbol{h}}_k)$. In addition, for the sake of simplicity, we will concentrate on the instantaneous SINR and leave the lower achievable bounds of Section 2.2.4 for future studies. Besides, MF filter is again considered for precoding and equalizing.

First, we will take a look at the results with the LS estimate and later we will focus on the LMMSE. Then, when setting $\hat{\boldsymbol{h}}_k = \boldsymbol{\phi}_k$, both filters result

$$\boldsymbol{g}_k = \frac{1}{\|\boldsymbol{\phi}_k\|_2}\boldsymbol{\phi}_k \quad \text{and} \quad \boldsymbol{p}_k = \beta\boldsymbol{\phi}_k \tag{3.8}$$

Hence, it can be seen that the corresponding SINRs are given by

$$\gamma_{k,\text{ul}} = \frac{|\boldsymbol{\phi}_k^{\text{H}}\boldsymbol{h}_k|^2}{\frac{\|\boldsymbol{\phi}_k\|_2^2}{\rho_{\text{ul}}} + \sum_{n\neq k}|\boldsymbol{\phi}_k^{\text{H}}\boldsymbol{h}_n|^2} \tag{3.9}$$

$$\gamma_{k,\text{dl}} = \frac{|\boldsymbol{h}_k^{\text{H}}\boldsymbol{\phi}_k|^2}{\frac{1}{\beta^2\rho_{\text{dl}}} + \sum_{n\neq k}|\boldsymbol{h}_k^{\text{H}}\boldsymbol{\phi}_n|^2} \tag{3.10}$$

Thereby, when M tends to infinity, we have that take special attention at the inner products, since they show that interference is not completely removed

$$\lim_{M\to\infty}\frac{1}{M}\boldsymbol{\phi}_k^{\text{H}}\boldsymbol{h}_n = \begin{cases} \|\boldsymbol{h}_k\|_2^2 & \text{if} \quad k = n \\ \sum_{n\in\mathcal{I}_k}\|\boldsymbol{h}_k\|_2^2 & \text{if} \quad k \neq n \end{cases} \tag{3.11}$$

$$\lim_{M\to\infty} \frac{1}{M}\boldsymbol{h}_k^{\mathrm{H}}\boldsymbol{\phi}_n = \begin{cases} \|\boldsymbol{h}_n\|_2^2 & \text{if} \quad n = k \\ \sum_{k\in\mathcal{I}_n} \|\boldsymbol{h}_k\|_2^2 & \text{if} \quad n \neq k \end{cases} \tag{3.12}$$

Consequently, as first shown by the author in [11], the SINR saturates in the large-scale regime in the following way

$$\gamma_{k,\text{ul}} = \frac{\frac{1}{M}|\boldsymbol{\phi}_k^{\mathrm{H}}\boldsymbol{h}_k|^2}{\frac{1}{M}\left(\frac{\|\boldsymbol{\phi}_k\|_2^2}{\rho_{\text{ul}}} + \sum_{n\neq k} |\boldsymbol{\phi}_k^{\mathrm{H}}\boldsymbol{h}_n|^2\right)} \approx \frac{\|\boldsymbol{h}_k\|_2^2}{\sum_{k\in\mathcal{I}_n} \|\boldsymbol{h}_n\|_2^2} \tag{3.13}$$

$$\gamma_{k,\text{dl}} = \frac{\frac{1}{M}|\boldsymbol{h}_k^{\mathrm{H}}\boldsymbol{\phi}_k|^2}{\frac{1}{M}\left(\frac{1}{\beta^2\rho_{\text{dl}}} + \sum_{n\neq k} |\boldsymbol{h}_k^{\mathrm{H}}\boldsymbol{\phi}_n|^2\right)} \approx \frac{\|\boldsymbol{h}_k\|_2^2}{\sum_{n\in\mathcal{I}_k} \|\boldsymbol{h}_n\|_2^2} \tag{3.14}$$

Note then, that in either ways, we obtain the same saturation. This is deeply explained in [11], where the author claims that L2-norms are expected to grow faster (proportional to M) than the inner products of uncorrelated vectors, e.g. different channels and noise. Hence, these terms vanish and only users with the same pilot sequence as the desired remain as interference. As expected, rates will also saturate in presence of this contamination.

On the other hand, regarding the LMMSE estimate, we have already discussed that if users sharing the same pilot sequence have channels with completely distinct directions, the contamination can be removed and thus, we can still reach the asymptotic results in (2.21) and (2.22). In fact, as we will see in Section 4.2, this similarity can be translated to covariance matrices since they determine the structure of their corresponding channels.

Finally, even though we are not going to show it here, it can be seen that the lower bounds experience the same effect. For large M, noise terms and uncorrelated channels disappear. However, the SINR still saturates as the contaminated parts of the estimate remain as interference.

Chapter 4

Interference Reduction

In the previous chapter we saw how devastating pilot contamination can be and the tremendous effect it has on the SINR and data rate. Here we will present then the set of solutions proposed to help reduce this interference. It represents the main objective and topic of this thesis.

First, we introduce the use of filters and their design in our environment to try to solve this issue. Different approaches are discussed and a strong emphasis on power allocation schemes for the DL scenario are analyzed. They will serve as basis for the entire scenario. Second, an approach for assigning pilot sequences to users in an optimal manner will be studied. Several options are introduced and will be compared in detail. Later, a new strategy for combating pilot contamination is suggested and that could be interpreted as a partial Zero Forcing (ZF) processing, applied directly to the estimates of the channel so that a better quality and performance are achieved.

4.1 Filter Design

The first approach employed to fight against pilot contamination is the processing of the transmitted and received signals by means of linear schemes. In fact, all other improvements presented will assume these tools are used. We will start with an approach where CSI is exploited and later, a strategy depending only on the second-order statistics of the channel is presented. These two aim to minimize the MSE between symbol estimate in true value, following the

criterion in [18]. In addition, a simplified version of the approach that uses CDI is proposed, although no optimization is performed. Besides, solutions for both, precoding and equalizing are derived in each case. All three strategies are also finally compared in terms of performance and efficiency. Note however, that only qualitative observations are given, whereas real simulations are properly discussed in Chapter 5. Finally, an optimal power allocation is presented to enhance the transmitter performance from two points of view: sum rate maximization and rate balancing.

It is important to highlight that any of these techniques is performed at the BS exclusively, since we assume is the only entity provided with channel knowledge (see Section 3.1). Besides, note that we focus on linear processing given the special properties of massive MIMO explained in Chapter 2, fact that represents one of the main advantages of these systems indeed.

4.1.1 Linear Minimum Square Error

As mentioned above, the first approach for the filters is based on the knowledge of instantaneous measurements, i.e. estimates of the channel realizations. In particular, we opt for the linear MMSE given its good performance and robustness against different situations for the SINR. For instance, in [34] authors show that the MMSE approach behaves like the MF for low SNR, where the interference is meaningless in front of noise, i.e. SINR converges to SNR. On the contrary, it is comparable to the nature of ZF processing whenever the SNR is high, region where interference gains relevancy and noise can be contemptible, i.e. SINR $\rightarrow$ SIR. Additionally, it gives a good performance for intermediate values of SINR. Hence, it seems to be the best option for massive MIMO systems, where pilot contamination plays an important role and we need to filter it out, although noise must be always considered.

Moreover, it can be shown that in the case of the equalizer, the minimum sufficient statistics are delivered and thus, the system is provided with the ability to achieve capacity [16]. Nonetheless, as said in Section 2.1, we will concentrate on separate decoding, always worse than joint but easier to define at the same time. Besides, the corresponding precoder also gives satisfactory results, even though data rates are smaller than in the case of reception, where this strategy is optimal (see Section 4.1.4 and Chapter 5). This is the reason why, on top of that, a power allocation will be performed in order to approach both communications and get similar data rates.

4.1.1.1 Equalizer

Following the derivations from [18], the equalizer of the LMMMSE approach can be found easily. In fact, as we will see in the next section, the development here will not be as precise as in the case of transmission, since here the expression is already given.

Let us start then with the k-th transmit symbol x_k and its estimate $\hat{x}_k = \boldsymbol{g}_k^{\mathrm{H}} \boldsymbol{y}_{\text{ul}}$ w.r.t. which we want to minimize the MSE through the equalizer

$$\boldsymbol{g}_k^{\star} = \underset{\boldsymbol{g}_k}{\operatorname{argmin}}\, \varepsilon_k(\boldsymbol{g}_k) = \underset{\boldsymbol{g}_k}{\operatorname{argmin}}\, \mathrm{E}[|x_k - \boldsymbol{g}_k^{\mathrm{H}} \boldsymbol{y}_{\text{ul}}|^2 | \boldsymbol{\Phi}] \tag{4.1}$$

Note that here we use the whole set of LS estimates $\boldsymbol{\Phi}$ instead of only the k-th component $\boldsymbol{\phi}_k$, like in (3.4), since the solution depends strictly on all of them. Concerning the MSE $\varepsilon_k(\boldsymbol{g}_k)$, its expression can be written as

$$\varepsilon_k(\boldsymbol{g}_k) = 1 + \boldsymbol{g}_k^{\mathrm{H}} (\boldsymbol{C}_{\text{err}} + \sum_n \boldsymbol{\theta}_n \boldsymbol{\theta}_n^{\mathrm{H}})^{-1} \boldsymbol{g}_k - \boldsymbol{g}_k^{\mathrm{H}} \boldsymbol{\theta}_k - \boldsymbol{\theta}_k^{\mathrm{H}} \boldsymbol{g}_k \tag{4.2}$$

where $\boldsymbol{C}_{\text{err}} \in \mathbb{C}^{M \times M}$ is defined as the total error covariance matrix and contains all estimation errors, including the effect of pilot contamination

$$\boldsymbol{C}_{\text{err}} = \frac{1}{\rho_{\text{ul}}} \mathbf{I}_M + \sum_k \tilde{\boldsymbol{C}}_k \tag{4.3}$$

with $\tilde{\boldsymbol{C}}_k$ being the individual error covariance matrix from the LMMSE channel estimate of user k defined in (3.4). Therefore, regarding the k-th equalizer from (4.1), it is straightforward to obtain

$$\boldsymbol{g}_k^{\star} = (\boldsymbol{C}_{\text{err}} + \sum_n \boldsymbol{\theta}_n \boldsymbol{\theta}_n^{\mathrm{H}})^{-1} \boldsymbol{\theta}_k \tag{4.4}$$

and the optimal MSE then yields

$$\varepsilon_k^{\star} = 1 - \boldsymbol{\theta}_k (\boldsymbol{C}_{\text{err}} + \sum_n \boldsymbol{\theta}_n \boldsymbol{\theta}_n^{\mathrm{H}})^{-1} \boldsymbol{\theta}_k \tag{4.5}$$

which is shown in [18] to tend to zero for large M, revealing the optimal performance of the LMMSE equalizer in this regime and justifying the usage of this technique in presence of pilot contamination.

Furthermore, in order to reduce the complexity of the previous expressions, we take advantage of the Woodbury Matrix Identity [35], also known as Matrix

Inversion Lemma (MIL). It provides with an alternative to compute the inverse of matrices that follow a certain form [35]. We also need the matrix notation for the equalizer and LMMSE estimates, i.e. $\boldsymbol{G}$ and $\boldsymbol{\Theta}$. With all this, we can express the optimal equalizer as

$$\boldsymbol{G}^{\star} = (\boldsymbol{C}_{\text{err}} + \boldsymbol{\Theta}\boldsymbol{\Theta}^{\text{H}})^{-1}\boldsymbol{\Theta} = \boldsymbol{C}_{\text{err}}^{-1}\boldsymbol{\Theta}(\mathbf{I}_K + \boldsymbol{\Theta}^{\text{H}}\boldsymbol{C}_{\text{err}}^{-1}\boldsymbol{\Theta})^{-1} \tag{4.6}$$

As we can see, we go from an inversion of a square matrix of size M to a $K \times K$ matrix and, in the case of massive MIMO, where $M \gg K$, this makes a huge difference in resources. In addition, with the DFT approximation described in Section 2.3.2, all covariance matrices become diagonal and thus, the inverse $\boldsymbol{C}_{\text{err}}^{-1}$ is just the reciprocal of its elements. Note that given the additive noise, $\boldsymbol{C}_{\text{err}}$ is full-rank, unlike $\boldsymbol{C}_{\boldsymbol{h}_k}$ when $M \to \infty$ (see Section 3.1.2). Consequently, we can ensure this inverse exists. Overall, these facts together lead to a substantial improvement of the efficiency, since the necessary computations for obtaining the filters are highly diminished.

4.1.1.2 Precoder

In the case of the precoder, no explicit solution is provided in [18] and we must seek for one. Nevertheless, it can be obtained in a similar way as the equalizer but with a certain power constraint. This is imposed at the BS and will reflect the relation between UL and DL budgets.

Thereby, with the help of the findings from [34], a proper expression is derived. Unlike before, here we find a solution for the whole matrix and not for the k-th element. This is due to the fact that, for simplicity, power constraints are usually assumed to be total and not individual, possibility studied in [22], since we consider that restrictions apply to the entire BS transmission. Then, taking into account the model and notation stated in (2.13), the optimization problem leading to the precoder that aims to minimize the MSE under a total power constraint at the BS is given by

$$\{\boldsymbol{P}^{\star}, \beta^{\star}\} = \underset{\boldsymbol{P},\beta}{\operatorname{argmin}}\, \text{E}\big[\|\boldsymbol{s} - \beta^{-1}\boldsymbol{y}_{\text{dl}}\|_2^2 | \boldsymbol{\Phi}\big] \quad \text{s.t.} : \text{E}\big[\|\boldsymbol{P}\boldsymbol{s}\|_2^2\big] = E_{\text{tx}} \tag{4.7}$$

where E_{tx} is the total transmit power available in the forward link, which value will be found later, and β is the scaling factor to satisfy the power restrictions. Note that no conditioning is imposed on it since $\boldsymbol{P}$ will have

already the information about $\boldsymbol{\Phi}$. In addition, this constraint can be interpreted in the instantaneous case or average, i.e. whenever we consider transmission over slow or fast fading channels. In other words, if we design the system to be prepared for changes in the channel or only suitable in the case of constant values. On the one hand, when assuming that the communication is performed during a single channel coherence interval τ_c

$$\mathrm{E}\big[\|\boldsymbol{P}\boldsymbol{s}\|_2^2\big] = \mathrm{tr}(\boldsymbol{P}\boldsymbol{C}_{\boldsymbol{s}}\boldsymbol{P}^{\mathrm{H}}) = \mathrm{tr}(\boldsymbol{P}\boldsymbol{P}^{\mathrm{H}}) = E_{\mathrm{tx}} \tag{4.8}$$

where $\boldsymbol{C}_s$ is the covariance matrix of the input data stream $\boldsymbol{s}$ (see Section 2.2.2), also considered to be i.i.d., i.e. $\boldsymbol{C}_s = \mathbf{I}_K$. Note that the precoder can be pulled out from the expectation since it is based only on the current magnitudes. Notwithstanding, as we will see later, a more adequate approach is to consider several realizations of the channel as we adapt the filter to this variability. Hence, the power constraint for this scenario reads as

$$\mathrm{E}\big[\|\boldsymbol{P}\boldsymbol{s}\|_2^2\big] = \mathrm{tr}(\mathrm{E}[\boldsymbol{P}\boldsymbol{s}\boldsymbol{s}^{\mathrm{H}}\boldsymbol{P}^{\mathrm{H}}]) = \mathrm{tr}(\mathrm{E}[\boldsymbol{P}\boldsymbol{P}^{\mathrm{H}}]) = E_{\mathrm{tx}} \tag{4.9}$$

where we assumed that $\boldsymbol{s}$ is independent from the channels, present in the expression of $\boldsymbol{P}$, as seen expressions from (2.3). Nonetheless, note that the precoder is now a RV as an average constraint is imposed and several channel accesses are considered. Hence, time variations are present now, which means expectation must be applied at this magnitude.

On the other hand, given this constraint, we must employ the method of Lagrange multipliers. Thereby, the function representing this optimization problem can be formulated as

$$\mathcal{L}(\boldsymbol{P}, \beta, \lambda) = \varepsilon(\boldsymbol{P}) + \lambda(f(\boldsymbol{P}) - E_{\mathrm{tx}}) \tag{4.10}$$

where λ is the multiplier associated to the constraint, here represented by $f(\boldsymbol{P})$, valid for both aforementioned perspectives. Nevertheless, as later discussed, to ease derivations, we assume an instantaneous strategy is used, i.e. $f(\boldsymbol{P}) = \mathrm{tr}(\boldsymbol{P}\boldsymbol{P}^{\mathrm{H}})$. Besides, $\varepsilon(\boldsymbol{P}) = \mathrm{E}\big[\|\boldsymbol{s} - \beta^{-1}\boldsymbol{y}_{\mathrm{dl}}\|_2^2|\boldsymbol{\Phi}\big]$ corresponds to the objective MSE, which can be rewritten as

$$\begin{aligned}\varepsilon(\boldsymbol{P}) = K(1+\beta^{-2}) - 2\beta^{-1}\mathrm{Re}(\mathrm{tr}(\boldsymbol{P}\,\mathrm{E}\big[\boldsymbol{H}^{\mathrm{H}}|\boldsymbol{\Phi}\big])) \\ + \beta^{-2}\mathrm{tr}(\boldsymbol{P}\boldsymbol{P}^{\mathrm{H}}\mathrm{E}\big[\boldsymbol{H}\boldsymbol{H}^{\mathrm{H}}|\boldsymbol{\Phi}\big])\end{aligned} \tag{4.11}$$

Note that here we focus on final expressions only since more detailed and precise developments result irrelevant for our scope. Also, it is important to realize that the precoder itself will depend on the current channel realizations whereas the power constraint, as mentioned, can be either instantaneous or average. This will have an impact only on the expression for the scaling term β, as we will see at the end of this part and again in Section 4.1.2.

Next step is to compute the derivatives of the Lagrangian function

$$\frac{\partial \mathcal{L}(\boldsymbol{P},\beta,\lambda)}{\partial \boldsymbol{P}} = -\beta^{-1}(\mathrm{E}\big[\boldsymbol{H}^{\mathrm{H}}|\boldsymbol{\Phi}\big])^{\mathrm{T}} + \beta^{-2}\mathrm{E}\big[\boldsymbol{H}^{*}\boldsymbol{H}^{\mathrm{T}}|\boldsymbol{\Phi}\big]\boldsymbol{P}^{*} + \lambda\boldsymbol{P}^{*} \quad (4.12)$$

which, setting to zero, leads to the following result

$$\boldsymbol{P}(\lambda\beta^2) = \beta\tilde{\boldsymbol{P}}(\lambda\beta^2) = \beta(\mathrm{E}\big[\boldsymbol{H}\boldsymbol{H}^{\mathrm{H}}|\boldsymbol{\Phi}\big] + \lambda\beta^2\mathbf{I}_M)^{-1}\mathrm{E}\big[\boldsymbol{H}|\boldsymbol{\Phi}\big] \quad (4.13)$$

where $\tilde{\boldsymbol{P}}(\lambda\beta^2)$ represents the precoder not fulfilling the constraint. Having this, from the determination in (4.8), it is straightforward to obtain

$$E_{\mathrm{tx}} = \mathrm{tr}(\boldsymbol{P}(\lambda\beta^2)\boldsymbol{P}^{\mathrm{H}}(\lambda\beta^2)) = \beta^2\mathrm{tr}(\tilde{\boldsymbol{P}}(\lambda\beta^2)\tilde{\boldsymbol{P}}^{\mathrm{H}}(\lambda\beta^2)) \quad (4.14)$$

and consequently,

$$\beta = \sqrt{\frac{E_{\mathrm{tx}}}{\mathrm{tr}(\tilde{\boldsymbol{P}}(\lambda\beta^2)\tilde{\boldsymbol{P}}^{\mathrm{H}}(\lambda\beta^2))}} \quad (4.15)$$

Regarding the derivative of the part associated to the power constraint, it can be seen that it directly yields

$$\begin{aligned}\frac{\partial \mathcal{L}(\boldsymbol{P},\beta,\lambda)}{\partial \beta} &= \beta^2\mathrm{tr}(\lambda\beta^2\tilde{\boldsymbol{P}}(\lambda\beta^2)\tilde{\boldsymbol{P}}^{H}(\lambda\beta^2)) - K \\ &= \lambda\beta^2 E_{\mathrm{tx}} - K\end{aligned} \quad (4.16)$$

where we employed the determination found in (4.14). Hence, like in [34], by setting the previous derivative to zero it follows

$$\lambda\beta^2 = K/E_{\mathrm{tx}} \quad (4.17)$$

Furthermore, in order to make a fair comparison with the UL, as mentioned in Section 2.1.2, we fix $E_{\text{tx}} = K\rho_{\text{ul}}$, which implies $\rho_{\text{dl}} = 1$ to preserve coherence. As a result, in total, we transmit the same overall power in both directions and the term in (4.17) then reads as

$$\lambda\beta^2 = 1/\rho_{\text{ul}} \tag{4.18}$$

Consequently, we can express the solution to (4.7) in the following way

$$\boldsymbol{P}^\star = \beta^\star \boldsymbol{F}^{-1}\mathrm{E}\big[\boldsymbol{H}|\boldsymbol{\Phi}\big] \tag{4.19}$$

where

$$\beta^\star = \sqrt{\frac{E_{\text{tx}}}{\mathrm{tr}(\boldsymbol{F}^{-2}\mathrm{E}\big[\boldsymbol{H}|\boldsymbol{\Phi}\big]\mathrm{E}\big[\boldsymbol{H}^{\mathrm{H}}|\boldsymbol{\Phi}\big])}} \tag{4.20}$$

and

$$\boldsymbol{F} = \mathrm{E}\big[\boldsymbol{H}\boldsymbol{H}^{\mathrm{H}}|\boldsymbol{\Phi}\big] + \frac{1}{\rho_{\text{ul}}}\mathbf{I}_M \tag{4.21}$$

Finally, as well as before, taking into account that $\mathrm{E}\big[\boldsymbol{H}|\boldsymbol{\Phi}\big] = \boldsymbol{\Theta}$ and $\mathrm{E}\big[\boldsymbol{H}\boldsymbol{H}^{\mathrm{H}}|\boldsymbol{\Phi}\big] = \boldsymbol{\Theta}\boldsymbol{\Theta}^{\mathrm{H}} + \sum_k \tilde{\boldsymbol{C}}_k$, the definitive solution results

$$\boldsymbol{P}^\star = \beta^\star \boldsymbol{F}^{-1}\boldsymbol{\Theta} = \beta^\star(\boldsymbol{C}_{\text{err}} + \boldsymbol{\Theta}\boldsymbol{\Theta}^{\mathrm{H}})^{-1}\boldsymbol{\Theta} \tag{4.22}$$

with

$$\beta^\star = \sqrt{\frac{E_{\text{tx}}}{\mathrm{tr}(\boldsymbol{F}^{-2}\boldsymbol{\Theta}\boldsymbol{\Theta}^{\mathrm{H}})}} \tag{4.23}$$

To conclude this section, two more aspects have to be mentioned. First, the expression in (4.22) can be further simplified following the discussion in (4.8), i.e. by means of the DFT approximation and the MIL. In fact, both expressions are the same except for the scaling factor. Second, regarding this term, a more tedious expression can be found in the case of average constraint

$$\beta^\star = \sqrt{\frac{E_{\text{tx}}}{\mathrm{tr}(\mathrm{E}\big[\boldsymbol{F}^{-2}\boldsymbol{\Theta}\boldsymbol{\Theta}^{\mathrm{H}}\big])}} \tag{4.24}$$

However, it can be inferred that, given the expression of the matrix $\boldsymbol{F}$, an analytic solution for this factor cannot be found easily. That is the reason why,

as we will debate later in Section 5.2.1, Monte-Carlo simulations over several realizations must be employed to obtain a suitable value.

4.1.2 Generalized Matched Filter

The second approach presented in this work is the so-called Generalized Matched Filter (GMF), also introduced in [18]. Its design is based on a certain matrix $\boldsymbol{A}_k$, different for each user, together with the LS estimate of the k-th channel. This construction gives the filter its name: the common MF is formed with the known channel and the inverse of the noise covariance (here assumed to be an scaled identity). Then, instead of this matrix, here we employ $\boldsymbol{A}_k$.

For the same reasons as before, we also try to minimize the MSE between true and estimated symbol value, now by means of $\boldsymbol{A}_k$. However, considering the special structure of the filter, this matrix relies only on the second-order statistics of the channel or CDI, as we will see later. This way, the solution must be computed only when the distributions change and not at every realization, given that the estimates are always available. As we will discuss in Section 4.1.4, this aspect will be one of the major advantages of this proposal in front of the LMMSE, which delivers better results when looking at the throughput.

Moreover, here we also rely on separate decoding for obtaining an expression of the processing techniques. Unlike before, the corresponding precoder and equalizer, as we will observe later, have a close behavior. Nevertheless, we will still use a power allocation in the DL scheme for a better performance.

4.1.2.1 Equalizer

As mentioned above, the equalizer of user k has the following form

$$\boldsymbol{g}_k = \boldsymbol{A}_k \boldsymbol{\phi}_k \tag{4.25}$$

Note that matrix $\boldsymbol{A}_k \in \mathbb{C}^{M \times M}$ can be designed in different ways but here we construct it so that the MSE is minimized. Also, with this expression, it becomes evident why it receives the name of generalized MF. Thereby, the next derivations follow from [18], where the optimization problem is stated as

$$\boldsymbol{A}_k^{\star} = \underset{\boldsymbol{A}_k}{\operatorname{argmin}} \, \mathrm{E}[|x_k - \boldsymbol{g}_k^{\mathrm{H}} \boldsymbol{y}_{\mathrm{ul}}|^2] = \underset{\boldsymbol{A}_k}{\operatorname{argmin}} \, \mathrm{E}[|x_k - \boldsymbol{\phi}_k^{\mathrm{H}} \boldsymbol{A}_k^{\mathrm{H}} \boldsymbol{y}_{\mathrm{ul}}|^2] \tag{4.26}$$

Here, no conditioning over the LS estimates $\boldsymbol{\Phi}$ is required since this information is already present in the structure of $\boldsymbol{g}_k$. Then, with the help of the equivalences from (2.31) and using $\boldsymbol{A}_k\boldsymbol{\phi}_k$ as $\boldsymbol{x}$, we can write the following

$$\begin{aligned}\mathrm{E}[|x_k - \boldsymbol{\phi}_k^{\mathrm{H}}\boldsymbol{A}_k^{\mathrm{H}}\boldsymbol{y}_{\mathrm{ul}}|^2] = 1 - \mathrm{tr}(\boldsymbol{C}_{\boldsymbol{h}_k}\boldsymbol{A}_k) - \mathrm{tr}(\boldsymbol{A}_k^{\mathrm{H}}\boldsymbol{C}_{\boldsymbol{h}_k}) \\ + \mathrm{tr}(\boldsymbol{C}_{\boldsymbol{\phi}_k}\boldsymbol{A}_k^{\mathrm{H}}\boldsymbol{C}_{\boldsymbol{h}_k}\boldsymbol{A}_k) + \sum_{n\in\mathcal{I}_k}|\mathrm{tr}(\boldsymbol{A}_k^{\mathrm{H}}\boldsymbol{C}_{\boldsymbol{h}_k})|^2\end{aligned} \tag{4.27}$$

In order to obtain a proper solution, vector notation is required

$$\boldsymbol{c}_{\boldsymbol{h}_k} = \mathrm{vec}(\boldsymbol{C}_{\boldsymbol{h}_k}) \quad \text{and} \quad \boldsymbol{a}_k = \mathrm{vec}(\boldsymbol{A}_k) \tag{4.28}$$

which both will have length M^2. Also, given the operations and variables involved in the procedure, the following identities will be necessary

$$\mathrm{tr}(\boldsymbol{B}^{\mathrm{T}}\boldsymbol{D}) = \mathrm{vec}(\boldsymbol{B})^{\mathrm{T}}\mathrm{vec}(\boldsymbol{D}) \tag{4.29}$$

$$\mathrm{vec}(\boldsymbol{B}\boldsymbol{X}\boldsymbol{D}) = (\boldsymbol{D}^{\mathrm{T}} \otimes \boldsymbol{B})\mathrm{vec}(\boldsymbol{X}) \tag{4.30}$$

for any $\boldsymbol{B}$, $\boldsymbol{D}$ and $\boldsymbol{X}$. Note that (4.29) also holds for $\boldsymbol{B}^{\mathrm{H}}$. In addition, taking into account that the trace is invariant under cyclic permutations, e.g. $\mathrm{tr}(\boldsymbol{B}\boldsymbol{D}) = \mathrm{tr}(\boldsymbol{D}\boldsymbol{B})$, and the fact that covariance matrices are Hermitian, i.e. $\boldsymbol{C}^{\mathrm{H}} = \boldsymbol{C}$ or $\boldsymbol{C}^{\mathrm{T}} = \boldsymbol{C}^*$, we can transform the MSE in (4.27) as

$$1 - \boldsymbol{c}_{\boldsymbol{h}_k}^{\mathrm{H}}\boldsymbol{a}_k - \boldsymbol{a}_k^{\mathrm{H}}\boldsymbol{c}_{\boldsymbol{h}_k} + \boldsymbol{a}_k^{\mathrm{H}}(\boldsymbol{C}_{\boldsymbol{\phi}_k}^{\mathrm{T}} \otimes \boldsymbol{C}_{\boldsymbol{y}})\boldsymbol{a}_k + \sum_{n\in\mathcal{I}_k}\boldsymbol{a}_k^{\mathrm{H}}\boldsymbol{c}_{\boldsymbol{h}_k}\boldsymbol{c}_{\boldsymbol{h}_k}^{\mathrm{H}}\boldsymbol{a}_k \tag{4.31}$$

Therefore, when deriving w.r.t. $\boldsymbol{a}_k$ and setting the result to zero we get

$$\boldsymbol{a}_k^{\star} = (\boldsymbol{C}_{\boldsymbol{\phi}_k}^{*} \otimes \boldsymbol{C}_{\boldsymbol{y}} + \sum_{n\in\mathcal{I}_k}\boldsymbol{c}_{\boldsymbol{h}_k}\boldsymbol{c}_{\boldsymbol{h}_k}^{\mathrm{H}})^{-1}\boldsymbol{c}_{\boldsymbol{h}_k} \tag{4.32}$$

As shown in [18], this solution allows the MSE converge to zero for $M \to \infty$ under certain conditions. However, it decreases at a lesser rate than in the case of the LMMSE equalizer, leading to a strictly lower performance. Besides, just like before, a simplified solution can be found when using the DFT approximation together with the MIL.

Finally, it can inferred that this solution depends only on the second-order statistics of the channel, which barely change in comparison with the realization since it is assumed that $\tau_c \ll T_c$, as already discussed in Section 2.1.

4.1.2.2 Precoder

Likewise, an expression for the precoder can be found based on CDI knowledge only. However, this task results more laborious than the previous development in the case of the LMMSE providing the special structure of the filters.

First, we begin by stating the optimization problem, similar to the equalizer situation described above but now with total power constraint considered

$$\{\boldsymbol{P}^\star, \beta^\star\} = \underset{\boldsymbol{P},\beta}{\operatorname{argmin}} \, \mathrm{E}\big[\|\boldsymbol{s} - \beta^{-1}\boldsymbol{y}_{\mathrm{dl}}\|_2^2\big] \quad \text{s.t.} : \mathrm{E}\big[\|\boldsymbol{P}\boldsymbol{s}\|_2^2\big] = E_{\mathrm{tx}} \tag{4.33}$$

with the condition that the precoder must be constructed as follows

$$\boldsymbol{P} = [\boldsymbol{A}_1\boldsymbol{\phi}_1, \ldots, \boldsymbol{A}_K\boldsymbol{\phi}_K] = \boldsymbol{A}\bar{\boldsymbol{\Phi}} \tag{4.34}$$

where $\boldsymbol{A} = [\boldsymbol{A}_1, \ldots, \boldsymbol{A}_K]$ and $\bar{\boldsymbol{\Phi}} = \mathrm{blkdiag}(\boldsymbol{\phi}_1, \ldots, \boldsymbol{\phi}_K)$, with individual $\boldsymbol{A}_k \in \mathbb{C}^{M\times M}$. Once again, we will find a solution considering the whole matrix $\boldsymbol{P}$ and not a single precoder $\boldsymbol{p}_k = \beta\boldsymbol{A}_k\boldsymbol{\phi}_k$, since we deal with a total power constraint. Also, for the reasons aforementioned in the last section, no conditioning on $\boldsymbol{\Phi}$ is required neither in the MSE nor in the constraint.

Next step is to define the resulting MSE when using this compact matrix structure defined in (4.34). To do so, we first need to determine whether we use an instantaneous or average power constraint. The first one results

$$\mathrm{E}\big[\|\boldsymbol{P}\boldsymbol{s}\|_2^2\big] = \mathrm{tr}(\boldsymbol{A}\bar{\boldsymbol{\Phi}}\bar{\boldsymbol{\Phi}}^{\mathrm{H}}\boldsymbol{A}^{\mathrm{H}}) = E_{\mathrm{tx}} \tag{4.35}$$

whereas the second is given by

$$\mathrm{E}\big[\|\boldsymbol{P}\boldsymbol{s}\|_2^2\big] = \mathrm{tr}(\boldsymbol{A}\mathrm{E}\big[\bar{\boldsymbol{\Phi}}\bar{\boldsymbol{\Phi}}^{\mathrm{H}}\big]\boldsymbol{A}^{\mathrm{H}}) = \mathrm{tr}(\boldsymbol{A}\boldsymbol{C}_{\boldsymbol{\phi}}\boldsymbol{A}^{\mathrm{H}}) = E_{\mathrm{tx}} \tag{4.36}$$

with $\boldsymbol{C}_{\boldsymbol{\phi}} = \mathrm{blkdiag}(\boldsymbol{C}_{\boldsymbol{\phi}_1}, \ldots, \boldsymbol{C}_{\boldsymbol{\phi}_K})$. To comprehend both approaches, we define the matrix $\boldsymbol{C}$ that describes the outer product $\bar{\boldsymbol{\Phi}}\bar{\boldsymbol{\Phi}}^{\mathrm{H}}$ and the block diagonal covariance matrix $\boldsymbol{C}_{\boldsymbol{\phi}}$. At the end of this section we will discuss which one is more adequate for our scenario.

Therefore, the MSE $\varepsilon(\boldsymbol{P}) = \mathrm{E}\big[\|\boldsymbol{s} - \beta^{-1}\boldsymbol{y}_{\mathrm{dl}}\|_2^2\big]$ now can be ultimately expressed as follows

$$\varepsilon(\boldsymbol{P}) = K(1+\beta^{-2}) - \beta^{-1}[\mathrm{tr}(\boldsymbol{C}_{\boldsymbol{h}}\boldsymbol{A} + \boldsymbol{A}^{\mathrm{H}}\boldsymbol{C}_{\boldsymbol{h}}^{\mathrm{H}})] + \beta^{-2}\alpha \tag{4.37}$$

where $\boldsymbol{C}_{\boldsymbol{h}} = [\boldsymbol{C}_{\boldsymbol{h}_1}, \ldots, \boldsymbol{C}_{\boldsymbol{h}_K}]^{\mathrm{H}}$ and

$$\begin{aligned}\alpha &= \mathrm{tr}(\mathrm{E}[\boldsymbol{\Phi}^{\mathrm{H}}\boldsymbol{A}^{\mathrm{H}}\boldsymbol{H}\boldsymbol{H}^{\mathrm{H}}\boldsymbol{A}\boldsymbol{\Phi}]) = \sum_{k=1}^{K}\mathrm{E}[\boldsymbol{\phi}_k^{\mathrm{H}}\boldsymbol{A}_k^{\mathrm{H}}\boldsymbol{H}\boldsymbol{H}^{\mathrm{H}}\boldsymbol{A}_k\boldsymbol{\phi}_k] \\ &= \sum_{k=1}^{K}\sum_{i=1}^{K}\mathrm{E}[\boldsymbol{\phi}_k^{\mathrm{H}}\boldsymbol{A}_k^{\mathrm{H}}\boldsymbol{H}\boldsymbol{e}_i\boldsymbol{e}_i^{\mathrm{T}}\boldsymbol{H}^{\mathrm{H}}\boldsymbol{A}_k\boldsymbol{\phi}_k] = \sum_{k=1}^{K}\sum_{i=1}^{K}\alpha_{k,i}\end{aligned} \tag{4.38}$$

since $\mathbf{I}_K = \sum_{i=1}^{K}\boldsymbol{e}_i\boldsymbol{e}_i^{\mathrm{T}}$. Employing the determinations from (2.31) and considering uncorrelated noise, we can further develop the terms $\alpha_{k,i}$ as

$$\begin{aligned}\alpha_{k,i} &= \mathrm{tr}(\mathrm{E}[\boldsymbol{A}_k\boldsymbol{\phi}_k\boldsymbol{\phi}_k^{\mathrm{H}}\boldsymbol{A}_k^{\mathrm{H}}]\mathrm{E}[\boldsymbol{h}_i\boldsymbol{h}_i^{\mathrm{H}}]) + |\mathrm{tr}(\mathrm{E}[\boldsymbol{h}_i\boldsymbol{\phi}_k^{\mathrm{H}}\boldsymbol{A}_k^{\mathrm{H}}])|^2 \\ &= \mathrm{tr}(\boldsymbol{A}_k\boldsymbol{C}_{\boldsymbol{\phi}_k}\boldsymbol{A}_k^{\mathrm{H}}\boldsymbol{C}_{\boldsymbol{h}_i}) + |\mathrm{tr}(\mathrm{E}[\boldsymbol{h}_i(\boldsymbol{h}_k^{\mathrm{H}} + \sum_{n\in\mathcal{I}_k}\boldsymbol{h}_n^{\mathrm{H}} + \frac{1}{\sqrt{\rho_{\mathrm{tr}}}}\boldsymbol{v}_k^{\mathrm{H}})]\boldsymbol{A}_k^{\mathrm{H}})|^2 \\ &= \mathrm{tr}(\boldsymbol{A}_k\boldsymbol{C}_{\boldsymbol{\phi}_k}\boldsymbol{A}_k^{\mathrm{H}}\boldsymbol{C}_{\boldsymbol{h}_i}) + |\mathrm{tr}(\mathrm{E}[\boldsymbol{h}_i(\boldsymbol{h}_k^{\mathrm{H}} + \sum_{n\in\mathcal{I}_k}\boldsymbol{h}_n^{\mathrm{H}})]\boldsymbol{A}_k^{\mathrm{H}})|^2\end{aligned} \tag{4.39}$$

Hence, the expression in (4.38) yields

$$\begin{aligned}\alpha &= \sum_{k=1}^{K}\sum_{i=1}^{K}\mathrm{tr}(\boldsymbol{A}_k\boldsymbol{C}_{\boldsymbol{\phi}_k}\boldsymbol{A}_k^{\mathrm{H}}\boldsymbol{C}_{\boldsymbol{h}_i}) + \sum_{k=1}^{K}|\mathrm{tr}(\mathrm{E}[\boldsymbol{h}_k(\boldsymbol{h}_k^{\mathrm{H}} + \sum_{n\in\mathcal{I}_k}\boldsymbol{h}_n^{\mathrm{H}})]\boldsymbol{A}_k^{\mathrm{H}})|^2 \\ &+ \sum_{k=1}^{K}\sum_{i\neq k}^{K}|\mathrm{tr}(\mathrm{E}[\boldsymbol{h}_i(\boldsymbol{h}_k^{\mathrm{H}} + \sum_{n\in\mathcal{I}_k}\boldsymbol{h}_n^{\mathrm{H}})]\boldsymbol{A}_k^{\mathrm{H}})|^2 \\ &= \sum_{k=1}^{K}\sum_{i=1}^{K}\mathrm{tr}(\boldsymbol{A}_k\boldsymbol{C}_{\boldsymbol{\phi}_k}\boldsymbol{A}_k^{\mathrm{H}}\boldsymbol{C}_{\boldsymbol{h}_i}) + \sum_{i\in\mathcal{I}_k\cup\{k\}}|\mathrm{tr}(\boldsymbol{C}_{\boldsymbol{h}_i}\boldsymbol{A}_k^{\mathrm{H}})|^2\end{aligned} \tag{4.40}$$

Note that the condition of $i \neq k \cap i \in \mathcal{I}_k$ is equal to $i \in \mathcal{I}_k$ since $k \notin \mathcal{I}_k$ by definition. Finally, the MSE from (4.37) reads as

$$\begin{aligned}\varepsilon(\boldsymbol{P}) = K(1+\beta^{-2}) - \beta^{-1}[\mathrm{tr}(\boldsymbol{C_h A} + \boldsymbol{A}^{\mathrm{H}}\boldsymbol{C}_{\boldsymbol{h}}^{\mathrm{H}})] \\ + \beta^{-2}\Big(\sum_{k=1}^{K}\sum_{i=1}^{K}\mathrm{tr}(\boldsymbol{A}_k\boldsymbol{C}_{\boldsymbol{\phi}_k}\boldsymbol{A}_k^{\mathrm{H}}\boldsymbol{C}_{\boldsymbol{h}_i}) + \sum_{i\in\mathcal{I}_k\cup\{k\}}|\mathrm{tr}(\boldsymbol{C}_{\boldsymbol{h}_i}\boldsymbol{A}_k^{\mathrm{H}})|^2\Big)\end{aligned} \tag{4.41}$$

As before, to find an optimal to the constrained problem stated in (4.33), the following Lagrangian function must be defined

$$\mathcal{L}(\boldsymbol{A},\beta,\lambda) = \varepsilon(\boldsymbol{P}) + \lambda(\mathrm{tr}(\boldsymbol{ACA}^{\mathrm{H}}) - E_{\mathrm{tx}}) \tag{4.42}$$

which can be rewritten in vector notation

$$\begin{aligned}\mathcal{L}(\boldsymbol{a}_k,\beta,\lambda) = K(1+\beta^{-2}) - \beta^{-1}[a+b] \\ + \beta^{-2}\Big(\sum_{k=1}^{K}\sum_{i=1}^{K}c_{k,i} + \sum_{i\in\mathcal{I}_k\cup\{k\}}d_{k,i}\Big) + \lambda\Big(\sum_{k=1}^{K}e_k - E_{\mathrm{tx}}\Big)\end{aligned} \tag{4.43}$$

with

$$\begin{aligned} a &= \mathrm{tr}(\boldsymbol{C_h A}) = \sum_{k=1}^{K}\boldsymbol{c}_{\boldsymbol{h}_k}^{\mathrm{H}}\boldsymbol{a}_k \quad b = \mathrm{tr}(\boldsymbol{A}^{\mathrm{H}}\boldsymbol{C}_{\boldsymbol{h}}^{\mathrm{H}}) = \sum_{k=1}^{K}\boldsymbol{a}_k^{\mathrm{H}}\boldsymbol{c}_{\boldsymbol{h}_k} \\ c_{k,i} &= \mathrm{tr}(\boldsymbol{A}_k\boldsymbol{C}_{\boldsymbol{\phi}_k}\boldsymbol{A}_k^{\mathrm{H}}\boldsymbol{C}_{\boldsymbol{h}_i}) = \boldsymbol{a}_k^{\mathrm{H}}(\boldsymbol{C}_{\boldsymbol{\phi}_k}^{*}\otimes\boldsymbol{C}_{\boldsymbol{h}_i})\boldsymbol{a}_k \\ d_{k,i} &= |\mathrm{tr}(\boldsymbol{C}_{\boldsymbol{h}_i}\boldsymbol{A}_k^{\mathrm{H}})|^2 = \boldsymbol{a}_k^{\mathrm{H}}\boldsymbol{c}_{\boldsymbol{h}_i}\boldsymbol{c}_{\boldsymbol{h}_i}^{\mathrm{H}}\boldsymbol{a}_k \\ e_k &= \mathrm{tr}(\boldsymbol{A}_k\boldsymbol{C}_k\boldsymbol{A}_k^{\mathrm{H}}) = \boldsymbol{a}_k^{\mathrm{H}}(\boldsymbol{C}_k^{*}\otimes\mathbf{I}_M)\boldsymbol{a}_k \end{aligned} \tag{4.44}$$

where $\boldsymbol{C}_k$ can be either $\boldsymbol{\phi}_k\boldsymbol{\phi}_k^{\mathrm{H}}$ or $\boldsymbol{C}_{\boldsymbol{\phi}_k}$. Consequently, when taking the derivatives of the Lagrangian function we get the following

$$\begin{aligned}\frac{\partial \mathcal{L}(\boldsymbol{a}_k, \beta, \lambda)}{\partial \boldsymbol{a}_k} &= -\beta^{-1}\boldsymbol{c}_{\boldsymbol{h}_k}^{\mathrm{H}} + \beta^{-2}\boldsymbol{a}_k^{\mathrm{H}} \sum_{i=1}^{K} (\boldsymbol{C}_{\boldsymbol{\phi}_k}^{*} \otimes \boldsymbol{C}_{\boldsymbol{h}_i}) \\ &\quad + \beta^{-2}\boldsymbol{a}_k^{\mathrm{H}} \Big[\sum_{i \in \mathcal{I}_k \cup \{k\}} \boldsymbol{c}_{\boldsymbol{h}_i} \boldsymbol{c}_{\boldsymbol{h}_i}^{\mathrm{H}} + \lambda\beta^2 (\boldsymbol{C}_{\boldsymbol{\phi}_k}^{*} \otimes \mathbf{I}_M) \Big]\end{aligned} \tag{4.45}$$

Setting this to zero leads to the expression of $\boldsymbol{a}_k$

$$\boldsymbol{a}_k(\lambda\beta^2) = \beta\tilde{\boldsymbol{a}}_k(\lambda\beta^2) = \beta \boldsymbol{F}_k^{-1}(\lambda\beta^2)\boldsymbol{c}_{\boldsymbol{h}_k} \tag{4.46}$$

with

$$\boldsymbol{F}_k(\lambda\beta^2) = \sum_{i=1}^{K} (\boldsymbol{C}_{\boldsymbol{\phi}_k}^{*} \otimes \boldsymbol{C}_{\boldsymbol{h}_i}) + \sum_{i \in \mathcal{I}_k \cup \{k\}} \boldsymbol{c}_{\boldsymbol{h}_i} \boldsymbol{c}_{\boldsymbol{h}_i}^{\mathrm{H}} + \lambda\beta^2 (\boldsymbol{C}_k^{*} \otimes \boldsymbol{I}_M) \tag{4.47}$$

Moreover, from the power constraint

$$E_{\mathrm{tr}} = \mathrm{tr}(\boldsymbol{A}\boldsymbol{C}\boldsymbol{A}^{\mathrm{H}}) = \beta^2 \sum_{k=1}^{K} \tilde{\boldsymbol{a}}_k^{\mathrm{H}}(\lambda\beta^2)(\boldsymbol{C}_k^{*} \otimes \boldsymbol{I}_M)\tilde{\boldsymbol{a}}_k(\lambda\beta^2) \tag{4.48}$$

we directly see that

$$\beta = \sqrt{\frac{E_{\mathrm{tr}}}{\sum_{k=1}^{K} \tilde{\boldsymbol{a}}_k^{\mathrm{H}}(\lambda\beta^2)(\boldsymbol{C}_k^{*} \otimes \boldsymbol{I}_M)\tilde{\boldsymbol{a}}_k(\lambda\beta^2)}} \tag{4.49}$$

On the other hand, regarding the derivative w.r.t. β, according to the expression in (4.46), we get

$$\begin{aligned}\frac{\partial \mathcal{L}(\boldsymbol{a}_k, \beta, \lambda)}{\partial \beta} &= K - \lambda\beta^2 \sum_{k=1}^{K} \beta^2 \tilde{\boldsymbol{a}}_k^{\mathrm{H}}(\lambda\beta^2)(\boldsymbol{C}_k^{*} \otimes \mathbf{I}_M)\tilde{\boldsymbol{a}}_k(\lambda\beta^2) \\ &= K - \lambda\beta^2 E_{\mathrm{tx}}\end{aligned} \tag{4.50}$$

where we make use of the determination from (4.48). Then, we realize that again, $\lambda\beta^2 = K/E_{\mathrm{tx}}$, with $E_{\mathrm{tx}} = K\rho_{\mathrm{ul}}$ to allow fairness between link budgets, as mentioned in the analogous section of the LMMSE filter.

We can express then the optimal solution as follows

$$\boldsymbol{a}_k^\star = \beta^\star \boldsymbol{F}_k^{-1} \boldsymbol{c}_{\boldsymbol{h}_k} \tag{4.51}$$

with

$$\beta^\star = \sqrt{\frac{E_{\text{tx}}}{\sum_{k=1}^{K} \boldsymbol{c}_{\boldsymbol{h}_k}^{\text{H}} \boldsymbol{F}_k^{-1} (\boldsymbol{C}_k^* \otimes \boldsymbol{I}_M) \boldsymbol{F}_k^{-1} \boldsymbol{c}_{\boldsymbol{h}_k}}} \tag{4.52}$$

and

$$\boldsymbol{F}_k = \sum_{i=1}^{K} (\boldsymbol{C}_{\boldsymbol{\phi}_k}^* \otimes \boldsymbol{C}_{\boldsymbol{h}_i}) + \sum_{i \in \mathcal{I}_k \cup \{k\}} \boldsymbol{c}_{\boldsymbol{h}_i} \boldsymbol{c}_{\boldsymbol{h}_i}^{\text{H}} + \frac{K}{E_{\text{tr}}} (\boldsymbol{C}_k^* \otimes \mathbf{I}_M) \tag{4.53}$$

Finally, we need to clarify which kind of constraint we will be considering in the rest of the project. As already said, the main advantage of this technique w.r.t. the LMMSE is that the solution can be computed only when the second-order statistics change. However, this is not true for the instantaneous case since the matrix $\boldsymbol{C} = \bar{\boldsymbol{\Phi}} \bar{\boldsymbol{\Phi}}^{\text{H}}$ varies with the channel. Also, it cannot be approximated by a diagonal with the DFT, fact that increases complexity considerably. Therefore, from now on, we will restrict to the average approach, i.e. $\boldsymbol{C} = \boldsymbol{C}_{\boldsymbol{\phi}}$. In addition, it represents the strategy with more physical and realistic sense. Consequently, we will require Monte-Carlo simulations for computing the scaling factor β in the LMMSE case (see Section 4.1.1). Note that in the average case, $\boldsymbol{F}_k$ from (4.53) could be expressed in terms of $\boldsymbol{C}_{\boldsymbol{y}}$, defined in (2.2), to get a similar expression than the equalizer. However, this would not make sense as such information is not available at the transmitter, i.e. in general noise is unknown.

Furthermore, the solution can be found in a more compact form if we employ a matrix notation. Nevertheless, this additional step is presented in Appendix A.1. In both cases, expressions can be also simplified by the DFT approximation and the MIL, which lead to a considerable efficiency enhancement, i.e. number of operations is highly reduced.

4.1.3 Simplified Generalized Matched Filter

The last filter solution we are discussing in this section is the simplified version of the GMF. It relies on the lower bound, on the achievable bound defined in (2.26) and (2.27) when considering a CDI based approach.

Let us first start then by rewriting these bounds when using $\boldsymbol{g}_k = \boldsymbol{A}_k\boldsymbol{\phi}_k$ and $\boldsymbol{p}_k = \beta\boldsymbol{A}_k\boldsymbol{\phi}_k$. In that case, it can be shown that they result

$$\underline{\gamma}_{k,\text{ul}}^{\text{CDI}} = \frac{|\text{tr}(\boldsymbol{A}_k^{\text{H}}\boldsymbol{C}_{\boldsymbol{h}_k})|^2}{\frac{\text{tr}(\boldsymbol{A}_k^{\text{H}}\boldsymbol{C}_{\boldsymbol{h}_k}\boldsymbol{A}_k)}{\rho_{\text{ul}}} + \sum_n \text{tr}(\boldsymbol{A}_k\boldsymbol{C}_{\boldsymbol{\phi}_k}\boldsymbol{A}_k^{\text{H}}\boldsymbol{C}_{\boldsymbol{h}_n}) + \sum_{n\in\mathcal{I}_k} |\text{tr}(\boldsymbol{A}_k^{\text{H}}\boldsymbol{C}_{\boldsymbol{h}_n})|^2} \tag{4.54}$$

$$\underline{\gamma}_{k,\text{dl}}^{\text{CDI}} = \frac{|\text{tr}(\boldsymbol{C}_{\boldsymbol{h}_k}\boldsymbol{A}_k)|^2}{\frac{1}{\beta^2\rho_{\text{dl}}} + \sum_n \text{tr}(\boldsymbol{C}_{\boldsymbol{h}_k}\boldsymbol{A}_n\boldsymbol{C}_{\boldsymbol{\phi}_n}\boldsymbol{A}_n^{\text{H}}) + \sum_{n\in\mathcal{I}_k} |\text{tr}(\boldsymbol{C}_{\boldsymbol{h}_k}\boldsymbol{A}_n)|^2} \tag{4.55}$$

Note that from these expressions and with the help of the Multiple Access Channel - Broadcast Channel (MAC-BC) duality [36], we can find the optimal filters that maximize the SINR [37]. However, they will be just scaled versions of the solutions in Section 4.1.2, meaning data results will not change. Hence, we skip this approach to avoid redundancy.

On the other hand, since we are interested in large-scale antenna scenarios, we can focus only on eliminating the remaining interfering terms at that regimes, i.e. addends from $\sum_{n\in\mathcal{I}_k}$. Then, the special properties of the covariance matrices apply. In [33], taking into account the channel model described in Section 2.3 (ULA), it is shown that covariance matrices of users with a completely distinct structure become orthogonal for $M \to \infty$. This is due to their rank deficiency we discussed before in Section 3.1.2, which implies a null space is created, which is where other users matrices land. In fact, for those situations, we are able to distinguish more directions and thus, all users can be separated eventually. This issue can be represented by the following

$$\boldsymbol{C}_{\boldsymbol{h}_i}^{\text{H}}\boldsymbol{C}_{\boldsymbol{h}_j} \to \boldsymbol{0}\,\forall i \neq j \tag{4.56}$$

Thereby, a simple approach for the design of $\boldsymbol{A}_k$ can be to choose it equal to the covariance matrix of user k, i.e. $\boldsymbol{A}_k = \boldsymbol{C}_{\boldsymbol{h}_k}$. This way, we can get rid of the aforementioned terms and maintain desired signals. In other words, in the large scale regime we can simply write

$$\text{tr}(\boldsymbol{C}_{\boldsymbol{h}_k}\boldsymbol{C}_{\boldsymbol{h}_n}) = \text{tr}(\boldsymbol{C}_{\boldsymbol{h}_n}\boldsymbol{C}_{\boldsymbol{h}_k}) = \begin{cases} \|\boldsymbol{C}_{\boldsymbol{h}_k}\|_{\text{F}}^2 & \text{if} \quad n = k \\ 0 & \text{if} \quad n \in \mathcal{I}_k \end{cases} \tag{4.57}$$

However, as we will see in Chapter 5, this solution does not provide really good results given its poor adaptability, specially for a finite number of BS antennas. In that case, covariances in the set $\mathcal{I}_k \cup \{k\}$ are not completely orthogonal and (4.57) does not hold. Thus, the main advantage to point out is that no operations are needed for finding the solution. Also, regarding the scaling factor in the DL, it can be obtained like in Section 4.1.2

$$\beta^{\star} = \sqrt{\frac{E_{\text{tx}}}{\sum_{k=1}^{K} \boldsymbol{c}_{\boldsymbol{h}_k}^{\text{H}} (\boldsymbol{C}_k^{*} \otimes \boldsymbol{I}_M) \boldsymbol{c}_{\boldsymbol{h}_k}}} \tag{4.58}$$

This leads to an enormous increase of the system efficiency at the price of low performance. Besides, it is important to realize that covariance matrices are also present in the GMF filters found in Section 4.1.2. As a result, interference can be canceled the same way and thanks to the inverse term, this mitigation is further improved. Thus, data rates are much higher in that case.

Another similar strategy, yet more complex, to eliminate this interference would be to design the matrix $\boldsymbol{A}_k$ such that the following is fulfilled

$$\boldsymbol{A}_k \tilde{\boldsymbol{C}}_k = \boldsymbol{0} \tag{4.59}$$

where $\tilde{\boldsymbol{C}}_k$ contains the covariance matrices from users in the set $\mathcal{I}_k$

$$\tilde{\boldsymbol{C}}_k = [\boldsymbol{C}_{\boldsymbol{h}_{n_1}}, \ldots, \boldsymbol{C}_{\boldsymbol{h}_{n_L}}] \quad \forall n_i \in \mathcal{I}_k \quad L = |\mathcal{I}_k| \tag{4.60}$$

Considering the structure of this equation, a solution can be found whenever this wide $\tilde{\boldsymbol{C}}_k$ matrix is rank-deficient . As already seen, this condition can be fulfilled given that usually there are not enough multipaths as possible channel directions, i.e. $M \gg N_P$. Consequently, when computing the *singular value decomposition* (SVD) of $\boldsymbol{C}_k$

$$\boldsymbol{C}_k = \boldsymbol{U}\boldsymbol{\Sigma}\boldsymbol{V}^{\text{H}} \quad \text{with} \quad \boldsymbol{\Sigma} = \text{diag}(\sigma_1, \ldots, \sigma_K) \tag{4.61}$$

it can be easily inferred that there will exist some non-empty set $\mathcal{Z}_k$ of zero singular values σ_i. Then, a possible choice for our matrix $\boldsymbol{A}_k$ would be just to use the left-singular vectors associated to those null singular values as basis for our matrix. Alternatively, given the reduced SVD form $\boldsymbol{C}_k = \boldsymbol{U}_r \boldsymbol{\Sigma}_r \boldsymbol{V}_r^{\text{H}}$, a more suitable approach can be to express $\boldsymbol{A}_k$ as

$$\boldsymbol{A}_k = \boldsymbol{A}_k' (\mathbf{I} - \boldsymbol{U}_r \boldsymbol{U}_r^{\text{H}}) \tag{4.62}$$

for some $\boldsymbol{A}'_k$. Note that since $\boldsymbol{\Sigma}_r \succeq \mathbf{0}$, all its singular values will be non-zero. Then, this solution can lead orthogonality to be achieved more rapidly. Nevertheless, it has been seen that this approach does not behave well in our scenario. The main reason behind it, is that when constructing $\tilde{\boldsymbol{C}}_k$ with lots of users, it can quickly become full-rank. That is the reason why we skip this processing scheme in our analysis. Despite that, it will become useful in Section 4.3, where a similar perspective is exploited and a deeper study is elaborated. It will help us introduce and understand related concepts.

4.1.4 Results I

In this project, given the large amount of different scenarios and approaches, we opted for presenting all the numerical results in a different fifth chapter. Nevertheless, here we will make a qualitative analysis with the help of those numerical results. In particular, we will review the comparison between the three different strategies in terms of rate and efficiency.

To begin with, it is important to highlight that none of the equalizers presented are normalized. This additional step is done with MATLAB at the simulations part. Also, in all three cases, the DL results are lower than the UL given the absence of an optimal power allocation and the lack of noise information. That is why the first approach is performed and analyzed later, in Section 4.1.5.

On the other hand, it can be seen that the LMMSE approach will always deliver a better result than the GMF, and its simplified version, since it relies on the current channel realization and thus, interference can be reduced more effectively. In other words, the GMF does not have the same statistical properties as the LMMSE as it is based on second-order moments, which suppress non desired (instantaneous) signals more poorly and slowly. This will be clearly reflected in Section 5.2, where numerical values are given.

However, as already mentioned, when looking at the efficiency of the solutions, the GMF supposes a great breakthrough as less computations are required along large periods of time, i.e. when several different channel and covariance matrix realizations are considered. Obviously, the simplified case is the best in this aspect, but a lot of performance is sacrificed.

4.1.5 Power Allocation

At the transmitter side, employing an uniform power allocation is far from being optimal, specially when the SINR is not at a high regime. Then, in order to approach both links data rates, we announce a way to allocate power in a more proper manner. This will be the perspective of sum-rate maximization. At the second part of this section, we will discuss the possibility of using a rate balancing approach to distribute power more fairly. Note that this operation can only be performed at the BS and thus, in the DL, since all information is only available there, i.e. users are blind for any processing.

4.1.5.1 Sum Rate Maximization

To take into account the power allocation optimization we introduce a new precoder $\boldsymbol{T} = \boldsymbol{P}\boldsymbol{D}^{1/2}$ based on the previous found precoders, which are fixed, and on a diagonal matrix $\boldsymbol{D} = \text{diag}(d_1, \ldots, d_K) \in \mathbb{R}^{K \times K}$ that reflects the distribution of power, e.g. in the case of uniform, it is simply an identity. In fact, each k-th element d_k represents the portion of the total power destined to user k. Besides, to preserve the system requirements, $\boldsymbol{T}$ must fulfill the same power constraint as before

$$\text{E}[\|\boldsymbol{T}\boldsymbol{s}\|_2^2] = \text{tr}(\text{E}[\boldsymbol{P}\boldsymbol{D}\boldsymbol{P}^{\text{H}}]) = E_{\text{tx}} \tag{4.63}$$

For simplicity, we will consider an instantaneous power constraint, even though an average would be more appropriate for the GMF case. Hence, the expectation can be dropped in the previous expression

$$\text{tr}(\boldsymbol{P}\boldsymbol{D}\boldsymbol{P}^{\text{H}}) = E_{\text{tx}} \tag{4.64}$$

In addition, with the new precoder, the expression of the individual rates for the users, depending on $\boldsymbol{D}$, read as

$$R_k(\boldsymbol{D}) = \log_2(1 + \gamma_k(\boldsymbol{D})) \tag{4.65}$$

with

$$\gamma_k(\boldsymbol{D}) = \frac{|\boldsymbol{h}_k^{\text{H}}\boldsymbol{t}_k|^2}{\frac{1}{\rho_{\text{dl}}} + \sum_{n \neq k} |\boldsymbol{h}_k^{\text{H}}\boldsymbol{t}_n|^2} = \frac{d_k|\boldsymbol{h}_k^{\text{H}}\boldsymbol{t}_k|^2}{\frac{1}{\rho_{\text{dl}}} + \sum_{n \neq k} d_n|\boldsymbol{h}_k^{\text{H}}\boldsymbol{p}_n|^2} = \frac{N_k}{D_k} \tag{4.66}$$

where we employed $\boldsymbol{t}_k = \sqrt{d_k}\boldsymbol{p}_k$. Thereby, since we aim to optimize the sum rate w.r.t. the matrix $\boldsymbol{D}$, we can state the problem as follows

$$\boldsymbol{D}^{\star} = \underset{\boldsymbol{D}}{\operatorname{argmax}} \sum_{k=1}^{K} R_k(\boldsymbol{D}) = \underset{\boldsymbol{D}}{\operatorname{argmax}}\, R_{\text{sum}}(\boldsymbol{D}) \quad \text{s.t. : } \text{tr}(\boldsymbol{P}\boldsymbol{D}\boldsymbol{D}\boldsymbol{P}^{\text{H}}) = E_{\text{tx}} \tag{4.67}$$

As we can see, this sum rate maximization (BC) under a total power constraint is a non-convex optimization problem [16]. This is due to the fact that d_k not only affects the SINR of its corresponding user but also the value of the others. Then, we need to find the solution by means of suboptimal approaches. We opted for the gradient projection based method [38]

$$\boldsymbol{D}^{(n+1)} = \mathcal{P}_{\mathcal{C}}\left(\boldsymbol{D}^{(n)} + s^{(n)} \frac{\partial_w R_{\text{sum}}(\boldsymbol{D})}{\partial_w \boldsymbol{D}}\Big|_{\boldsymbol{D}=\boldsymbol{D}^{(n)}}\right) \tag{4.68}$$

where $\mathcal{P}_{\mathcal{C}}(\cdot)$ represents the orthogonal projection operator onto the convex constrained set $\boldsymbol{D} \in \mathcal{C} : \text{tr}(\boldsymbol{P}\boldsymbol{D}\boldsymbol{D}\boldsymbol{P}^{\text{H}}) = E_{\text{tx}}$ and $s^{(n)} > 0$ the iteration-dependent step-size. These terms are defined below.

On the one hand, since the given $\boldsymbol{P}$ already satisfies the total power constraint, we can express the orthogonal projection operator as follows

$$\mathcal{P}_{\mathcal{C}}(\boldsymbol{D}) = \begin{cases} \boldsymbol{D} & \text{if} \quad \text{tr}(\boldsymbol{P}\boldsymbol{D}\boldsymbol{D}\boldsymbol{P}^{\text{H}}) = E_{\text{tx}} \\ \frac{E_{\text{tx}}}{\text{tr}(\boldsymbol{P}\boldsymbol{D}\boldsymbol{D}\boldsymbol{P}^{\text{H}})}\boldsymbol{D} & \text{if} \quad \text{tr}(\boldsymbol{P}\boldsymbol{D}\boldsymbol{D}\boldsymbol{P}^{\text{H}}) \neq E_{\text{tx}} \end{cases} \tag{4.69}$$

This way, whenever the precoder $\boldsymbol{T}$ does not fulfill the constraint, $\boldsymbol{D}$ is projected onto the constraint set $\mathcal{C}$. Note also that this operation is just a scaling of the matrix $\boldsymbol{D}$ to ensure the sum power condition is satisfied.

On the other hand, regarding the step-size parameter, different approaches can be used to design a proper value so that convergence of the algorithm onto a stationary point is achieved. In our case, for the sake of simplicity, we choose the open loop approach [38], i.e. $s^{(n)} = 1/n$. Nonetheless, one could seek for more optimal strategies that accelerate the speed of this convergence and that result more efficient, e.g. the Armijo method [38].

Finally, another important term in the algorithm described in (4.68) is the Wirtiger derivative [35] of the utility function $R_{\text{sum}}(\boldsymbol{D})$. It can be expressed as the summation of derivatives of the individual rates defined in (4.65)

$$\begin{aligned}\frac{\partial_w R_{\text{sum}}(\boldsymbol{D})}{\partial_w \boldsymbol{D}} &= \sum_{k=1}^{K} \frac{\partial_w R_k(\boldsymbol{D})}{\partial_w \boldsymbol{D}} = \sum_{k=1}^{K} \frac{\partial_w}{\partial_w \boldsymbol{D}} \log_2(1+\gamma_k(\boldsymbol{D})) \\ &= \sum_{k=1}^{K} \frac{1}{(1+\gamma_k(\boldsymbol{D}))\ln 2} \frac{\partial_w \gamma_k}{\partial_w \boldsymbol{D}}\end{aligned} \tag{4.70}$$

where

$$\frac{\partial_w \gamma_k}{\partial_w \boldsymbol{D}} = \frac{1}{N_k^2} |\boldsymbol{h}_k^{\mathrm{H}} \boldsymbol{t}_k|^2 (\boldsymbol{e}_k \boldsymbol{e}_k^{\mathrm{T}} N_k - d_k \sum_{n \neq k} |\boldsymbol{h}_k^{\mathrm{H}} \boldsymbol{p}_n|^2 \boldsymbol{e}_n \boldsymbol{e}_n^{\mathrm{T}}) \tag{4.71}$$

Overall, the steps of this iterative procedure are defined in Algorithm 1. It is no surprise that we start with a uniform power allocation, i.e. $\boldsymbol{D} = \mathbf{I}$. Also, to speed up the whole process, we could double n each time instead of increasing it by one. However, this practice is favorable only when the solution is close enough since otherwise, lots of steps would be necessary.

Algorithm 1 Gradient Projection Algorithm

initialize
  $\boldsymbol{D}^{(0)} \leftarrow \mathbf{I}$ and $n = 0$
repeat
  $n \leftarrow n + 1$
  $s \leftarrow 1/n$
  $\boldsymbol{D}^{(n+1)} \leftarrow$ (4.68)
until $R_{\text{sum}}(\boldsymbol{D}^{(n+1)}) - R_{\text{sum}}(\boldsymbol{D}^{(n)}) \leq \xi$

Note that, at each step of this algorithm, we go in the direction of the steepest gradient decent to find the solution. Then, if the power constraint is compromised, the projection is applied.

Moreover, since in reality we will employ average restraints, we will use the following approach, yet heuristic, to take this into account. In particular, we will substitute the total transmit power E_{tx} by the term $\text{tr}(\boldsymbol{P}\boldsymbol{P}^{\mathrm{H}})$, which are equal only in the instantaneous case. Thereby, we impose that the overall power constraint is satisfied but restricting each value to be equal to the power of the old precoder $\boldsymbol{P}$ at each channel realization.

The optimal strategy would be to allow the new precoder $\boldsymbol{T}$ to have any instantaneous power, regardless of $\boldsymbol{P}$. However, this seems to be significantly more complicated and the benefits we could get would not be that relevant.

As we will see in Section 5.2.4, this optimization enables the transmitter to improve its data rates and get closer to the receiver performance. Major advances are experienced in the case of the LMMSE, where the gap between both links was larger. Therefore, the necessity of a proper power allocation is justified. Nevertheless, in the case of the GMF, given their close behavior, it is observed that the equalizer is surpassed by the precoder.

4.1.5.2 Rate Balancing

Until now, an opportunistic communication scheme is employed since we focus on sum rate. Nonetheless, this approach results too aggressive for users with a poor channel quality. In the extreme case, this set might not even be served, which is unreasonable for real systems with high demand.

To solve this issue, we propose a rate balancing approach for the power allocation. Thereby, now we will be able to satisfy Quality of Service (QoS) requirements and users will experience similar performances. In fact, we will concentrate on the case where all users have the same rate targets. To measure the improvement here, we focus on the variance reduction achieved in comparison with the sum rate approach. Empirical values will be seen also in Section 5.2.4 whereas a qualitative comparison is given at the end of this section. Furthermore, different solutions depending on the type of perspective are presented. Therefore, let us first begin with the CDI approach.

In the case of a statistical point of view, we rely on the lower bound on the achievable rate of the DL defined in (2.27). Then, considering a GMF solution is employed (see Section 4.1.2), given its suitability for this scenario, the rate balancing problem can be stated as follows

$$\boldsymbol{A}^{\star} = \underset{\boldsymbol{A}}{\operatorname{argmax}}\, \delta \quad \text{s.t.} : \log_2(1 + \underline{\gamma}_k^{\text{CDI}}) \geq \delta \varphi_k,\ \text{tr}(\boldsymbol{A}\boldsymbol{C}_{\boldsymbol{\phi}}\boldsymbol{A}^{\text{H}}) = E_{\text{tx}} \quad (4.72)$$

where $\boldsymbol{A}$ and $\boldsymbol{C}_{\boldsymbol{\phi}}$ are defined in (4.34) and φ_k represents the rate target for the k-th user. Note that the SINR is given by the expression in (4.55). The solution to the problem in (4.72) is constituted by two steps. First, find the optimal optimal UL filter $\boldsymbol{A}$ by means of the BC-MAC duality [36]. To do so,

we need to write the SINR in vector notation with the help of the equivalences given in (4.44). Later, obtain the optimal power allocation and translate the resulting solution to the DL. Nevertheless, we will focus only on the power allocation since we assume that $\boldsymbol{A}$ is already given, e.g. from Sections 4.1.2 or 4.1.3. Hence, we will use a new precoder $\boldsymbol{t}_k = \sqrt{d_k}\boldsymbol{p}_k$, where d_k are analogous to the previous one and determine the set of powers destined to each user. Note that no duality will be needed in this process.

In that case, it can be shown that the optimal powers can be found via a fixed-point iteration [37]. We just need to define an effective interference function that considers the new allocation

$$\mathcal{J}_k(\boldsymbol{d}) = \frac{\frac{1}{\beta^2\rho_{\text{dl}}} + \sum_n d_n \text{tr}(\boldsymbol{C}_{\boldsymbol{h}_k}\boldsymbol{A}_n\boldsymbol{C}_{\boldsymbol{\phi}_n}\boldsymbol{A}_n^{\text{H}}) + \sum_{n\in\mathcal{I}_k} d_k|\text{tr}(\boldsymbol{C}_{\boldsymbol{h}_k}\boldsymbol{A}_n)|^2}{|\text{tr}(\boldsymbol{C}_{\boldsymbol{h}_k}\boldsymbol{A}_k)|^2} \tag{4.73}$$

such that $\underline{\gamma}_k^{\text{CDI}} = d_k/\mathcal{J}_k(\boldsymbol{d})$. Note that β is the scaling factor that ensures the old power constraint from (4.72) is fulfilled and it is already defined by (4.52). Despite that, an adjustment must be done when introducing $\boldsymbol{d} = [d_1, \ldots, d_K]^{\text{T}}$, as discussed later on. Moreover, we define the SINR targets as follows

$$\omega(\delta) = [2^{\delta\varphi_1} - 1, \ldots, 2^{\delta\varphi_K} - 1]^{\text{T}} \tag{4.74}$$

Thereby, according to [37], the solution for $\boldsymbol{d}$ can be found in two steps with any initial values. At the beginning, we choose δ so that the power constraint is fulfilled also in the case of the new precoder. Later, we find $\boldsymbol{d}$ with a fixed-point iteration and the effective interference from (4.73)

$$\delta \leftarrow \delta : \omega(\delta)^{\text{T}}\mathcal{J}(\boldsymbol{d}) - 1 = 0 \tag{4.75}$$

$$\boldsymbol{d} \leftarrow \text{diag}(\omega(\delta))\mathcal{J}(\boldsymbol{d}) \tag{4.76}$$

where $\mathcal{J}(\boldsymbol{d}) = [\mathcal{J}_1(\boldsymbol{d}), \ldots, \mathcal{J}_K(\boldsymbol{d})]^{\text{T}}$. It is important to realize that the first stage is comparable to the orthogonal projection defined in (4.69). In the case of having the old precoders $\boldsymbol{p}_k$ with unit norm, we should use E_{tx} instead of one in equation (4.75). Additionally, following the arguments stated in [37], to find δ, we can employ the Newton-Raphson method as it converges globally. The second step is then the fixed-point iteration and the entire process is repeated until $\boldsymbol{d}$ stabilizes. All this is reflected in Algorithm 2.

Algorithm 2 Statistical Rate Balancing

initialize
$\boldsymbol{d} \leftarrow \mathbf{1}$ and $\varphi_k = 1 \, \forall k$
repeat
$\delta \leftarrow \delta : \omega(\delta)^{\mathrm{T}} \mathcal{J}(\boldsymbol{d}) - 1 = 0$
$\boldsymbol{d} \leftarrow \mathrm{diag}(\omega(\delta)) \mathcal{J}(\boldsymbol{d})$
until convergence

Note that, unlike before, the same power allocation is maintained during all channel realizations as long as the covariance matrices do not vary. Also, $\boldsymbol{d}$ is uniformly initialized to be coherent, even though it could be any arbitrary number. Besides, rate targets are assumed equal, no matter its value, i.e. $\varphi_k = \varphi \, \forall k$. In fact, it is the best way to go as no priorities are established and users obtain more similar results, leading to the lowest variance and highest sum rate too.

On the other hand, the same can be done for the CSI approach, directly related to the LMMSE filter since its based on channel realizations. Then, following the reasoning from [39] and considering the lower bound from (2.36), a similar optimization problem can be formulated

$$\boldsymbol{T}^{\star} = \underset{\boldsymbol{T}}{\mathrm{argmax}} \, \delta \quad \text{s.t.} : \log_2(1 + \underline{\gamma}_k^{\mathrm{CSI}}) \geq \delta \varphi_k, \, \mathrm{tr}(\boldsymbol{T}\boldsymbol{T}^{\mathrm{H}}) = E_{\mathrm{tx}} \tag{4.77}$$

where $\boldsymbol{T}$ is the new precoder we are seeking. Likewise, we assume the precoder $\boldsymbol{P}$ from (4.22) is given, despite the fact that two steps are needed to solve the problem in (4.77), i.e. optimal filter and power allocation. Hence, we will work with $\boldsymbol{t}_k = \sqrt{d_k}\boldsymbol{p}_k$ and focus on the power allocation, which can be derived as before with the two-iterative step [39] described in (4.75) and (4.76). This is then, a new and simpler problem. Nevertheless, now the effective interference $\mathcal{J}(\boldsymbol{d})$ that satisfies $\underline{\gamma}_k^{\mathrm{CSI}} = d_k / \mathcal{J}_k(\boldsymbol{d}) \, \forall k$ is determined by

$$\mathcal{J}_k(\boldsymbol{d}) = \frac{\frac{1}{\rho_{\mathrm{dl}}} + \sum_n d_n \boldsymbol{p}_n^{\mathrm{H}} \boldsymbol{C}_{\tilde{\boldsymbol{h}}_k} \boldsymbol{p}_n + \sum_{n \neq k} d_n |\hat{\boldsymbol{h}}_k^{\mathrm{H}} \boldsymbol{p}_n|^2}{|\hat{\boldsymbol{h}}_k^{\mathrm{H}} \boldsymbol{p}_k|^2} \tag{4.78}$$

Thereby, Algoritm 2 with random targets still holds and we can apply it to obtain the proper allocation. However, it can inferred that the solution must be computed every time the channel changes as it depends strongly on the realization. This is again, the main inconvenient when comparing with CDI. As expected, in terms of rate, a similar behavior to that of CDI is observed.

4.1.6 Results II

In the last two sections we have seen two approaches for allocating power depending on the system goals and customer needs. This requirements cannot be reached with a uniform strategy, and that is why the optimization is needed. Thereby, like in Section 4.1.4, here we will make a review and comparison of these two perspectives. Also, in Chapter 5, Section 5.2.4, numerical values from both will be presented and conclusions will be drawn too.

In particular, when we aim to maximize the total throughput, the best option is the one described at the beginning of Section 4.1.5. This aggressive strategy leads to high sum rates and approaches the performance of DL and UL, which in the case of the LMMSE are considerably far away. There is an improvement when using the GMF precoder as well, but not as significant.

On the other hand, if the purpose is to deliver a certain QoS or fixed performance to all users, we must employ the rate balancing approach, described in the last part. In that scenario, power is distributed so that variance of the user rates decreases considerably. This means users get more similar and realistic results and none of them is dismissed. However, as already mentioned, system performance is evaluated by means of sum rate and thus, this strategy would not be very useful in that sense as a part is sacrificed.

4.2 User Allocation

Another important part of our project is user allocation. It consists on grouping particular users together and assigning them certain pilots. Then, members within a group will share the same training sequences and contamination will be created among them. However, to mitigate this interference, this allocation must not be done randomly, but taking into consideration system characteristics.

In this section, we will present several approaches to perform user allocation. First, a discussion about random assignation is given. There, reasons for not using this strategy will be announced. Second, we will introduce two methods to perform this task optimally. One is based on the covariance matrices and channel properties whereas the other relies on the sum rate as principal target. We will see how user rates can be improved and how performance can reach the pilot contamination free case. In other words, this dramatic effect can be highly reduced with these two strategies. Finally, a qualitative analysis is provided to clearly understand the relevancy of this practice. Note that pilot assignation will

depend on channel statistics and thus, it is performed every time they change and maintained during the corresponding realizations.

4.2.1 Random Assignation

The first approach for assigning users to groups is to do it randomly. This way, none of the communication features are considered and pilot contamination effects become clearly dominant. This naive strategy is the one considered in Chapter 3 while analyzing the problem and its impact. It was shown that we can become strongly sensitive to this interference given the saturation that takes place over the SINR for large M. As a result, the system performance is highly compromised and low user data rates are obtained.

To overcome this issue, it has been observed that distributing users with certain smart criteria improves considerably the individual and overall throughputs [32]. Then, in the following we will explore different ways that exploit our scenario and try to cancel the interference created by pilot contamination.

4.2.2 Covariance Matrix Method

The first way to efficiently allocate users is based on the covariance matrix and its properties discussed in Sections 2.3 and 4.1.3. Here, we take benefit of the asymptotic orthogonality of these magnitudes, defined in (4.56). Therefore, the optimal approach is to gather together users with distinct structures so that pilot contamination is filtered out within the LMMSE estimate, thanks to the covariance (see Section 3.1.2). In turn, users with similar matrices and channels will be separated and thus, their interference will be diminished. Note that, as we will see later, this decision will be based exclusively on the covariance matrices, since they contain channel structure and propagation directions.

We will see this with a simple example. Let $K = 4$ be the number of users and $T_{\text{tr}} = 2$ the training time. This means we have two groups with two users each that share one pilot sequence. From this, it is easy to see that the optimal number of users per group, assuming all of them have the same size, will be given by $G = T_{\text{tr}}$, and the number of groups is then K/T_{tr}. Note that employing different sizes would be more complicated and no clear benefit would be obtained. In addition, consider users 1 and 3 have different structures as well as 2 and 4. On the contrary, 1 and 2 are similar, like 3 and 4. Consequently, the best way to go is to distribute users in the following pairs: $1-3$ and $2-4$. This way, the covariance matrix $\boldsymbol{C}_{\boldsymbol{h}_1}$ of the first user will suppress the interference

coming from the third when estimating the channel. Same happens with the other groups and users, where pilot contamination is removed. In fact, in the extreme case that they are orthogonal, this effect disappears completely.

This strategy is also employed in [32], where covariance matrices must be estimated as well. It is shown that, in this case, the best setting is to use groups of size $G' = G/2$. However, since we assume this information is given, the previous size G is already suitable. That is why we rely only on this magnitudes for our analysis, since they are the certain channel knowledge we have. Then, the need for covariance comparison appears and is stated in [32] too. In particular, users are allocated depending only on these matrices and specifically, on the measurement [32] employed to distinguish them. We will study this approach together with other criteria to try to solve this first problem. Moreover, once the measures are computed, a proper algorithm is required to find the optimal allocation. Given the large amount of possibilities, a greedy approach will be chosen to perform this task [32].

As a result, in this section, we will first introduce several of the metrics used to compare covariance matrices and determine their likeliness. Thereby, in the second part, a greedy algorithm will be presented to allocate users according to the previously calculated measurements.

4.2.2.1 Comparison Metrics

Here the metrics to compare covariance matrices, in terms of structure and orthogonality, will be presented. In particular, we will focus on a set of ratios $\Delta_{i,j}^{(n)}$, with $n = (1, \dots, 5)$, between different functions of matrices $\boldsymbol{C}_{\boldsymbol{h}_i}$ and $\boldsymbol{C}_{\boldsymbol{h}_j}$ that satisfy $0 \leq \Delta_{i,j}^{(n)} \leq 1$. Then, when both matrices become more similar, this ratio will increase and it will decrease otherwise. In fact, $\Delta_{i,j}^{(n)} = 1$ means the two matrices are equal while $\Delta_{i,j}^{(n)} = 0$ reveals they are completely distant and orthogonal. We are interested then in channel directions and propagation features. Thereby, we will also concentrate on the eigenvalues and eigenvectors of these matrices, since the same data is stored.

The first metric to be discussed, introduced in [40], is given by

$$\Delta_{i,j}^{(1)} = \frac{\text{tr}(\boldsymbol{C}_{\boldsymbol{h}_i}\boldsymbol{C}_{\boldsymbol{h}_j})}{\|\boldsymbol{C}_{\boldsymbol{h}_i}\|_{\text{F}}\|\boldsymbol{C}_{\boldsymbol{h}_j}\|_{\text{F}}} \tag{4.79}$$

We can see that only when $\boldsymbol{C}_{\boldsymbol{h}_i} = \boldsymbol{C}_{\boldsymbol{h}_j}$ this ratio will become one. In general we have that $\text{tr}(\boldsymbol{C}_{\boldsymbol{h}_i}\boldsymbol{C}_{\boldsymbol{h}_j}) \leq \|\boldsymbol{C}_{\boldsymbol{h}_i}\|_{\text{F}}\|\boldsymbol{C}_{\boldsymbol{h}_j}\|_{\text{F}}$. Note that from this measurement,

two simpler approaches can be derived if the *eigenvalue decomposition* (EVD) of the matrices is used, i.e. $\boldsymbol{C}_{\boldsymbol{h}_k} = \boldsymbol{U}_k \boldsymbol{\Lambda}_k \boldsymbol{U}_k^{\mathrm{H}}$ with $\boldsymbol{\Lambda}_k = \mathrm{diag}(\lambda_{k,1}, \ldots, \lambda_{k,M})$. Particularly, we could simply substitute $\boldsymbol{C}_{\boldsymbol{h}_k}$ by either $\boldsymbol{U}_k$ or $\boldsymbol{\Lambda}_k$ to make the comparison in an eigenvector or eigenvalue basis respectively. Nevertheless, when dealing with the whole matrix, we are taking into account both characteristics and therefore, the metric contains more information.

A second option is to work directly with the eigenvalues $\lambda_{k,i}$ from these two matrices. For ease of notation, we define $\boldsymbol{\lambda}_k$ as the vector containing all these elements. Then, we can formulate the following measurement

$$\Delta_{i,j}^{(2)} = 1 - \frac{\|\boldsymbol{\lambda}_i - \boldsymbol{\lambda}_j\|}{\|\boldsymbol{\lambda}_i + \boldsymbol{\lambda}_j\|} \tag{4.80}$$

Again, only when the eigenvalues are equal, meaning both matrices are the same, we will have $\Delta_{i,j}^{(2)} = 1$. In addition, it is important to remember that eigenvalues are not usually ordered. Therefore, we need arrange them, for instance, in descending order to make a coherent comparison. Otherwise, our measurements would be inconsistent and unclear. With this approach, we study the power of the different channel propagations only. Hence, information regarding their directions, contained in the eigenvectors, is ignored.

The third strategy could be to use another of the Frobenius norm inequalities

$$\begin{aligned} \|\boldsymbol{C}_{\boldsymbol{h}_i} + \boldsymbol{C}_{\boldsymbol{h}_j}\|_{\mathrm{F}}^2 &= \|\boldsymbol{C}_{\boldsymbol{h}_i}\|_{\mathrm{F}}^2 + \|\boldsymbol{C}_{\boldsymbol{h}_j}\|_F^2 + 2\langle \boldsymbol{C}_{\boldsymbol{h}_i}, \boldsymbol{C}_{\boldsymbol{h}_j} \rangle_{\mathrm{F}} \\ &\geq \|\boldsymbol{C}_{\boldsymbol{h}_i}\|_{\mathrm{F}}^2 + \|\boldsymbol{C}_{\boldsymbol{h}_j}\|_{\mathrm{F}}^2 \end{aligned} \tag{4.81}$$

where $\langle \bullet, \bullet \rangle_{\mathrm{F}}$ is the Frobenius inner product. Thereby, with the previous, the following metric can be defined

$$\Delta_{i,j}^{(3)} = 2\tilde{\Delta}_{i,j}^{(3)} \quad \text{with} \quad \tilde{\Delta}_{i,j}^{(3)} = 1 - \frac{\|\boldsymbol{C}_{\boldsymbol{h}_i}\|_F^2 + \|\boldsymbol{C}_{\boldsymbol{h}_j}\|_F^2}{\|\boldsymbol{C}_{\boldsymbol{h}_j} + \boldsymbol{C}_{\boldsymbol{h}_j}\|_F^2} \tag{4.82}$$

Note that we need the scaling factor 2 to ensure we achieve $\Delta_{i,i}^{(3)} = 1$ since in that situation, we have $\tilde{\Delta}_{i,i}^{(3)} = 1/2$. In addition, we will achieve values near zero whenever the two matrices are quite different. This comparison takes into account all the data, but it does not focus on the orthogonality itself.

Thereby, we can also take a look at the maximum singular values

$$\Delta_{i,j}^{(4)} = \frac{\sigma_{ij,\max}}{\sigma_{i,\max}\,\sigma_{j,\max}} = \frac{\|\boldsymbol{C}_{\boldsymbol{h}_i}\boldsymbol{C}_{\boldsymbol{h}_j}\|_2}{\|\boldsymbol{C}_{\boldsymbol{h}_i}\|_2\|\boldsymbol{C}_{\boldsymbol{h}_j}\|_2} \tag{4.83}$$

where $\sigma_{ij,\max}$ refers to the maximum singular value of the product $\boldsymbol{C}_{\boldsymbol{h}_i}\boldsymbol{C}_{\boldsymbol{h}_j}$ and $\sigma_{i,\max}$ to the one from $\|\boldsymbol{C}_{\boldsymbol{h}_j}\|_2$. Alternatively, we can use the eigenvalues to compute a similar ratio since $\sigma_{i,\max} = \lambda_{i,\max}$ and $\sigma_{j,\max} = \lambda_{j,\max}$, although equality does not hold for the product matrix: $\sigma_{ij,\max} \neq \lambda_{ij,\max}$. Nevertheless, in both cases, $\Delta_{i,i}^{(4)} = 1$ is fulfilled. Also, here we can distinguish clearly when covariance matrices are completely far apart.

The fifth metric we also consider is the one defined below

$$\Delta_{i,j}^{(5)} = 1 - \frac{\|\boldsymbol{C}_{\boldsymbol{h}_i} - \boldsymbol{C}_{\boldsymbol{h}_j}\|_{\mathrm{F}}}{\|\boldsymbol{C}_{\boldsymbol{h}_i} + \boldsymbol{C}_{\boldsymbol{h}_j}\|_{\mathrm{F}}} \tag{4.84}$$

which results one for $i = j$. Moreover, instead of using the Frobenius norm, we can also employ the trace to compare the diagonal elements instead of the whole matrix. However, we would require the absolute value of the difference of matrices to have a positive result. Besides, we can use the eigenvectors $\boldsymbol{U}_k$ to compute such ratio too but power information would be neglected.

Moreover, note that if the order of the eigenvalues remains unchanged, metrics 2 and 5 are equivalent for the diagonal covariance matrices case, e.g. when considering i.i.d. channels or when employing the DFT approximation. In that situation, we have $\boldsymbol{C}_{\boldsymbol{h}_k} = \boldsymbol{\Lambda}_k$ and operations can be further simplified. In fact, this approximation reduces the complexity of all the aforementioned metrics, since diagonal matrices are much easier to manipulate. For instance, for any matrices $\boldsymbol{D} = \mathrm{diag}(\boldsymbol{d})$ and $\boldsymbol{E} = \mathrm{diag}(\boldsymbol{e})$, we have

$$\mathrm{tr}(\boldsymbol{D}\boldsymbol{E}) = \boldsymbol{d}^{\mathrm{T}}\boldsymbol{e} \quad \text{and} \quad \|\boldsymbol{D}\|_{\mathrm{F}}^2 = \|\boldsymbol{d}\|_2^2 \tag{4.85}$$

Finally, some of the metrics could be combined to obtain new comparison values, for instance, by multiplying two of them, i.e. $\Delta_{i,j}^{(n)}\Delta_{i,j}^{(m)}$. However, it has been observed that this is not a suitable approach. Besides, at the end of this section, we will compare all these approaches, again qualitatively. Numerical results and conclusions can be found in Chapter 5, Section 5.3.1.

4.2.2.2 Greedy Algorithm

The previous information will be used at this point to separate users into different groups, each of them associated to a pilot sequence so that they do not interfere with each other. As mentioned, users will be allocated in the same group whenever their correlation is low, meaning their covariance matrices present scarce similarities, or equivalently, when $\Delta_{i,j}^{(n)} \to 0$. This way, even sharing the same sequence, the interference created within a group will be highly reduced if the LMMSE estimator of the channel is employed.

Given the magnitude of this problem, suboptimal approaches must be employed. A good option for the allocation algorithm seems to be the strategy proposed in [32]. It consists in two main steps. First, we fill in all empty groups Ω_g with one user, where $g = (1, \ldots, G)$ is the corresponding indexing. To make this decision, we start by finding the ones leading to the maximum metric $\Delta_{i,j}^{(n)}$ and separate them in two different groups. Then, we select the one with the highest sum of $\Delta_{i,j}^{(n)}$ w.r.t. to the previous allocated users. This user is assigned to the other empty groups and we continue until there are no left. Later, the rest of users are greedily allocated by means of a certain utility function U. In particular, it is defined as the negative value of the sum of all metrics once we introduce a new user into a certain group

$$U(\Omega_1, \ldots, \Omega_G) = -\sum_{g=1}^{G} \sum_{i,j \in \Omega_g} \Delta_{i,j}^{(n)} \tag{4.86}$$

Somehow, it measures the impact of inserting a new user into the system, i.e. see the performance deterioration. Hence, we try all possible combinations and choose the user-group tuple that reaches the largest value

$$(g^\star, k^\star) \leftarrow \underset{g \in \Gamma, k \in \Xi}{\operatorname{argmax}} U(\Omega_1, \ldots, \Omega_g \cup \{k\}, \ldots, \Omega_G) \tag{4.87}$$

where we denote Ξ and Γ to the set of remaining users and available groups, respectively. In addition, we remove a group from the possibilities whenever it is full, i.e. $|\Omega_g| = K/G$. This way, users with distinct covariances are grouped together and similar ones are separated efficiently, i.e. the resulting mapping reduces interference. The detailed procedure, from which we will take benefit of, is perfectly described in [32]. Nonetheless, in Section 4.2.3, a modified version will be presented, which will help understand the situation.

4.2.3 Sum Rate Optimization

Instead of concentrating on the group allocation based on covariance matrices and their asymptotic properties, we could assign users to pilots by means of other approaches with different objectives. Then, since we are mainly interested in sum rate, we could think of a method that maximizes this magnitude when distributing training sequences.

Here, two strategies to perform this task are introduced. As seen before, both rely on second-order statistics since it is the information from the channel we have got certain. That is why, we will define new metrics and utility functions based on an upper and lower bound of the SINR and sum rate. In fact, the first case will be an approximated version whereas the second will use the findings from Section 2.2.4. Besides, given the complexity of these two scenarios, the SINR will be simplified to reduce the number of computations. Finally, a greedy algorithm based on [32] is presented to perform this assignation. It is important to highlight that depending on the direction, UL or DL, a different user allocation will be obtained as the SINR varies accordingly.

4.2.3.1 Upper Bound

The first approach based on the sum rate as principal target relies on a simplified version of this measure, defined in Section 2.1. Then, in the following, by means of some approximations, we will find an upper bound for the total throughput and we will later exploit it for user allocation.

To begin with, recall the expression of the individual user rates R_k defined in (2.5). Then, it is straightforward to see that these are concave functions due to the logarithm nature. As a result, Jensen's inequality [16] can be applied and the sum rate, both for UL and DL, can be upper bounded as follows

$$R_{\text{sum}} = \sum_{k=1}^{K} \mathrm{E}[\log_2(1+\gamma_k)] \leq \sum_{k=1}^{K} \log_2(1+\mathrm{E}[\gamma_k]) = \bar{R}_{\text{sum}} \tag{4.88}$$

Note that when maximizing the upper bound, we are also allowing the real value to be higher and thus, we optimize it somehow. Furthermore, as proven in Appendix A.2, we can approximate the term $\mathrm{E}[\gamma_k]$ by means of the first-order Taylor series expansion around the mean of the instantaneous SINR

$$\mathrm{E}[\gamma_k] = \mathrm{E}\left[\frac{X_k}{Y_k}\right] \approx \frac{\mathrm{E}[X_k]}{\mathrm{E}[Y_k]} = \mathrm{E}[\tilde{\gamma}_k] \tag{4.89}$$

where X_k and Y_k represent the numerator and denominator from the ratio γ_k respectively. Note that we consider perfect channel knowledge and leave the achievable lower bound for the second approach. Therefore, the right hand side term of the equation in (4.88) results

$$\bar{R}_{\text{sum}} \approx \sum_{k=1}^{K} \log_2(1 + \mathrm{E}[\tilde{\gamma}_k]) = \sum_{k=1}^{K} \tilde{R}_k = \tilde{R}_{\text{sum}} \tag{4.90}$$

On the other hand, for the sake of simplicity, as precoder and equalizer we will employ common MF based on the channel estimates, i.e. $\boldsymbol{g}_k = \hat{\boldsymbol{h}}_k$ and $\boldsymbol{p}_k = \beta\hat{\boldsymbol{h}}_k$. Following a similar reasoning than in Section 4.1.1, it can be shown that for an average power constraint, $\beta = \sqrt{E_{\text{tr}}/\text{tr}\big(\sum_k \boldsymbol{C}_{\hat{\boldsymbol{h}}_k}\big)}$ is the resulting scaling factor with $\boldsymbol{C}_{\hat{\boldsymbol{h}}_k} \in \mathbb{C}^{M\times M}$ being the covariance matrix of $\hat{\boldsymbol{h}}_k$. Besides, a similar expression of the SINR in (2.20) and (2.21) can be formulated

$$\gamma_{k,\text{ul}} = \frac{|\hat{\boldsymbol{h}}_k^{\text{H}}\boldsymbol{h}_k|^2}{\frac{\|\hat{\boldsymbol{h}}_k\|_2^2}{\rho_{\text{ul}}} + \sum_{n\neq k} |\hat{\boldsymbol{h}}_k^{\text{H}}\boldsymbol{h}_n|^2} \tag{4.91}$$

$$\gamma_{k,\text{dl}} = \frac{|\boldsymbol{h}_k^{\text{H}}\hat{\boldsymbol{h}}_k|^2}{\frac{1}{\beta^2\rho_{\text{dl}}} + \sum_{n\neq k} |\boldsymbol{h}_k^{\text{H}}\hat{\boldsymbol{h}}_n|^2} \tag{4.92}$$

Thereby, with regard to the approximation in (4.89), we can write

$$\mathrm{E}[\tilde{\gamma}_{k,\text{ul}}] = \frac{\mathrm{E}[|\hat{\boldsymbol{h}}_k^{\text{H}}\boldsymbol{h}_k|^2]}{\frac{\mathrm{E}[\|\hat{\boldsymbol{h}}_k\|_2^2]}{\rho_{\text{ul}}} + \sum_{n\neq k} \mathrm{E}[|\hat{\boldsymbol{h}}_k^{\text{H}}\boldsymbol{h}_n|^2]} \tag{4.93}$$

$$\mathrm{E}[\tilde{\gamma}_{k,\text{dl}}] = \frac{\mathrm{E}[|\boldsymbol{h}_k^{\text{H}}\hat{\boldsymbol{h}}_k|^2]}{\frac{1}{\beta^2\rho_{\text{dl}}} + \sum_{n\neq k} \mathrm{E}[|\boldsymbol{h}_k^{\text{H}}\hat{\boldsymbol{h}}_n|^2]} \tag{4.94}$$

where it can be shown that, regardless of which channel estimate we use, the expectation of the norm in (4.93) yields $\mathrm{E}[\|\hat{\boldsymbol{h}}_k\|_2^2] = \text{tr}(\boldsymbol{C}_{\hat{\boldsymbol{h}}_k})$. Also, the set of different expectations will depend on the covariance matrices of these estimates, which can either be the LS, $\hat{\boldsymbol{h}}_k = \boldsymbol{\phi}_k$, or the LMMSE $\hat{\boldsymbol{h}}_k = \boldsymbol{\theta}_k$, already defined in Section 3.1. In particular, taking into account the pilot contaminated estimates from (3.7) and with the help of the equivalencies described in (2.31), it follows that, in the case of the UL, we have

$$\mathrm{E}[|\boldsymbol{\phi}_k^{\mathrm{H}}\boldsymbol{h}_n|^2] = \begin{cases} \mathrm{tr}(\boldsymbol{C}_{\boldsymbol{\phi}_k}\boldsymbol{C}_{\boldsymbol{h}_k}) + |\mathrm{tr}(\boldsymbol{C}_{\boldsymbol{h}_k})|^2 & \text{if} \quad n = k \\ \mathrm{tr}(\boldsymbol{C}_{\boldsymbol{\phi}_k}\boldsymbol{C}_{\boldsymbol{h}_n}) + |\mathrm{tr}(\boldsymbol{C}_{\boldsymbol{h}_n}|n \in \mathcal{I}_k)|^2 & \text{if} \quad n \neq k \end{cases} \tag{4.95}$$

or

$$\mathrm{E}[|\boldsymbol{\theta}_k^{\mathrm{H}}\boldsymbol{h}_n|^2] = \begin{cases} \mathrm{tr}(\boldsymbol{C}_{\boldsymbol{\theta}_k}\boldsymbol{C}_{\boldsymbol{h}_k}) + |\mathrm{tr}(\boldsymbol{C}_{\boldsymbol{\theta}_k})|^2 & \text{if} \quad n = k \\ \mathrm{tr}(\boldsymbol{C}_{\boldsymbol{\theta}_k}\boldsymbol{C}_{\boldsymbol{h}_n}) + |\mathrm{tr}(\boldsymbol{C}_{\boldsymbol{\theta}_n}|n \in \mathcal{I}_k)|^2 & \text{if} \quad n \neq k \end{cases} \tag{4.96}$$

Likewise, we can do the same for the DL scenario

$$\mathrm{E}[|\boldsymbol{h}_k^{\mathrm{H}}\boldsymbol{\phi}_n|^2] = \begin{cases} \mathrm{tr}(\boldsymbol{C}_{\boldsymbol{h}_k}\boldsymbol{C}_{\boldsymbol{\phi}_k}) + |\mathrm{tr}(\boldsymbol{C}_{\boldsymbol{h}_k})|^2 & \text{if} \quad k = n \\ \mathrm{tr}(\boldsymbol{C}_{\boldsymbol{h}_k}\boldsymbol{C}_{\boldsymbol{\phi}_n}) + |\mathrm{tr}(\boldsymbol{C}_{\boldsymbol{h}_k}|k \in \mathcal{I}_n)|^2 & \text{if} \quad k \neq n \end{cases} \tag{4.97}$$

and

$$\mathrm{E}[|\boldsymbol{h}_k^{\mathrm{H}}\boldsymbol{\theta}_n|^2] = \begin{cases} \mathrm{tr}(\boldsymbol{C}_{\boldsymbol{h}_k}\boldsymbol{C}_{\boldsymbol{\theta}_k}) + |\mathrm{tr}(\boldsymbol{C}_{\boldsymbol{\theta}_k})|^2 & \text{if} \quad k = n \\ \mathrm{tr}(\boldsymbol{C}_{\boldsymbol{h}_k}\boldsymbol{C}_{\boldsymbol{\theta}_n}) + |\mathrm{tr}(\boldsymbol{C}_{\boldsymbol{\theta}_k}|k \in \mathcal{I}_n)|^2 & \text{if} \quad k \neq n \end{cases} \tag{4.98}$$

where $\boldsymbol{C}_{\boldsymbol{\theta}_k} = \boldsymbol{C}_{\boldsymbol{h}_k}\boldsymbol{C}_{\boldsymbol{\phi}_k}^{-1}\boldsymbol{C}_{\boldsymbol{h}_k}$. Note that now, unlike the expression in (3.5), the matrix $\boldsymbol{C}_{\boldsymbol{\phi}_k}$ contains interfering terms we must consider

$$\boldsymbol{C}_{\boldsymbol{\phi}_k} = \boldsymbol{C}_{\boldsymbol{h}_k} + \sum_{n \in \mathcal{I}_k} \boldsymbol{C}_{\boldsymbol{h}_n} + \frac{1}{\rho_{\mathrm{tr}}}\boldsymbol{C}_{\boldsymbol{v}_k} \tag{4.99}$$

At this point, one could suggest that the utility function must be the approximated upper bound of the sum rate $\tilde{R}_{\mathrm{sum}}$, defined in (4.90). Nonetheless, here we opt for allocating users like before, progressively. Therefore, smaller metrics similar to $\Delta_{i,j}^{(n)}$ are required to determine the influence of the new assigned pilots at each stage for later, by means of the greedy algorithm, obtain a proper distribution. This way, the combinatorial problem, which is to find the mapping user-group that maximizes the aforementioned total throughput, can be solved suboptimally. As a result, we can choose the utility function to be

$$U(\Omega_1, \ldots, \Omega_G) = \sum_{g=1}^{G} \sum_{i,j \in \Omega_g} R_{i,j} \tag{4.100}$$

where $R_{i,j}$ are the new metrics employed here. Thereby, it can be foreseen that they will be based on the rates from (4.90). In our case, we use the individual magnitudes $\tilde{R}_i$ to define these terms

$$R_{i,j} = \tilde{R}_i + \tilde{R}_j \tag{4.101}$$

Note that, thanks to this decision, these measurements will be symmetric, i.e. $R_{i,j} = R_{j,i}$, and when all users are allocated, the utility function will simply become twice the sum of all user rates

$$U(\Omega_1, \ldots, \Omega_G) = \sum_{i,j} R_{i,j} = 2 \sum_{k=1}^{K} \tilde{R}_k = 2\tilde{R}_{\text{sum}} \tag{4.102}$$

Thereby, at every step of the optimization from (4.87), we will maximize a portion of the total sum rate since only combinations leading to highest throughput are kept. In the end, this solution leads to the largest $\tilde{R}_{\text{sum}}$. As we will see, the entire procedure will be summarized at the end of this section in Algorithm 3, where all phases will be collected.

Furthermore, it can be seen that this version reduces the complexity of the computations when compared to the original sum rate, since only second order moments are needed and they are indeed known. In the other case, expectations of the individual rates R_k must be computed and using Monte-Carlo simulations to do so, which implies a considerable increase of execution time and resources. Besides, if we were in the low SINR regime, we could linearize the logarithm, i.e. $\ln(x+1) \approx x$, so that the upper bound would no longer be necessary. In that scenario, both approaches would be equivalent. However, we would still require the Taylor approximation for computing the SINR expectations and get a CDI based solution. This will not be the case in massive MIMO, given the high array gains of these systems. Consequently, we stick to our proposal to efficiently perform pilot assignation.

Finally, in order to further reduce the computational complexity of the previous approach, we present a simplification of the approximated SINR given in (4.93) and (4.94). In particular, instead of consider all users different from k as interfering, we could simply employ the ones sharing the same training sequence, given that we are interested in measuring their impact when allocating pilots to avoid saturation in the large-scale regime. Then, the SINR read as

$$\mathrm{E}[\tilde{\gamma}_{k,\mathrm{ul}}] \approx \frac{\mathrm{E}[|\hat{\boldsymbol{h}}_k^{\mathrm{H}}\boldsymbol{h}_k|^2]}{\frac{1}{\rho_{\mathrm{ul}}} + \sum_{n\in\mathcal{I}_k}\mathrm{E}[|\hat{\boldsymbol{h}}_k^{\mathrm{H}}\boldsymbol{h}_n|^2]} \tag{4.103}$$

$$\mathrm{E}[\tilde{\gamma}_{k,\mathrm{dl}}] \approx \frac{\mathrm{E}[|\boldsymbol{h}_k^{\mathrm{H}}\hat{\boldsymbol{h}}_k|^2]}{\frac{1}{\beta^2\rho_{\mathrm{dl}}} + \sum_{n\in\mathcal{I}_k}\mathrm{E}[|\boldsymbol{h}_k^{\mathrm{H}}\hat{\boldsymbol{h}}_n|^2]} \tag{4.104}$$

where we can simply substitute the determinations from (4.95)(4.97) or (4.96)(4.98) to get the expression w.r.t. each estimate respectively.

4.2.3.2 Lower Bound

A similar but more rigorous approach is the one that uses the lower bound on the achievable rate described in Section 2.2.4. The only things changing are the expressions of the SINR and resulting user rates, since the whole procedure and the previous reasoning still hold. Then, instead of employing an upper bound we can use the inequality given in (2.25)

$$R_{\mathrm{sum}} \geq \sum_{k=1}^{K}\log_2(1+\underline{\gamma}_k^{\mathrm{CDI}}) = \sum_{k=1}^{K}\underline{R}_k^{\mathrm{CDI}} = \underline{R}_{\mathrm{sum}}^{\mathrm{CDI}} \tag{4.105}$$

This makes more sense than the first strategy since maximizing the lower bound always implies an increase of the original magnitude. As before, we get rid of the expectations and only second-order statistics are required to find the solution. In addition, considering the previous MF filters are again used as processing technique, the expressions for both SINR are already derived and can be found in (2.32) and (2.33). However, we must include the errors due to channel estimation and specially, the ones coming from effect of pilot contamination Therefore, the SINR read as follows

$$\underline{\gamma}_{k,\mathrm{ul}}^{\mathrm{CDI}} = \frac{|\mathrm{E}[\hat{\boldsymbol{h}}_k^{\mathrm{H}}\boldsymbol{h}_k]|^2}{\frac{\mathrm{E}[\|\hat{\boldsymbol{h}}_k\|_2^2]}{\rho_{\mathrm{ul}}} + \mathrm{var}\{\hat{\boldsymbol{h}}_k^{\mathrm{H}}\boldsymbol{h}_k\} + \sum_{n\neq k}\mathrm{E}[|\hat{\boldsymbol{h}}_k^{\mathrm{H}}\boldsymbol{h}_n|^2]} \tag{4.106}$$

$$\underline{\gamma}_{k,\mathrm{dl}}^{\mathrm{CDI}} = \frac{|\mathrm{E}[\boldsymbol{h}_k^{\mathrm{H}}\hat{\boldsymbol{h}}_k]|^2}{\frac{1}{\beta^2\rho_{\mathrm{dl}}} + \mathrm{var}\{\boldsymbol{h}_k^{\mathrm{H}}\hat{\boldsymbol{h}}_k\} + \sum_{n\neq k}\mathrm{E}[|\boldsymbol{h}_k^{\mathrm{H}}\hat{\boldsymbol{h}}_n|^2]} \tag{4.107}$$

where we are only adding an extra term in the denominator w.r.t. the expressions in (4.93) and (4.94) respectively: the variance. Then, we just need to find this value to complete our approach. In particular, let us first write

$$\text{var}\{\hat{\boldsymbol{h}}_k^{\text{H}}\boldsymbol{h}_k\} = \text{E}[|\hat{\boldsymbol{h}}_k^{\text{H}}\boldsymbol{h}_k|^2] - \text{E}[\hat{\boldsymbol{h}}_k^{\text{H}}\boldsymbol{h}_k]^2 \tag{4.108}$$

$$\text{var}\{\boldsymbol{h}_k^{\text{H}}\hat{\boldsymbol{h}}_k\} = \text{E}[|\boldsymbol{h}_k^{\text{H}}\hat{\boldsymbol{h}}_k|^2] - \text{E}[\boldsymbol{h}_k^{\text{H}}\hat{\boldsymbol{h}}_k]^2 \tag{4.109}$$

As we can see, the square mean is the term remaining unknown. In both links, this magnitude results the same for the LS and LMMSE estimates

$$\text{E}[\boldsymbol{\phi}_k^{\text{H}}\boldsymbol{h}_k] = \text{tr}(\boldsymbol{C}_{\boldsymbol{h}_k}) = \text{E}[\boldsymbol{h}_k^{\text{H}}\boldsymbol{\phi}_k] \tag{4.110}$$

$$\text{E}[\boldsymbol{\theta}_k^{\text{H}}\boldsymbol{h}_k] = \text{tr}(\boldsymbol{C}_{\boldsymbol{\theta}_k}) = \text{E}[\boldsymbol{h}_k^{\text{H}}\boldsymbol{\theta}_k] \tag{4.111}$$

Furthermore, given the expressions from (4.95),(4.97),(4.96) and (4.98), it can be easily inferred that the variances in (4.108) and (4.109) will result the same in both cases, UL and DL respectively

$$\text{var}\{\boldsymbol{\phi}_k^{\text{H}}\boldsymbol{h}_k\} = \text{tr}(\boldsymbol{C}_{\boldsymbol{\phi}_k}\boldsymbol{C}_{\boldsymbol{h}_k}) = \text{var}\{\boldsymbol{h}_k^{\text{H}}\boldsymbol{\phi}_k\} \tag{4.112}$$

$$\text{var}\{\boldsymbol{\theta}_k^{\text{H}}\boldsymbol{h}_k\} = \text{tr}(\boldsymbol{C}_{\boldsymbol{\theta}_k}\boldsymbol{C}_{\boldsymbol{h}_k}) = \text{var}\{\boldsymbol{h}_k^{\text{H}}\boldsymbol{\theta}_k\} \tag{4.113}$$

Hence, in this approach we are only adding an extra term w.r.t. the previous upper bound. This way, all users will experience a decrease of their SINR in every scenario. Nonetheless, as we will comment later in Section 4.2.4 and Chapter 5, Section 5.3.2 the user allocation returned here will not be much different from the previous one. This is due to covariances having close magnitudes, which implies similar deterioration is observed in all ratios.

Finally, we define the utility function as before, i.e. expression in (4.100), but now the associated metrics change. Instead of employing the previous individual user rates $\tilde{R}_i$, we use the ones defined in (4.105) to compute the small sum rate, i.e. $R_{i,j} = \underline{R}_i^{\text{CDI}} + \underline{R}_j^{\text{CDI}}$. As a result, the same discussion applies here with regard to the optimization problem and the greedy algorithm. In addition, we can also use a simplified version of the lower bound on the achievable SINR in (4.106) and (4.107). Then, we will restrict the interference to come from the same group only, i.e. use $n \in \mathcal{I}_k$ in the summation.

4.2.3.3 Greedy Algorithm

In order to allocate users, one can always use a naive approach and try all possibilities. Then, we would choose the one leading to the optimal utility function. However, this becomes highly inefficient and quickly unfeasible for increasing number of users K. That is why here we present an efficient way, yet sub-optimal, to allocate users that maximizes our target. It consists on a greedy approach, formed by several steps, which will be commented below. In fact, it is similar to the one described in Section 4.2.2 and that is based on [32].

Thereby, as already mentioned, we will fill up progressively all groups, optimizing the sum of the intermediate rates until reaching $\tilde{R}_{\text{sum}}$. Initially, we assign one user to each group so that none of them are empty for the second stage. To do so, we first select the pair leading to the smallest sum rate metric $R_{i,j}$ and separate them into different groups. Note that in both bounds, $R_{i,j}$ reflects the impact and sensitivity of the rates for such allocation. Then, for the other groups, we choose the user with the lowest sum of metrics w.r.t. the assignation performed until then. Once this stage is finished, we start by greedily allocating the remaining users. Then, we employ the previous utility functions and look for the combination that maximizes them. In particular, the same strategy as before is used, i.e. add one user to a certain group and compute the resulting function U. This is necessary to see how users affect each other and be able to separate them accordingly. Besides, whenever a group is full, it is removed. Consequently, we end up with a proper user allocation that maximizes a version of the sum rate. Such procedure is given in Algorithm 3.

Alternatively, instead of maximizing the sum rate, we could opt for an approach where the metric is defined as the product of rates, i.e. $R_{i,j} = \check{R}_i \check{R}_j$ with $\check{R}_i$ equal to $\tilde{R}_i$ or $\underline{R}_i^{\text{CDI}}$. In contrast to the previous arithmetic strategies, this measurement somehow represents the geometric mean. Thus, for this magnitude to be large, both users must have a good (high) similar rate and not only one of them. This way, a fairer distribution could be achieved, following the line of a rate balancing solution. Moreover, the procedure presented above and shown in Algorithm 3 would still be valid. Notwithstanding, it has been observed, with numerical experiments (not included in this work), that this approach does not provide a really good performance. In fact, the resulting data rates are lower and the objective, which would be to reduce the variance, is not satisfactorily achieved. Consequently, we will skip it in our investigation and concentrate on the sum rate as principal goal.

Algorithm 3 Greedy User Allocation

Require: Set of users $\Xi = \{1, \dots, K\}$ and groups $\Gamma = \{1, \dots, G\}$

First Assignation

$$(k_1^\star, k_2^\star) \leftarrow \underset{k_1,k_2 \in \Xi, k_1 \neq k_2}{\operatorname{argmin}} R_{k_1 k_2} \quad \text{s.t.} : k_1, k_2 \in \Omega_g{}^1$$
$$\Omega_1 \leftarrow \{k_1^\star\} \quad \Omega_2 \leftarrow \{k_2^\star\} \quad \Xi \leftarrow \Xi \setminus \{k_1^\star, k_2^\star\}$$

for $g = 3 : G$ **do**

$$k_g^\star \leftarrow \underset{k_g \in \Xi}{\operatorname{argmin}} \sum_{i=1}^{g-1} R_{k_i^\star k_g} \quad \text{s.t.} : k_i^\star, k_g \in \Omega_g$$
$$\Omega_g \leftarrow \{k_g^\star\} \quad \Xi \leftarrow \Xi \setminus \{k_g^\star\}$$

Remaining Users

while $\Theta \neq \varnothing$ **do**

$$(g^\star, k^\star) \leftarrow \underset{g \in \Gamma, k \in \Xi}{\operatorname{argmax}} U(\Omega_1, \dots, \Omega_g \cup \{k\}, \dots, \Omega_G)$$
$$\Omega_{g^\star} \leftarrow \Omega_{g^\star} \cup \{k^\star\} \quad \Xi \leftarrow \Xi \setminus \{k^\star\}$$

if $|\Omega_{g^\star}| = L$ **then**

$$\Gamma \leftarrow \Gamma \setminus \{g^\star\}$$

Furthermore, note that since these solutions also rely on CDI knowledge, the DFT approximation helps to reduce complexity, as discussed before. In this case, it simplifies the calculus of the SINR and sum rate metrics.

4.2.4 Results

In this last part of the section, a review and comparison of the previous techniques, covariance and sum rates, is given. Later, in Chapter 5, Section 5.3, the following statements are corroborated. As expected, both approaches do not deliver the same mapping. This is due to the fact that one relies on the correlation between users and their covariance structure whereas the other are based simply on the maximization of the sum rate. In fact, the original purpose of the second was to justify the allocation obtained with the first. Thereby, we

[1] As long as both users are assigned to the same group, it does no matter which, 1 or 2

would be able to assure its performance was optimal. Nevertheless, let us first start by analyzing both approaches separately and then compare them.

On the one hand, when focusing on the covariance based method, it can be seen that the best metrics are the first and the fifth, since the entire matrix information is included. Then, orthogonality can be easily studied and consequently, both of them become a reliable representative of the channel properties and are suitable for user allocation. This is clearly revealed in the simulations part, where it results with $\Delta_{i,j}^{(5)}$ are slightly better than in the case of using $\Delta_{i,j}^{(1)}$. The main reason behind is that a different assignation is obtained in each case. Hence, we will show only those of the fifth in Section 5.3.1.

On the other hand, regarding the sum rate optimization approach, very similar results are obtained with both, lower and upper bounds. As mentioned before, the only aspect changing between them is the extra variance term in the denominator. Thereby, given the channel model used here (see Section 2.3), the variation of the SINR results barely relevant for the distribution of groups. Note that we are considering the simplified version of these ratios, since the reduction of complexity is substantial. Also, it has been observed that, when compared to the original complete solution, performance is not compromised.

Finally, when comparing both procedures, two main aspects must be pointed out. In particular, sum rate approaches are preferable when looking at the throughput. Also, the possibility of using different allocations for the UL and DL has to be highlighted, since the other method is not capable to offer it. On the contrary, the covariance matrix based solution represents a significant lower complexity enhancement. Hence, since the rate improvement is not very considerable, we decide for the user correlation strategy as best option.

4.3 User Projection

The last strategy introduced in this thesis to cope with pilot contamination is the so-called user projection. It consists on applying a certain transformation to the channel estimates to remove this interference. Somehow, it can be understood as a partial ZF to fight against this effect directly. To this end, two perspectives will be presented and later compared. They are based on the *eigenvalue decomposition* (EVD) and *rank-revealing* QR (RRQR) decomposition [41] respectively. In fact, both exploit the channel model and the aforementioned properties of the covariance matrices. Thereby, as we will see later, these projections can only be used and work under certain circumstances.

More precisely, the idea here is to mitigate undesired directions or, in our case, even cancel them. That is why a strong emphasis must be done in this aspect as inadequate decisions can become critical. For instance, if most of the directions are eliminated, few place for communication would be left, even if the remaining portions are interference-free. On the contrary, when almost all directions are kept, no improvement is achieved. This will be of special interest in the second approach and will be reflected in the matrix rank. We will select those directions that represent the null space of the covariance, which existence is a necessary condition for this proposal to be useful. In other words, we require these matrices to be rank deficient, also in the EVD scenario. Besides, note that we will focus on the LS estimate but the same analysis still holds for the LMMSE. Despite that, no significant changes are be observed in that case and that is why we avoid the corresponding derivation.

4.3.1 Eigenvalue Decomposition

The first approach of user projection attempts to remove the interference coming from pilot contamination, clearly evident in the LS estimate (see Section 3.2.1), by means of the EVD of the channel covariance matrix $\boldsymbol{C}_{\boldsymbol{h}_k} = \boldsymbol{U}_k \boldsymbol{\Lambda}_k \boldsymbol{U}_k^{\mathrm{H}}$ with eigenvector basis $\boldsymbol{U}_k = [\boldsymbol{u}_{k,1}, \ldots, \boldsymbol{u}_{k,M}]$.

To begin with, we define a certain projection matrix $\boldsymbol{\mathcal{P}}_k \in \mathbb{C}^{M \times M}$, which will be constructed with the set of eigenvectors exclusive to one user. In particular, as we will argue later, we select those directions satisfying $\boldsymbol{u}_{k,m}^{\mathrm{H}} \boldsymbol{C}_{\boldsymbol{h}_n}^{1/2} = \boldsymbol{0}$ $\forall n \in \mathcal{I}_k$ given that $\boldsymbol{C}_{\boldsymbol{h}_k}^{\mathrm{H}} \boldsymbol{C}_{\boldsymbol{h}_n} \to \boldsymbol{0}$ when $n \neq k$ for $M \to \infty$. However, this requirement can only be accomplished in the asymptotic (ideal) case, where covariance matrices become truly orthogonal.

Therefore, in real systems, this condition results too strong and needs to be relaxed. In our case, we first opted for using the following feasible one

$$\boldsymbol{u}_{k,m}^{\mathrm{H}} \boldsymbol{C}_{\boldsymbol{h}_k}^{1/2} \gg \boldsymbol{u}_{k,m}^{\mathrm{H}} \boldsymbol{C}_{\boldsymbol{h}_n}^{1/2} \quad \forall n \in \mathcal{I}_k \tag{4.114}$$

This allows more directions to be chosen, all of which form the basis of a new subspace that we denote as $\tilde{\boldsymbol{U}}_k$. For a clearer notation, let $\mathcal{U}_k$ be the set of index associated to these eigenvectors of the k-th user, so that we can write $\tilde{\boldsymbol{U}}_k = [\boldsymbol{u}_{k,1}, \ldots, \boldsymbol{u}_{k,|\mathcal{U}_k|}] \in \mathbb{C}^{M \times |\mathcal{U}_k|}$ for $\boldsymbol{u}_{k,i}$ with $i \in \mathcal{U}_k$. Then, we will project the LS channel estimates into this subspace by means of the projection matrix. To this end, we set $\boldsymbol{\mathcal{P}}_k = \tilde{\boldsymbol{U}}_k \tilde{\boldsymbol{U}}_k^{\mathrm{H}}$, which also ensures all required properties of these operators are satisfied [41]. As a result, with the definition

from (3.7), we can formulate the transformation as

$$\boldsymbol{\phi}'_k = \boldsymbol{\mathcal{P}}_k \boldsymbol{\phi}_k = \boldsymbol{\mathcal{P}}_k \boldsymbol{h}_k + \sum_{n \in \mathcal{I}_k} \boldsymbol{\mathcal{P}}_k \boldsymbol{h}_n + \frac{1}{\sqrt{\rho_{\text{tr}}}} \boldsymbol{n}'_k \tag{4.115}$$

where $\boldsymbol{\phi}'_k$ and $\boldsymbol{n}'_k = \boldsymbol{\mathcal{P}}_k \boldsymbol{n}_k$ are the transformed versions of the LS estimate and noise, respectively. That being said, the justification of the approach can be at this point understood, and it is given in the following.

Recall first that channels contain their covariance matrices since they can be expressed as $\boldsymbol{h}_k = \boldsymbol{C}_{\boldsymbol{h}_k}^{1/2} \boldsymbol{h}'_k$ (see Section 2.2.2). Then, instead of using the condition in (4.114), we use a more restrictive one. In particular, we will employ as basis for our projection the eigenvectors of $\boldsymbol{C}_{\boldsymbol{h}_k}^{1/2}$ that satisfy

$$\boldsymbol{u}_{k,m}^{\text{H}} \boldsymbol{C}_{\boldsymbol{h}_k}^{1/2} \gg \sum_{n \in \mathcal{I}_k} \boldsymbol{u}_{k,m}^{\text{H}} \boldsymbol{C}_{\boldsymbol{h}_n}^{1/2} \tag{4.116}$$

which has sense only when matrices are rank deficient. That is why it is a requirement in this approach. Note also that $\boldsymbol{u}_{k,m}$ are the same for $\boldsymbol{C}_{\boldsymbol{h}_k}$, since only eigenvalues change. Then, with (4.116) the subspace $\tilde{\boldsymbol{U}}_k$ will be modified and consequently, after applying the transformation $\boldsymbol{\mathcal{P}}_k$, directions where our desired signal is stronger than the interference will be prioritized

$$\boldsymbol{\mathcal{P}}_k \boldsymbol{h}_k = \boldsymbol{\mathcal{P}}_k \boldsymbol{C}_{\boldsymbol{h}_k}^{1/2} \boldsymbol{h}'_k \gg \sum_{n} \boldsymbol{\mathcal{P}}_k \boldsymbol{C}_{\boldsymbol{h}_n}^{1/2} \boldsymbol{h}'_n = \sum_{n \in \mathcal{I}_k} \boldsymbol{\mathcal{P}}_k \boldsymbol{h}_n \tag{4.117}$$

This way, the effect of pilot contamination can be highly mitigated. In fact, an easier explanation arises when working with diagonal covariance matrices, which result from the DFT approximation. It is important to realize that, since this simplification is used throughout the project, we need to apply the transformation after so that conditions (Toeplitz form) from Section 2.3.2 are respected. Then, eigenvectors will be canonical unitary vectors, i.e. $\boldsymbol{U}_k = \mathbf{I}_M \, \forall k$. Hence, given its construction, after choosing the suitable basis $\tilde{\boldsymbol{U}}_k$, the projection matrix $\boldsymbol{\mathcal{P}}_k$ will be a diagonal matrix with ones in the desired directions. Thereby, zeros are set in the elements where interference is larger so that these portions are completely removed and not only mitigated. For instance, if we end up with $\mathcal{U}_k = \{1, 3\}$, only the first and third directions will be preserved, i.e. $\boldsymbol{\mathcal{P}}_k = \text{diag}(1, 0, 1, 0, \ldots, 0)$. In addition, another possibility for the selection criterion could be to use those directions where the power of the total projected

interference is (also) smaller than that of the transformed noise.

Finally, we need to find a measurement to determine which eigenvectors will be selected according to (4.116). A simple way to do it is to use the square norm of the product between eigenvector and covariance matrix, which measures the power of the resulting projected signals

$$\|\boldsymbol{u}_{k,m}^{\mathrm{H}}\boldsymbol{C}_{\boldsymbol{h}_k}^{1/2}\|_2^2 = \boldsymbol{u}_{k,m}^{\mathrm{H}}\boldsymbol{C}_{\boldsymbol{h}_k}\boldsymbol{u}_{k,m} \tag{4.118}$$

Overall, our goal is to design a filter, exclusive for each user, that ensures no overlapping between training signals takes place. This way, pilot contaminated interference can be reduced, i.e. $\sum_{n\in\mathcal{I}_k}\boldsymbol{\mathcal{P}}_k\boldsymbol{h}_n \to \mathbf{0}$. Nevertheless, as we will discuss later, we must take into account that the number of available directions also diminishes and a certain balance must be established. The whole process is then summarized in Algorithm 4.

Algorithm 4 EVD Projection

Require: Set of empty matrices $\boldsymbol{E}_k$, with $k = \{1, \ldots, K\}$

for $k = 1 : K$ **do**

for $m = 1 : M$ **do**

if $\|\boldsymbol{u}_{k,m}^{\mathrm{H}}\boldsymbol{C}_{\boldsymbol{h}_k}^{1/2}\|_2^2 \gg \sum_{k'\in\mathcal{I}_k}\|\boldsymbol{u}_{k,m}^{\mathrm{H}}\boldsymbol{C}_{\boldsymbol{h}_{k'}}^{1/2}\|_2^2$ **then**

$\boldsymbol{E}_k \leftarrow \begin{bmatrix}\boldsymbol{E}_k & \boldsymbol{e}_m\end{bmatrix}$

$\boldsymbol{P}_k \leftarrow \boldsymbol{U}_k\boldsymbol{E}_k\boldsymbol{E}_k^{\mathrm{H}}\boldsymbol{U}_k^{\mathrm{H}} = \tilde{\boldsymbol{U}}_k\tilde{\boldsymbol{U}}_k^{\mathrm{H}}$

Furthermore, note that, to be consistent, covariances matrices of the LS estimates must be transformed too, i.e. $\boldsymbol{C}_{\boldsymbol{\phi}_k'} = \boldsymbol{\mathcal{P}}_k\boldsymbol{C}_{\boldsymbol{\phi}_k}\boldsymbol{\mathcal{P}}_k^{\mathrm{H}}$.

4.3.2 Rank-Revealing QR Decomposition

The other alternative we present here to design the user projection approach is based on the RRQR decomposition and it becomes highly useful in our scenario assuming covariance matrices become rank deficient. Therefore, we will start by introducing this particular concept. Later, the relation to our application will be pointed out with the construction of the linear transformation $\boldsymbol{\mathcal{P}}_k$.

Thereby, let us first, given a certain covariance matrix $\boldsymbol{C}_{\boldsymbol{h}_k}$, formulate its RRQR decomposition as follows

$$\boldsymbol{C}_{\boldsymbol{h}_k}\boldsymbol{\Pi}_k = \boldsymbol{Q}_k\boldsymbol{R}_k \tag{4.119}$$

where $\boldsymbol{\Pi}_k \in \mathbb{R}^{M\times M}$ corresponds to the matrix of permutations we will use later and $\boldsymbol{Q}_k, \boldsymbol{R}_k \in \mathbb{C}^{M\times M}$ are defined as

$$\boldsymbol{Q}_k = \begin{bmatrix} \boldsymbol{Q}_{k,11} & \boldsymbol{Q}_{k,12} \\ \boldsymbol{Q}_{k,21} & \boldsymbol{Q}_{k,22} \end{bmatrix} \quad \text{and} \quad \boldsymbol{R}_k = \begin{bmatrix} \boldsymbol{R}_{k,11} & \boldsymbol{R}_{k,12} \\ \mathbf{0} & \boldsymbol{R}_{k,22} \end{bmatrix} \tag{4.120}$$

Note that $\boldsymbol{R}_k$ is an upper triangular matrix and, in the case of the covariance matrices not being full rank, we have also that $\boldsymbol{R}_{k,22} = \mathbf{0}$. Then, considering that the submatrices from $\boldsymbol{Q}_k$ and $\boldsymbol{R}_k$ have all the same size, the expression in (4.120) is simplified. As a result, a reduced form can be derived

$$\boldsymbol{C}_{\boldsymbol{h}_k}\boldsymbol{\Pi}_k = \begin{bmatrix} \boldsymbol{Q}_{k,11} \\ \boldsymbol{Q}_{k,21} \end{bmatrix} [\boldsymbol{R}_{k,11}, \boldsymbol{R}_{k,12}] = \boldsymbol{Q}_{k,\text{red}}\boldsymbol{R}_{k,\text{red}} \tag{4.121}$$

where $\boldsymbol{Q}_{k,\text{red}} \in \mathbb{C}^{M\times r_k}$, $\boldsymbol{R}_{k,\text{red}} \in \mathbb{C}^{r_k\times M}$ and $r_k = \text{rank}(\boldsymbol{C}_{\boldsymbol{h}_k}) \leq M$. At this point, we need a proper approach to find this decomposition. In our case, we opted for the Householder method with column pivoting [41] described in Algorithm 5. It consists on computing the ordinary QR factorization but permuting the columns of $\boldsymbol{R}_k$ at each step so that they are sorted in descending order w.r.t. the L2-norm. This is where the matrix $\boldsymbol{\Pi}_k$ comes into play, as it reflects these changes. In addition, regarding the rest of the procedure, it is widely described e.g. in [41]. Finally, once the decomposition is found, we remove the zero rows of $\boldsymbol{R}_k$ and the corresponding columns of $\boldsymbol{Q}_k$ to determine the reduced matrix expressions. This is done when truncating these matrices with the rank r_k, which computation will be discussed later.

Note also that, with the process below, we are computing the Hermitian of the $\boldsymbol{Q}_k$ given that with this method we get $\boldsymbol{R}_k$ and not $\boldsymbol{C}_{\boldsymbol{h}_k}$

$$\boldsymbol{Q}_k\boldsymbol{C}_{\boldsymbol{h}_k}\boldsymbol{\Pi}_k = \boldsymbol{R}_k \tag{4.122}$$

Then, it can be seen that the Q and permutation matrices are sub-unitary and unitary respectively, i.e. $\boldsymbol{Q}_k^{\text{H}}\boldsymbol{Q}_k = \mathbf{I}$ and $\boldsymbol{\Pi}_k\boldsymbol{\Pi}_k^{\text{H}} = \boldsymbol{\Pi}_k^{\text{H}}\boldsymbol{\Pi}_k = \mathbf{I}$.

$$\boldsymbol{C}_{\boldsymbol{h}_k}\boldsymbol{\Pi}_k = \boldsymbol{Q}_k^{\text{H}}\boldsymbol{R}_k \tag{4.123}$$

or equivalently

$$\boldsymbol{C}_{\boldsymbol{h}_k} = \boldsymbol{Q}_k^{\text{H}}\boldsymbol{R}_k\boldsymbol{\Pi}_k^{\text{H}} \tag{4.124}$$

Algorithm 5 Householder QR decomposition with column pivoting

Require: Covariance matrices $\boldsymbol{C}_{\boldsymbol{h}_k}$, with $k = \{1, \dots, K\}$

initialize

$\boldsymbol{Q}_k \leftarrow \mathbf{I}$, $\boldsymbol{R}_k \leftarrow \boldsymbol{C}_{\boldsymbol{h}_k}$ and $\boldsymbol{\Pi}_k \leftarrow \mathbf{I}\ \forall k$

for $k = 1 : K$ **do**

$r_k = \text{rank}(\boldsymbol{C}_{\boldsymbol{h}_k})$

for $m = 1 : M$ **do**

$[\boldsymbol{n}]_j = \sqrt{\sum_{i=m}^{M} |[\boldsymbol{R}_k]_{i,j}|^2}\ \forall j \in [m, M]$

$m^\star = \underset{j \in [m,M]}{\text{argmax}}\, \boldsymbol{n}$

$[\boldsymbol{R}_k]_{1:M,[m,m^\star]} \leftarrow [\boldsymbol{R}_k]_{1:M,[m^\star,m]}$

$\boldsymbol{\pi} = \mathbf{I}$

$[\boldsymbol{\pi}]_{1:M,[m,m^\star]} \leftarrow [\boldsymbol{\pi}]_{1:M,[m^\star,m]}$

$\boldsymbol{\Pi}_k \leftarrow \boldsymbol{\Pi}_k \boldsymbol{\pi}$

$\boldsymbol{u} = \|[\boldsymbol{R}_k]_{m:M,m}\|_2 \boldsymbol{e}_1 - [\boldsymbol{R}_k]_{m:M,m}$

$\boldsymbol{H} = \mathbf{I} - \frac{2}{\|\boldsymbol{u}\|_2^2} \boldsymbol{u}\boldsymbol{u}^{\text{H}}$

$\boldsymbol{R}_{m:M,m:M} \leftarrow \boldsymbol{H}\boldsymbol{R}_{m:M,m:M}$

$\boldsymbol{Q}_k \leftarrow \boldsymbol{H}\boldsymbol{Q}_k$

$\boldsymbol{Q}_k \leftarrow \boldsymbol{Q}_k^{\text{H}}$

$\boldsymbol{Q}_{k,\text{red}} = [\boldsymbol{Q}_k]_{1:M,1:r_k}$

We are interested in the reduced form of this last Q-matrix, which from now on we will call $\boldsymbol{Q}_{k,\text{red}}$. Note that we omit the Hermitian operator for the ease of notation but it should be included in the actual calculus. With this, we can now construct the projection matrix, procedure similar to the one studied in Section 4.1.3. In particular, for each user we define a matrix $\tilde{\boldsymbol{Q}}_k$ that includes all the reduced Q-matrices of the interfering ones. As before, we we focus exclusively on those sharing the same pilots. Therefore, like in (4.60), we will concatenate just this set of matrices to obtain the aforementioned magnitude

$$\tilde{\boldsymbol{Q}}_k = [\boldsymbol{Q}_{n_1,\text{red}}, \dots, \boldsymbol{Q}_{n_L,\text{red}}] \quad \forall n_i \in \mathcal{I}_k \quad L = |\mathcal{I}_k| \tag{4.125}$$

Finally, we will build the operator $\boldsymbol{\mathcal{P}}_k$ so that it projects the LS channel estimate into the orthogonal complement of the previous matrix. Hence, the resulting projection yields

$$\boldsymbol{\mathcal{P}}_k = \mathbf{I} - \tilde{\boldsymbol{Q}}_k(\tilde{\boldsymbol{Q}}_k^{\mathrm{H}}\tilde{\boldsymbol{Q}}_k)^{-1}\tilde{\boldsymbol{Q}}_k^{\mathrm{H}} \tag{4.126}$$

which again, only works when the matrices $\boldsymbol{C}_{\boldsymbol{h}_k}$ are rank deficient. Otherwise, we would have $\boldsymbol{Q}_{k,\text{red}} = \boldsymbol{Q}_k$ and thus, we would end with $\boldsymbol{\mathcal{P}}_k = \mathbf{0}$ so that no data transfer would be possible. In addition, following the discussion in Section 4.3.1, for this approach to have a physical sense we need to compute the decomposition w.r.t. the square root of the covariances, i.e. $\boldsymbol{C}_{\boldsymbol{h}_k}^{1/2}$. Besides, we will restrict all matrices included in $\tilde{\boldsymbol{Q}}_k$ to be rank deficient to eliminate all the interference and not just the part coming only from some users in the same group. Also, it can be inferred that if this matrix results in a not reduced form eventually, we would need to perform its RRQR decomposition and use the resulting Q-matrix as the new $\tilde{\boldsymbol{Q}}_k$ to obtain $\boldsymbol{\mathcal{P}}_k$ in (4.126). Also, to avoid it to become full rank, only the first directions of each interfering user should be kept, i.e. we will truncate at lower values than r_k. However, this is beyond the scope of this project as we consider only a single one is contaminating.

On the other hand, it can observed that the rank plays a transcendental role in the whole analysis. In particular, it determines the number of directions we are going to strengthen or, equivalently, filter out. Then, given that the tools used to compute this parameter, MATLAB in our case, are inaccurate, we need to establish some method to obtain this value properly. A heuristic approach would be to compare the magnitude of the eigenvalues and set to zero those below a certain arbitrary threshold ν. However, we go a step further and try to find a strategy that adapts the result to the SINR experienced. For instance, r_k must be small in the low regime since there the interference is meaningless and all possible directions must be used. On the contrary, it must be large if the amount of contamination in the same group is comparable, equal or larger, to that of the noise in order to discard more directions and avoid interference. Note that when referring to the rank of our desired user, this criterion should be applied conversely: large with strong noise and low when interference predominates.

In our case, we will also rely on a threshold υ to find the rank r_k and determine the null eigenvalues. Notwithstanding, the method we will present takes into account the different SINR scenarios. Then, we will first compute a certain threshold ν_k for each user and average them to obtain ν. In particular, we propose the following expression for the individual magnitudes

$$\nu_k = \left|\frac{\lambda_{k,1}}{\lambda_{k,\upsilon}}\right| \tag{4.127}$$

where $\lambda_{k,m}$ is the m-th eigenvalue of the covariance matrix of user k and the index υ is designed such that noise and interference are contemplated while finding the threshold. Then, defining $\boldsymbol{\lambda}_k = [\lambda_{k,1}, \ldots, \lambda_{k,M}]^{\mathrm{T}}$ as the vector of eigenvalues sorted in descending order and taking into account the expression of the LS estimate defined in (3.7), an adequate option comes from the vector

$$\boldsymbol{\upsilon} = \begin{cases} \arg\big(\rho_{\text{tr}}\boldsymbol{\lambda}_k < 1\big) & \text{if} \quad \sum_{n\in\mathcal{I}_k} \mathbf{1}^T\boldsymbol{\lambda}_n < K/\rho_{\text{tr}} \\ M - \arg\big(\boldsymbol{\lambda}_k < \sum_{n\in\mathcal{I}_k} \boldsymbol{\lambda}_n\big) & \text{otherwise} \end{cases} \tag{4.128}$$

from which we take the first element, i.e. $\upsilon = \boldsymbol{\upsilon}\{1\}$. This way, we compare the power of the noise and that of the interference w.r.t. the k-th user (contamination of the desired one indeed), both available at the BS since SNR and CDI knowledge are assumed. Note that they refer to the signals from the training phase and thus, we use ρ_{tr} and $n \in \mathcal{I}_k$. Finally, the threshold ν reads as

$$\nu = \frac{1}{K}\sum_{k=1}^{K} \nu_k \tag{4.129}$$

and the resulting rank is then given by

$$r_k = \underset{m\in\{1,M\}}{\arg}\left(\left|\frac{\boldsymbol{\lambda}_k}{\lambda_{k,1}}\right| < \frac{1}{\nu}\right) - 1 \tag{4.130}$$

Overall, the definition of the parameter υ relies on the pilot contamination effect and represents a critical step in this approach. This makes us very sensitive to changes in the environment. In turn, the EVD based method also benefits from this rank computations but it results more robust against possible SINR variations given that no truncation is performed. However, there we rely on the main user itself whereas here we compute the rank of the interfering ones, for later find the orthogonal complement. Therefore, since we want the opposite behavior, instead of the index obtained from (4.128) we have $M - \upsilon$. Note that in that scenario, r_k is only used to determine whether we can apply the projection or not; it does not really influence the directions employed.

Furthermore, whenever the DFT approximation is applied, the covariance matrices will become diagonal and so will do the corresponding Q and R matrices. This simplifies considerably the number of operations involved in the entire procedure and, as before, it will be the scenario studied here.

4.3.3 Results

Here the two approaches for user projection will be reviewed and compared qualitatively. Numerical results are reserved to Chapter 5, Section 5.4. As we will see, both strategies result in a system performance enhancement as data rates are increased and get closer to the pilot contamination free case.

On the one hand, in the strategy relying on the EVD, a proper analysis is performed since we focus exactly on the signals, and their power, relevant for the pilot contamination scenario. In fact, only those directions where the desired user is stronger are kept. As a result, it gives a better throughput than the other approach. The main problem of the RRQR decomposition based method is its sensitivity towards the rank threshold ν, which determines the directions employed and that are somehow similar to the other preferred ones. However, there is still a gap between both. Then, to achieve higher results, we could adjust this parameter correctly or even choose a more optimal perspective.

On the other hand, regarding efficiency, the computational cost of the EVD is larger than that of the RRQR [41]. Nevertheless, when more than two users share pilots, the second strategy quickly becomes disadvantageous since $|L| > 1$ decompositions must be computed in front of the single one employed in the first case. Additionally, even though it is used in both cases, the rank and threshold must be found multiple times, fact that increases complexity of the two procedures significantly.

In other words, relying on the covariance matrices of the interfering users instead of the main one might be not the best approach in terms of both, throughput and resources. That is why we would choose the first option for the design of a practical system. As already mentioned, this insight will be also corroborated in the simulations chapter.

Chapter 5

Simulations

In the previous chapter, we have presented the set of approaches used in this project to reduce the interference coming from pilot contamination. A qualitative analysis was given at the end of each section to understand the theory behind all solutions. Nevertheless, to get clear insights and justify these findings, in this chapter we show the numerical results obtained with every strategy. Realistic parameters together with Monte-Carlo simulations will then be employed to provide this data accurate and reliably.

First, we will state the set of parameters concerning the communication scenario, e.g. propagation, energy and users status, for which International Telecommunication Union (ITU) standards will be used. General parameters and a brief comment about the simulations employed will be also included in that section. Second, we will start with the set of empirical values that result from each approach. In addition, quantitative conclusions will be drawn accordingly. Besides, we will follow the structure of the previous chapter while presenting the outcomes, i.e. filters, user allocation and projection. Note that we are going to construct the scenario progressively by adding one solution on top of the other. This way, we will end with the highest performance this thesis can provide. Execution time and computational resource measurements are left for further experiments and investigations. In all cases, MATLAB is employed.

5.1 System Parameters

In this section, we will first present the aforementioned standard parameters related to the channel model described in Section 2.3.1. Later, a discussion of the general settings is also included. Finally, few words about the Monte-Carlo simulations, common to all scenarios, will be given as well.

5.1.1 ITU Standard

Throughout all the simulations, the same standard parameters defined in the ITU-R report from [42] will be used. This way, we will rely on a widely accepted and revised basis. Hence, the upcoming numerical values from this chapter can be used as solid representatives of practical scenarios. Note that further updates of this document are not contemplated.

On the one hand, once the covariance matrices are obtained through the spatial model, proper SNRs must be included so that second-order statistics values are realistic. To this end, we multiply these covariance matrices with the term ρ_k, different for each user. In a logarithmic scale, it is defined as follows

$$\rho_k = \mathrm{AG_{BS}} + \mathrm{NF_{BS}} + \mathrm{AG_{UT}} - \mathrm{PL}_k - \mathrm{TN} - 10\log_{10}(\mathrm{BW}) \tag{5.1}$$

where AG, NF, PL and BW stand for Antenna Gain, Noise Figure, Path Loss and Bandwidth respectively. Note that user NF is not included because we focus only on the UL channel, where estimation takes place. Thereby, it could be translated to the DL just by changing this scaling factor ρ_k.

All parameters are given in dB except for the TN, which units are dBm/Hz. That is why we have the term including the BW. As mentioned in Section 2.3.1, we assume a urban macro scenario (8 degree) is established and thus, most of the parameters can be found in Table 8-4 from [42]

BS AG	**BS NF**	**UT AG**	**TN**
17 dBi	5 dB	0 dBi	-174 dBm/Hz

Table 5.1: ITU-R Standard Parameters

In turn, PL_k is already defined in Section 2.3.1 and, with regard to BW, we assume we work with typical values for a common TDD systems. We will employ 20 MHz as dictated in Table 8-5. Furthermore, a decisive parameter

is the power each user transmits. In particular, we will be using the value according to Table 8-2 from [42], i.e. $\rho_{\text{ul}} = 24$ dBm.

5.1.2 General Settings

Here we will announce the settings employed in the Monte-Carlos simulations, from which two main types can be clearly distinguished: sweep over number of BS antennas, maintaining number of users constant; and sweep over K for a fixed M. In particular, we will work with the following cases

Sweep	M	K
A	20 - 200	20
B	100	10 - 50

Table 5.2: Sweep Cases

As already mentioned, regarding the simulations, we will use a Monte-Carlo approach to compute the object of study in our thesis, i.e. sum rate R_{sum} defined in (2.4) and given in [bps/Hz]. To do so, 100 accesses or symbols with distinct channels will be averaged over 100 different statistics. In other words, we will change the covariance matrices several times (100) and from each of them, numerous channels (100). This way, a smooth curve will be obtained for our system performance metric as many realizations (10^4) are considered.

Moreover, we need to define the number of symbols destined to training. In our case, we employed $T_{\text{tr}} = 10$ for all the computations, which means groups will have size $G = 2$ in the case of Sweep A. Thereby, two users will share the same pilot and they will interfere with each other, i.e. $|L| = 1$. Likewise, in Sweep B we will have $G = [1, 2, 3, 4, 5]$, where the situation worsens.

5.2 Filters

In this section, the numerical results obtained with the proposed filters are shown. We will begin with the LMMSE for the pilot-free ($T_{\text{tr}} = K$) and contaminated cases. The same will be done for the GMF scenario and its simplification. We will not separate transmitter from receiver side since we are interested in the difference between performance. This will be useful in the power allocation case, presented at the end. Note at each point, outcomes will be discussed and compared. In addition, no user allocation or projection is considered.

5.2.1 Linear Minimum Mean Square Error

The first plot shows the results obtained with the LMMSE strategy in both links, UL and DL, by means of the equalizer and precoder respectively. Then, we will use this notation to refer to each scenario. Also, the cases pilot-free and pilot contamination will be denoted as PF and PC in all figures. In particular, in Fig. 5.1 we represent the sum rate for the Sweep A and the B case in Fig. 5.2

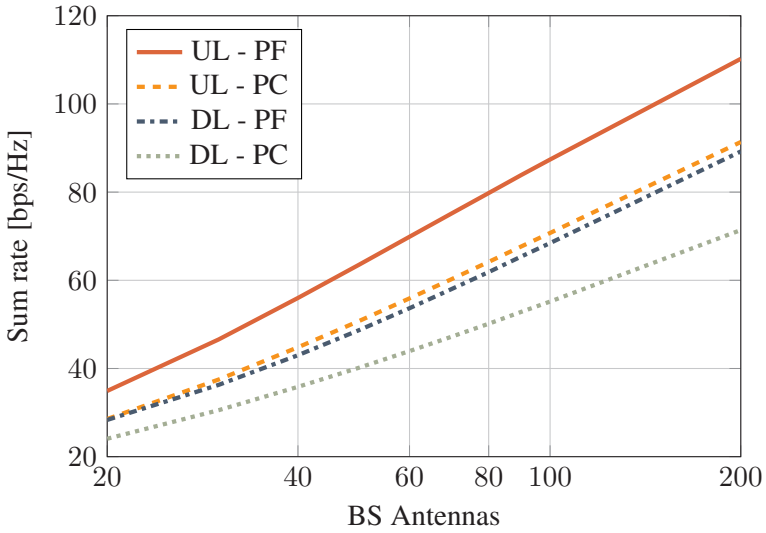

Figure 5.1: Sweep A: LMMSE Precoder (DL) and Equalizer (UL)

As expected, the rates obtained are higher in the case of the equalizer since sufficient minimum statistics are provided with this solution and thus, it results optimal. In both scenarios, we can observe the impact that pilot contamination has on the system performance as it worsens considerably. For instance, when looking at the precoder, there is a decrease of more than 10 bps/Hz between PF and PC around $M = 100$. In fact, the gap increases with higher M due to the SINR saturation. Thus, the problematic of this effect is revealed.

On the other hand, the same is experienced in the Sweep B case, where the previous discussion holds. Additionally, in both links, we can see how performance deteriorates the more users we include in the same group without increasing the available pilots (rate saturates). In that case, more terminals share the same unique pilot, leading to a major interference and poorer estimate.

Note that in both cases, since an average power constraint is used, the scaling factor β defined in (4.24) is computed numerically with these simulations.

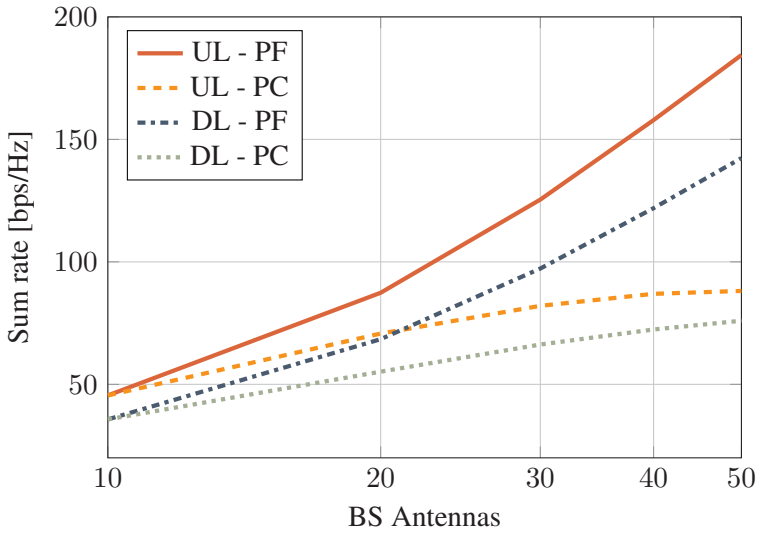

Figure 5.2: Sweep B: LMMSE Precoder (DL) and Equalizer (UL)

5.2.2 Generalized Matched Filter

Similarly to before, here the results with the GMF approach are shown. First, in Fig. 5.3 we plot the Sweep A case and later, in Fig. 5.4 the Sweep B scenario.

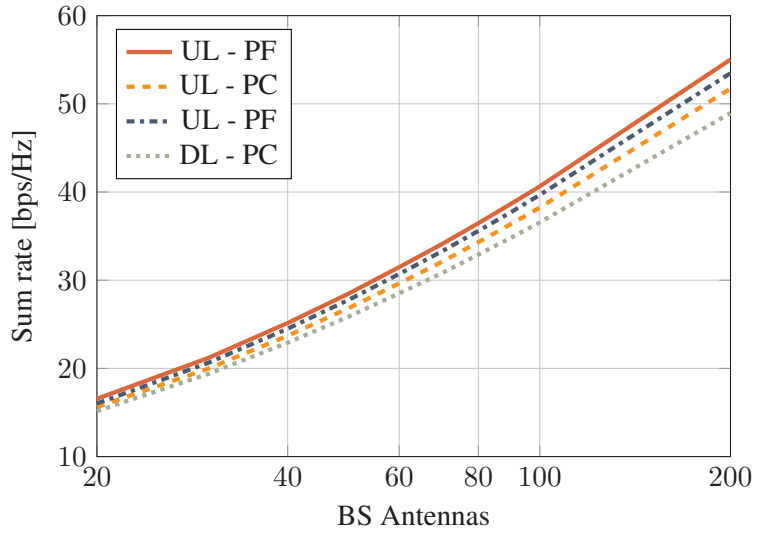

Figure 5.3: Sweep A: GMF Precoder (DL) and Equalizer (UL)

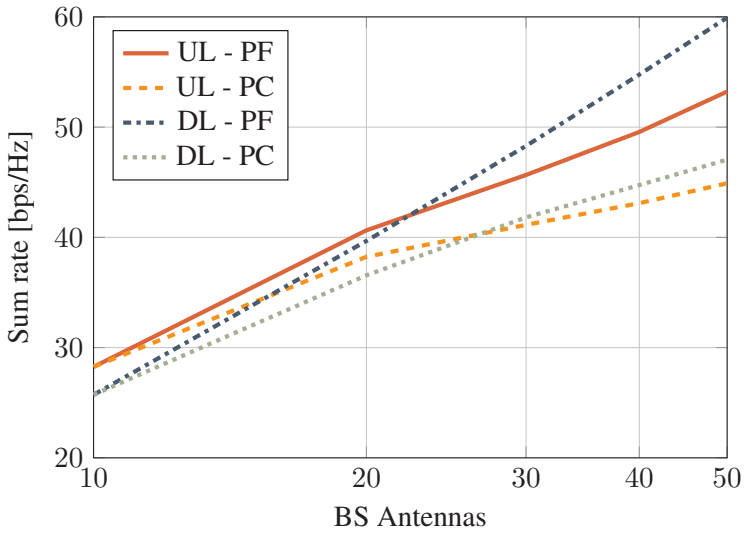

Figure 5.4: Sweep B: GMF Precoder (DL) and Equalizer (UL)

As we discussed before, in Fig. 5.3 there is also a difference between transmitter and receiver but now it is not as significant as that in LMMSE. In addition, a minor, but existent, decrease of the rates is observed in the contaminated case. This is because it relies on CDI and not on instantaneous realizations, which vary more abruptly and increase the system sensitivity. Hence, all curves here result very close as a good robustness against pilot contamination and a similar performance in UL and DL is delivered with this solution. As expected, both gaps increase with M. Nonetheless, rate values are lower than in LMMSE for the same aforementioned reasons, i.e. CSI is better in front of a statistical basis. Besides, regarding Sweep B depicted in Fig. 5.4, we can also observe the impact of including more users in the same group, given the deterioration, yet smaller, in the overall performance.

5.2.3 Simplified GMF

In this section, we present the results obtained with the simplified GMF. As we will see, the results are worse than in the case of GMF and obviously, much more when comparing with the LMMSE solution. Thereby, in Fig. 5.5 Sweep A is shown. Outcomes from Sweep B are however skipped since no relevant findings are observed. In addition, we will not consider this solution in further scenarios as we will focus on the LMMSE and GMF only.

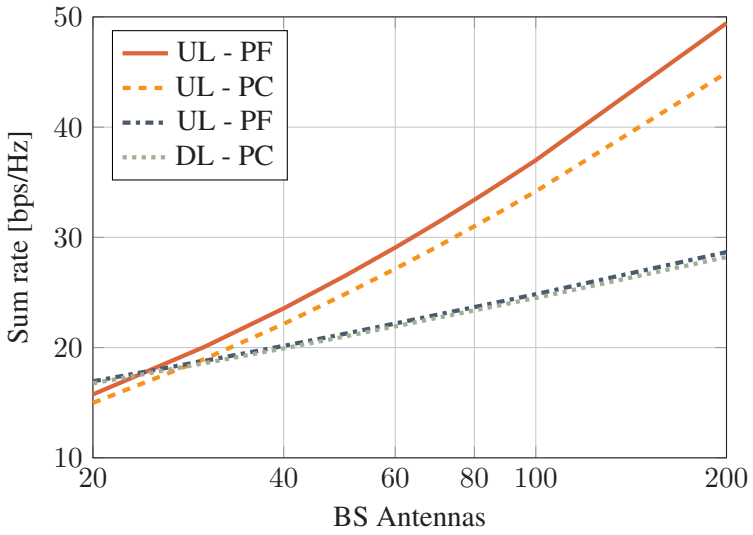

Figure 5.5: Sweep A: Simplified GMF Precoder (DL) and Equalizer (UL)

Differently from before, now the GMF equalizer surpasses the precoder for large number of antennas. This is due to the fact that interference comes from distinct users through the same channel and from different directions. Hence, with this filtering we are able to remove interference more suitably. In the case of the transmitter, a poorer performance is obtained. Nevertheless, a more robust behavior towards pilot contamination is achieved in the DL. As mentioned, this strategy will not be further studied given the small interest it draws.

5.2.4 Power Allocation

As we discussed in Section 4.1.5, an optimal power allocation is necessary for approaching precoder and equalizer performances in the case of sum rate maximization. Then, we will first show the results with the LMMSE and GMF strategies in Fig. 5.6 and 5.7 respectively. Note that, in order to avoid curves to collapse, only the pilot contaminated case is shown. Also, as said, the equalizer performance is included to really appreciate the enhancement. Then, to represent power allocation usage, we will employ the initials PAU and PAN to determine whether power allocation is used or not.

On the other hand, the results with the rate-balancing approach are shown. To this end, we will use the variance as measure to reflect the new distribution of rates and the fairness achieved. This magnitude is also computed by means

of Monte-Carlo simulations, with the settings defined in Section 5.1.2, depicted in Fig. 5.8 (LMMSE) and 5.9 (GMF). Here, pilot free and contaminated results are represented to show its impact. We can observe that, as expected, variance increases in the contaminated case, which always worsens the situation. Moreover, note that we first compute the individual variance, defined below in (5.2), and then we average over all users to find the total value. However, these moments are found by means of sample measurements. Besides, in both strategies, only Sweep A is shown.

$$\text{var}\{R_k\} = \text{E}[|R_k - \text{E}[R_k]|^2] \tag{5.2}$$

5.2.4.1 Sum Rate Maximization

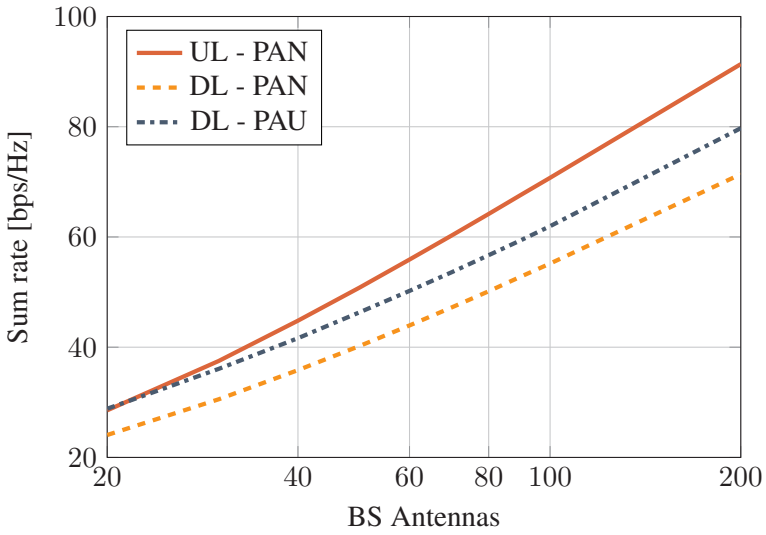

Figure 5.6: Sweep A: LMMSE Precoder (DL) and Equalizer (UL) Sum Rate Power Allocation (PA)

As we can see, a substantial improvement is obtained in both scenarios. In fact, in the GMF case, power allocation enables transmitter rates to exceed those from the receiver. This clearly justifies the usage of this technique to enhance overall performance and the seek for more optimal approaches. However, given the large number of possibilities that could result, from now on we will assume no allocation is performed. In addition, this practice implies numerous computations to find the final allocation (see Section 4.1.5).

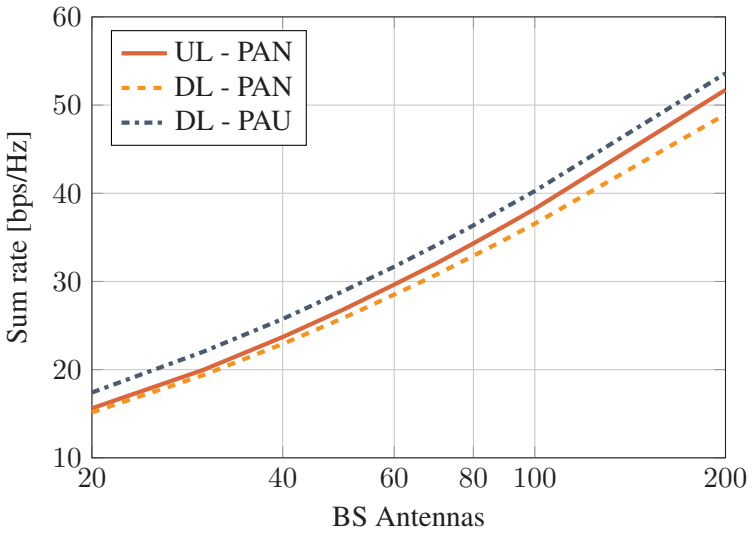

Figure 5.7: Sweep A: GMF Precoder (DL) and Equalizer (UL) Sum Rate Power Allocation (PA)

5.2.4.2 Rate Balancing

The decrease in the variance shows that resources are distributed more evenly and a fairer performance is experienced from the point of view of each user. This achievement can be seen in Fig. 5.8 and 5.9, where it is reflected that the GMF reaches a larger enhancement for the entire range of BS antennas. Nonetheless, as expected, magnitudes in both cases diminish considerably, specially for low M values. In addition, note that only the transmitter is shown as we want to focus on this improvement regardless of the receiver. Besides, when looking at the rates, one could see that a similar behavior and set of values, lower, than those of the sum rate case, are obtained. We skip this plot as it does not reflect the main point here, i.e. impartial division of resources.

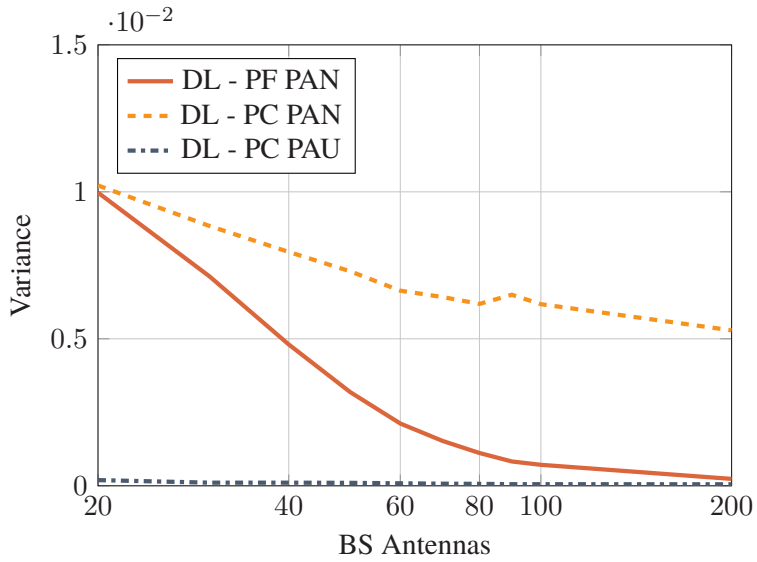

Figure 5.8: Sweep A: LMMSE Precoder (DL) and Equalizer (UL) Rate Balancing Power Allocation (PA)

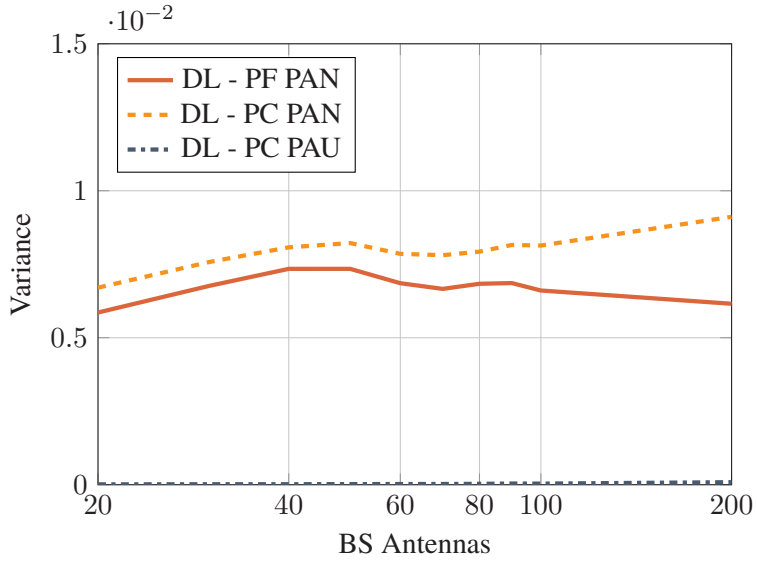

Figure 5.9: Sweep A: GMF Precoder (DL) and Equalizer (UL) Rate Balancing Power Allocation (PA)

5.3 User Allocation

In the following, results obtained with user allocation are shown. As we will see, this approach is decisive for pilot contamination mitigation since rates are boosted significantly. First, we will start with the covariance matrix based method. There, outcomes with LMMSE and GMF are presented in Fig. 5.10 and 5.11 respectively. Only metric 5 (M5) is shown since its the one delivering the best rates. Later, the sum rate approach is presented in Fig. 5.12 and 5.13. Also, to avoid redundancy, we will represent the results with the upper bound approach and leave those with the lower. In addition, given its higher performance, we will plot exclusively the curves of the DL allocation with the LMMSE estimate, denoted by SR. In both cases, we represent only the pilot contaminated curves since they are the main topic of this thesis. A comparison is made at the end of the section. Besides, Sweep B is again skipped as the same behavior as before is observed.

5.3.1 Covariance Matrix Method

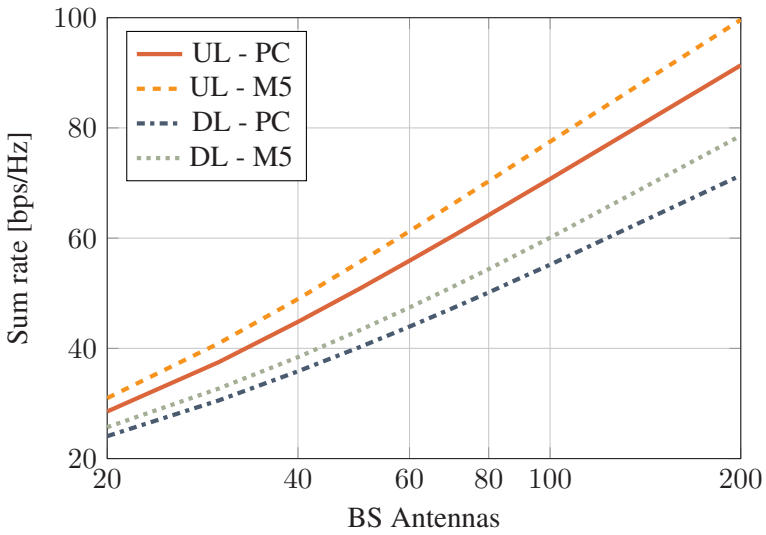

Figure 5.10: Sweep A: LMMSE Precoder (DL) and Equalizer (UL) Covariance Matrix User Allocation (M5)

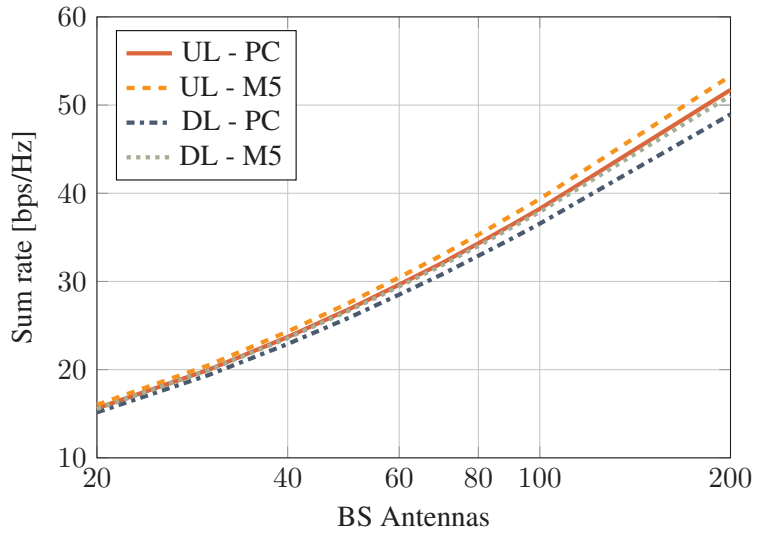

Figure 5.11: Sweep A: GMF Precoder (DL) and Equalizer (UL) Covariance Matrix User Allocation (M5)

5.3.2 Sum Rate Optimization

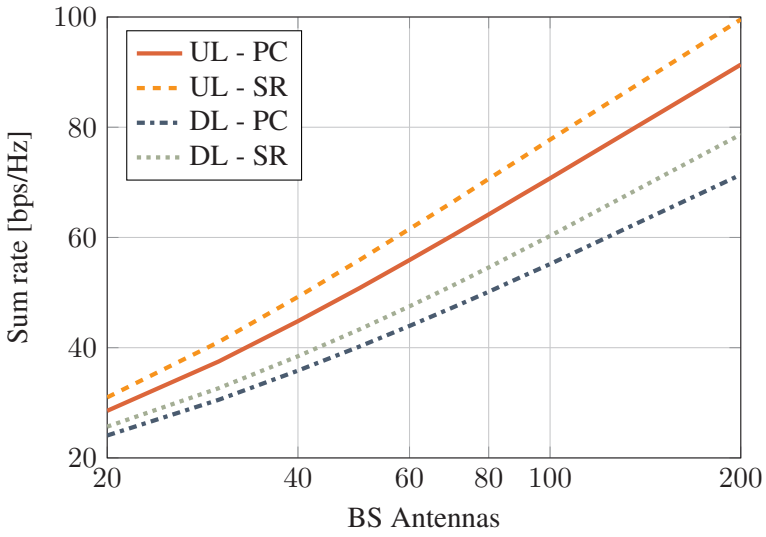

Figure 5.12: Sweep A: LMMSE Precoder (DL) and Equalizer (UL) Sum Rate User Allocation (SR)

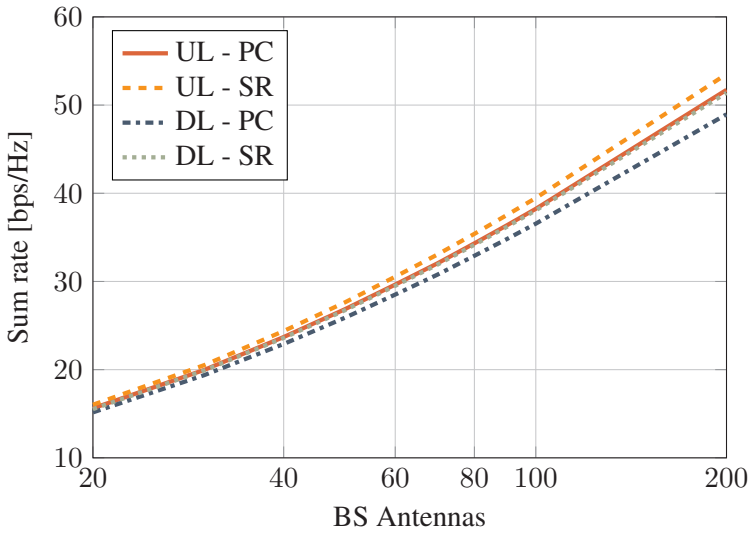

Figure 5.13: Sweep A: GMF Precoder (DL) and Equalizer (UL) Sum Rate User Allocation (SR)

We have already mentioned in Section 4.2.4 that both approaches should deliver similar results. As expected, close and substantial improvements are achieved, specially for large M where the orthogonality of covariance matrices arises considerably. This also benefits somehow the sum rate approach, apart from the first, since a proper assignation helps the LMMSE estimate filter the interference effectively. Hence, that is reason why user allocation becomes so crucial in the presence of pilot contamination in massive MIMO systems. Furthermore, as mentioned, the second method helps to justify the good performance and usage of the other strategy. As a result, given its lower complexity, the covariance based approach will be used in the following.

5.4 User Projection

In this last section, the results obtained with user projection strategies, EVD and RRQR, are plotted. Note first that we contemplate pilot contaminated scenarios. User allocation is also considered (covariance approach with metric 5). Then, we will begin with the eigenvalue approach for both filters, LMMSE and GMF. The corresponding numerical values are shown in Fig. 5.14 and 5.15. Later, the same will be done for the RRQR method in Fig. 5.16 and 5.17. Sweep B is not presented given its redundancy. At the end we will compare outcomes.

5.4.1 EVD Approach

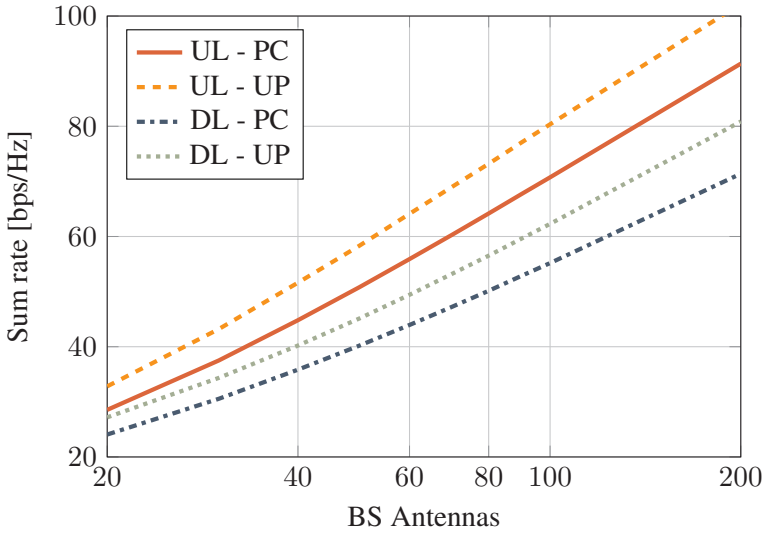

Figure 5.14: Sweep A: LMMSE Precoder (DL) and Equalizer (UL)
EVD User Projection (UP)

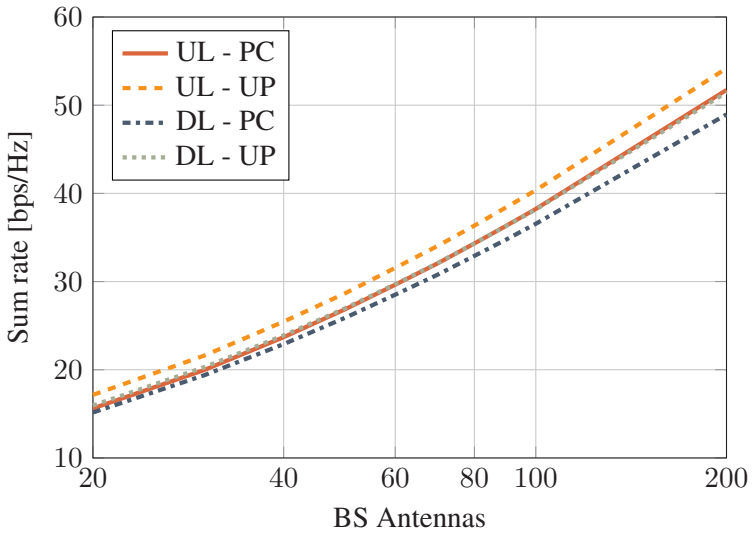

Figure 5.15: Sweep A: GMF Precoder (DL) and Equalizer (UL)
EVD User Projection (UP)

5.4.2 RRQR Approach

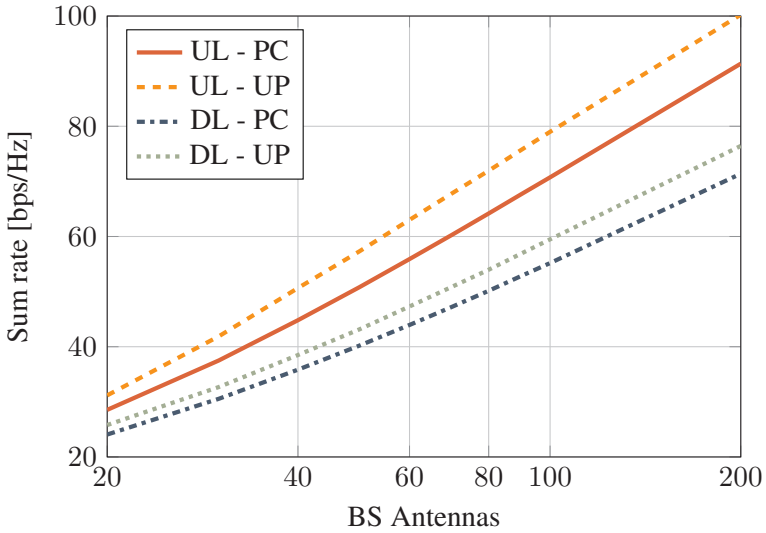

Figure 5.16: Sweep A: LMMSE Precoder (DL) and Equalizer (UL)
RRQR User Projection (UP)

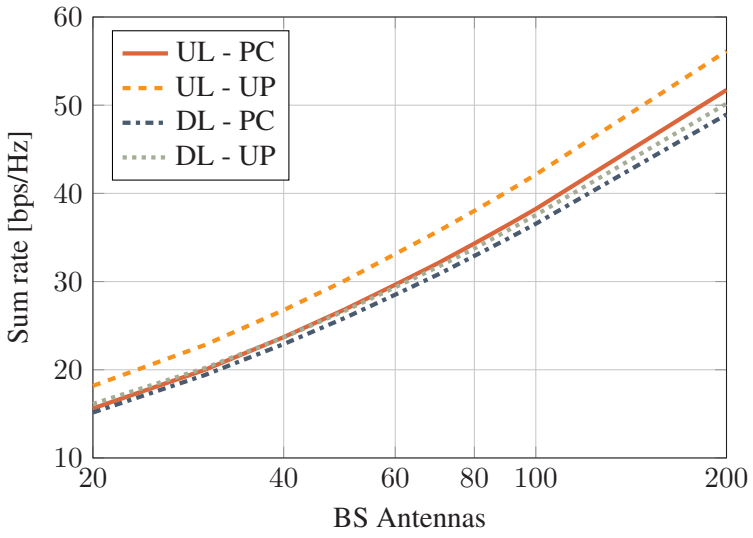

Figure 5.17: Sweep A: GMF Precoder (DL) and Equalizer (UL)
RRQR User Projection (UP)

As stated in Section 4.3.3, the EVD based approach delivers better rates than the RRQR method, specially with the LMMSE filter. The second approach helps in the GMF scenario. Nevertheless, both suppose an improvement of the data rates and thus, their usage is sustained. In fact, both of them attack the original problem, since the LS estimate is transformed with the projection. Hence, pilot contamination can be largely filtered, specially for large M, when covariance matrices really become distant and orthogonal. Overall, these achievements encourage further investigations following this line of research to be performed, from which we will propose some in the last chapter.

Chapter 6

Conclusions

In this chapter, we will first summarize the major points discussed in this thesis and highlight the findings discovered as well as the improvements achieved. Thereby, chapters will be listed and commented in order. The first one is, for obvious reasons, not included. Finally, we will present several lines of research which could be followed in the future. It will consist on expanding the investigations introduced here and on some new innovations we also propose.

6.1 Summary

First, in Chapter 2, we have presented the system used and some of its characteristics. Then, massive MIMO was introduced and its importance revealed since, in principle, this technology can deliver infinite rates if $M \to \infty$ with a simple MF as processing scheme. In addition, when assuming imperfect channel knowledge (CDI or CSI), SINR deteriorates for a finite number of BS antennas. Related to the channel, the standard spatial model we employ and its properties are described at the end.

Second, in Chapter 3, the main problem was stated. We realized that, since channels are unknown, they must be estimated and that, during the process, due to the lack of orthogonal training sequences, an interference appears as users must share pilots. That is why this effect is called pilot contamination and it limits the overall performance as the SINR, and consequently the throughput, saturate in the large-scale antenna regime. This justifies the issue relevance.

Later, in Chapter 4, we proposed different measures to cope with this effect and reduce its impact. We began with two filters as basis, from which we prefer the LMMSE given its statistical properties. The GMF solutions are suitable when looking at efficiency measurements. In addition, we saw that optimal power allocations are useful to enhance the transmitter rates, either with a total (aggressive) or individual (fair) point of view. Then, it has been seen that allocating users optimally into groups helps to filter pilot contamination and even cancel it completely for infinite number of BS antennas. Two approaches are discussed, from which the opportunistic, i.e. sum rate maximization, results better. It is based either on a lower or upper bound of the SINR, although no real difference is experienced. Nevertheless, thanks to the properties of the channels, the covariance matrix based strategy delivers almost the same results. Next, a transformation of the estimates based on projections is presented. It attempts to remove the contaminated directions of the channel and keep only those where interference is negligible. Two methods are also studied, based on the decomposition of the covariance matrices: EVD and RRQR. We also saw that the first one behaves better as it compares the parts of the signal relevant for the decision. The other results too sensitive to possible SINR variations.

Finally, in Chapter 5, the previous statements where corroborated with numerical results. To this end, we used Monte-Carlo simulations to compute the user rates by averaging over several realizations. Variance is also calculated in the rate-balancing environment, even though no special attention is paid. In the end, thanks to their features, we observed that the LMMSE filter with a sum rate power and user allocation (metric 5), together with a EVD projection, we can mitigate pilot contamination more substantially.

Overall, in this project, we have seen that pilot contamination supposes a large deterioration of the data rates in massive MIMO systems. Thereby, given the saturation of the SINR created due to this lack of channel knowledge, full potential of the technology cannot be exploited. In addition, several approaches, mostly based on channel properties, have been proposed to overcome this effect and improve the overall performance. Their behavior has been analyzed and later, with numerical results, it has been proved to be suitable for these realistic modern environments. Hence, we can conclude that with these strategies, we help communication in presence of interference to significantly enhance.

6.2 Future Work

Regarding future improvements, several ideas can be proposed to mitigate pilot contamination. One could think of further exploiting the approaches of user projection given that it represents the main contribution here. The other strategies are already deeply studied and more major achievements are difficult to be found. Then, for instance, we could try first to linearize the channels by multiplying with the whole eigenvector basis and then select those directions we are interested in. Likewise, we could use as projection the steering vector, which means we would require the estimation of angle of arrival. On the other hand, we could focus on applying these transformations at the filtering step, i.e. use them as precoder and equalizer to restrict the possible directions so that all the interference, and not just the pilot contamination part, could be canceled out. Another possibility could be to use some sort of time division strategy where users transmit or receive with all directions at a given instant and later, only with very few but the necessary to establish a useful communication. Then, the other users could do the same in a complementary manner, i.e. use the intervals where the rest barely interfere to boost their throughput. This way, we could reduce the total interference while transferring data continuously. Finally, there is always space for extending our simulation environments. We could expand the number of scenarios analyzed, e.g. sweep over different power settings. Besides, although they are unrealistic at the moment, experimental values with more BS antennas could be interesting to completely understand the asymptotic regimes. In other words, this project has left us with some open questions to be answered and doors to be explored in the near future.

Appendix A

A.1 GMF Precoder Solution with Matrix Notation

The GMF precoder can be presented in a more compact form. To this end, we first rewrite the terms in (4.44) considering the whole summation

$$
\begin{aligned}
a &= \sum_{k=1}^{K} \boldsymbol{c}_{\boldsymbol{h}_k}^{\mathrm{H}} \boldsymbol{a}_k = \mathrm{tr}(\boldsymbol{\Gamma}^{\mathrm{H}}\boldsymbol{\Xi})\,; \quad b = \sum_{k=1}^{K} \boldsymbol{a}_k^{\mathrm{H}} \boldsymbol{c}_{\boldsymbol{h}_k} = \mathrm{tr}(\boldsymbol{\Xi}^{\mathrm{H}}\boldsymbol{\Gamma}) \\
c &= \sum_{k=1}^{K}\sum_{i=1}^{K} c_{k,i} = \sum_{k=1}^{K}\sum_{i=1}^{K} \boldsymbol{a}_k^{\mathrm{H}}(\boldsymbol{C}_{\boldsymbol{\phi}_k}^{*} \otimes \boldsymbol{C}_{\boldsymbol{h}_i})\boldsymbol{a}_k = \mathrm{tr}(\boldsymbol{\Xi}^{\mathrm{H}}\boldsymbol{\Psi}\boldsymbol{\Xi}) \\
d &= \sum_{k=1}^{K} \sum_{i\in\mathcal{I}_k\cup\{k\}} d_{k,i} = \sum_{k=1}^{K} \sum_{i\in\mathcal{I}_k\cup\{k\}} \boldsymbol{a}_k^{\mathrm{H}} \boldsymbol{c}_{\boldsymbol{h}_i} \boldsymbol{c}_{\boldsymbol{h}_i}^{\mathrm{H}} \boldsymbol{a}_k = \mathrm{tr}(\boldsymbol{\Xi}^{\mathrm{H}}\boldsymbol{\Omega}\boldsymbol{\Xi}) \\
e &= \sum_{k=1}^{K} e_k = \sum_{k=1}^{K} \boldsymbol{a}_k^{\mathrm{H}}(\boldsymbol{C}_k^{*} \otimes \boldsymbol{I}_M)\boldsymbol{a}_k = \mathrm{tr}(\boldsymbol{\Xi}^{\mathrm{H}}\boldsymbol{\Sigma}\boldsymbol{\Xi})
\end{aligned}
\tag{A.1}
$$

where we defined the following auxiliary matrices

$$
\begin{gathered}
\boldsymbol{\Xi} = [\boldsymbol{a}_1, \ldots, \boldsymbol{a}_K] \qquad \boldsymbol{\Gamma} = [\boldsymbol{c}_{\boldsymbol{h}_1}, \ldots, \boldsymbol{c}_{\boldsymbol{h}_K}] \\
\boldsymbol{\Psi} = \boldsymbol{C}_{\boldsymbol{\phi}}^{*} \otimes \sum_{i=1}^{K} \boldsymbol{C}_{\boldsymbol{h}_i} \quad \boldsymbol{\Omega} = \sum_{i} \boldsymbol{c}_{\boldsymbol{h}_i} \boldsymbol{c}_{\boldsymbol{h}_i}^{\mathrm{H}} \quad \boldsymbol{\Sigma} = \boldsymbol{C}_k^{*} \otimes \mathbf{I}_M
\end{gathered}
\tag{A.2}
$$

Consequently, it can be shown that the Lagrangian yields

$$\begin{aligned}\mathcal{L}(\boldsymbol{\Xi},\beta,\lambda) = K(1+\beta^{-2}) - 2\beta^{-1}\mathrm{Re}(\mathrm{tr}(\boldsymbol{\Gamma}^{\mathrm{H}}\boldsymbol{\Xi})) \\ + \beta^{-2}\mathrm{tr}(\boldsymbol{\Xi}^{\mathrm{H}}\boldsymbol{\Psi}\boldsymbol{\Xi} + \boldsymbol{\Xi}^{\mathrm{H}}\boldsymbol{\Omega}\boldsymbol{\Xi}) + \lambda(\mathrm{tr}(\boldsymbol{\Xi}^{\mathrm{H}}\boldsymbol{\Sigma}\boldsymbol{\Xi}) - E_{\mathrm{tx}})\end{aligned} \tag{A.3}$$

Thereby, the derivatives result

$$\frac{\partial\mathcal{L}(\boldsymbol{\Xi},\beta,\lambda)}{\partial\boldsymbol{\Xi}} = -\beta^{-1}\boldsymbol{\Gamma}^{*} + \beta^{-2}(\boldsymbol{\Psi}^{\mathrm{T}}\boldsymbol{\Xi}^{*} + \boldsymbol{\Omega}^{\mathrm{T}}\boldsymbol{\Xi}^{*}) + \lambda\boldsymbol{\Sigma}^{\mathrm{T}}\boldsymbol{\Xi}^{*} \tag{A.4}$$

$$\frac{\partial\mathcal{L}(\boldsymbol{\Xi},\beta,\lambda)}{\partial\beta} = (-K + \beta\mathrm{tr}(\mathrm{Re}(\boldsymbol{\Gamma}^{\mathrm{H}}\boldsymbol{\Xi})) - \mathrm{tr}(\boldsymbol{\Xi}^{\mathrm{H}}\boldsymbol{\Psi}\boldsymbol{\Xi} + \boldsymbol{\Xi}^{\mathrm{H}}\boldsymbol{\Omega}\boldsymbol{\Xi}))2\beta^{-3} \tag{A.5}$$

By setting the first to zero it is straightforward to obtain

$$\boldsymbol{\Xi}(\lambda\beta^{2}) = \beta\tilde{\boldsymbol{\Xi}}(\lambda\beta^{2}) = \beta\boldsymbol{F}^{-1}(\lambda\beta^{2})\boldsymbol{\Gamma} \tag{A.6}$$

where

$$\boldsymbol{F}(\lambda\beta^{2}) = \boldsymbol{\Psi} + \boldsymbol{\Omega} + \lambda\beta^{2}\boldsymbol{\Sigma} \tag{A.7}$$

and the scaling factor is defined by the power constraint from (4.48)

$$\beta = \sqrt{\frac{E_{\mathrm{tr}}}{\mathrm{tr}(\tilde{\boldsymbol{\Xi}}^{\mathrm{H}}(\lambda\beta^{2})\boldsymbol{\Sigma}\tilde{\boldsymbol{\Xi}}(\lambda\beta^{2}))}} \tag{A.8}$$

At this point, together with the determination in (A.5), we can find $\lambda\beta^{2}$ like in equation (4.50), i.e. by setting the derivative to zero. Then, it follows that it is given by $\lambda\beta^{2} = K/E_{\mathrm{tx}}$. Finally, the optimal solution reads as

$$\boldsymbol{\Xi}^{\star} = \beta^{\star}\boldsymbol{F}^{-1}\boldsymbol{\Gamma} = \beta^{\star}\left(\boldsymbol{\Psi} + \boldsymbol{\Omega} + \frac{K}{E_{\mathrm{tx}}}\boldsymbol{\Sigma}\right)^{-1}\boldsymbol{\Gamma} \tag{A.9}$$

with

$$\beta^{\star} = \sqrt{\frac{E_{\mathrm{tr}}}{\mathrm{tr}(\boldsymbol{\Gamma}^{\mathrm{H}}\boldsymbol{F}^{-1}\boldsymbol{\Sigma}\boldsymbol{F}^{-1}\boldsymbol{\Gamma})}} \tag{A.10}$$

A.2 First Order Taylor Approximation

We aim to approximate the expectation of a ratio of different RV by the ratio of expectations of the corresponding numerator and denominator

$$\mathrm{E}\left[\frac{X}{Y}\right] \approx \frac{\mathrm{E}[X]}{\mathrm{E}[Y]} \tag{A.11}$$

To begin with, let the first order Taylor expansion around the point $A = (x_o, y_o)$ for any function $f(x, y)$ be

$$f(x, y) = f(A) + f'_x(A)(x - x_o) + f'_y(A)(y - y_o) + C \tag{A.12}$$

where f'_x and f'_y represent the derivatives of the function $f(x, y)$ with respect to x and y. The remainder C will be discarded to work directly with the first order Taylor series approximation, which then reads as

$$f(x, y) \approx f(A) + f'_x(A)(x - x_o) + f'_y(A)(y - y_o) \tag{A.13}$$

In addition, we define two RVs X and Y, with statistical means μ_x and μ_y respectively. Setting $A = (\mu_x, \mu_y)$, the approximation for $f(X, Y)$ yields

$$f(X, Y) \approx f(A) + f'_x(A)(X - \mu_x) + f'_y(A)(Y - \mu_y) \tag{A.14}$$

which is valid as long as we remain around the means. Hence, it is straightforward to see that the approximation for the expectation is given by

$$\begin{aligned} \mathrm{E}[f(X, Y)] &\approx \mathrm{E}[f(A) + f'_x(A)(X - \mu_x) + f'_y(A)(Y - \mu_y)] \\ &= f(A) + f'_x(A)(\mathrm{E}[X] - \mu_x) + f'_y(A)(\mathrm{E}[Y] - \mu_y) \\ &= f(A) = f(\mu_x, \mu_y) \end{aligned} \tag{A.15}$$

Finally, since our function is $f(X, Y) = X/Y$, the resulting approximation of its expectation will be the ratio of the corresponding expectations, i.e. $\mathrm{E}[X/Y] \approx \mathrm{E}[X]/\mathrm{E}[Y]$. In other words, by means of linearizing the previous function, we can simplify greatly its expectation. This concludes the proof.

List of Figures

List of Tables

Bibliography

[1] K. Tachikawa. A perspective on the evolution of mobile communications. *IEEE Commun. Mag.*, pages 66–73, Oct. 2003.

[2] E. Dahlman, S. Parkvall, J. Skold, and P. Beming. 3g evolution: Hspa and lte for mobile broadband, 2nd edition. *Elsevier*, 2008.

[3] L. Zheng and D. Tse. Communication on the Grassmann manifold: a geometric approach to the noncoherent multiple-antenna channel. *IEEE Trans. Inf. Theory*, 48:359–383, Feb. 2002.

[4] L. Lu, G. Y. Li, A. L. Swindlehurst, A. Ashikhmin, and R. Zhang. An Overview of Massive MIMO: Benefits and Challenges. *Special Issie on Massive MIMO of IEEE Journal of Selected Topics in Sign. Process.*, pages 1–18, 2014.

[5] H. Q. Ngo, E. G. Larsson, and T. L. Marzetta. Energy and Spectral Efficiency of Very Large Multiuser MIMO Systems. *IEEE Trans. Comm.*, 61(4), Apr. 2007.

[6] E. G. Larsson, O. Edfors, F. Tufvesson, and T.L Marzetta. Massive MIMO for Next Generation Wireless Systems. *IEEE Comm. Mag.*, 52(2):186–195, 2014.

[7] J. Hoydis, S. T. Brink, and M. Debbah. Massive MIMO in the UL/DL of Cellular Networks: How Many Antennas Do We Need? *IEEE Journal on selected Areas in Communications*, 31(2):160–171, 2013.

[8] T. Rappaport et al. Millimeter wave mobile communications for 5G cellular: It will work! *IEEE Access*, 1:335–349, May 2013.

[9] E. Björnson, E. G. Larsson, and T. L. Marzetta. Massive MIMO: Ten Myths and One Critical Question. *Accepted from Open Call in IEEE Communications Magazine*, Feb. 2016.

[10] J. Jose, A. Ashikhmin, T. L. Marzetta, and S. Vishwanath. Pilot contamination problem in multicell TDD systems. *UCSD Information Theory & Applications Workshop*, San Diego, Feb. 2009.

[11] T. L. Marzetta. Noncooperative Cellular Wireless with Unlimited Numbers of Base Station Antennas. *IEEE Trans. Wireless Commun.*, 9:3590–3600, Nov 2010.

[12] D. Gesbert, M. Kountouris, R. W. Heath Jr., C. Chae, and T. Salzer. From single user to multiuser communications: shifting the MIMO paradigm. *IEEE Signal Process. Mag.*, 24(5):36–36, Sep. 2007.

[13] H. Sampath, S. Talwar, J. Tellado, V. Erceg, and A. Paulraj. A fourth-generation MIMO-OFDM broadband wireless system: design, performance, and field trial results. *IEEE Commun. Mag.*, pages 143–149, Sep. 2002.

[14] T. L. Marzetta and B. M. Hochwald. Capacity of a mobile multiple antenna communications link in a Rayleigh flat-fading environment. *IEEE Trans. Inf. Theory*, 45(1):139–157, Jan. 1993.

[15] David Tse and Pramod Viswanath. *Fundamentals of Wireless Communication*. Cambridge University Press, 2005.

[16] Michael Joham. *MIMO Systems*. TUM, Aug. 2016.

[17] F. Rusek et al. Scaling Up MIMO: Opportunities and challenges with very large arrays. *IEEE Signal Process. Mag.*, 30(1):40–60, Jan. 2013.

[18] D. Neumann, M. Joham, and W. Utschick. On MSE based receiver design for massive MIMO. *Proceedings of 11th International ITG Conference on Systems, Communications and Coding (SCC)*, pages 1–6, Feb. 2016.

[19] A. Pastore and M. Joham. Mutual Information Bounds for MIMO Channels under Imperfect Receiver CSI. *Asilomar*, 2009.

[20] M. Medard. The effect upon channel capacity in wireless communications of perfect and imperfect knowledge of the channel. *IEEE Trans. Inf. Theory*, 46:933–946, May 2000.

[21] T. L. Marzetta. How much training is required for multiuser MIMO? *Fortieth Asilomar Conf. on Signals, Systems, & Computers*, Pacific Grove, CA, Oct. 2006.

[22] D. Neumann, A. Gründinger, M. Joham, and W. Utschick. CDI Rate-balancing with Per-base-station Constraints. *ITG Workshop on Smart Antennas (WSA)*, Munich, Mar. 2016.

[23] J. Jose, A. Ashikhmin, T. L. Marzetta, and S. Vishwanath. Pilot contamination problem in multicell TDD systems. *IEEE Trans. on Wireless Comm.*, 10(8), Aug. 2011.

[24] B. Hassibi and B. M. Hochwald. How Much Training is Needed in Multiple-Antenna Wireless Links? *IEEE Trans. Inf. Theory*, 49(3):951–963, Apr. 2003.

[25] K. Appaiah, A. Ashikhmin, and T. L. Marzetta. Pilot contamination reduction in multi-user TDD systems. *In Proc. IEEE Int. Conf. Commun. (ICC)*, Cape Town, South Africa, May 2010.

[26] D. Neumann, M. Joham, and W. Utschick. CDI Precoding for Massive MIMO. *Conf. Syst. Commun. and Coding*, pages 1–6, Feb. 2015.

[27] D. Neumann, M. Joham, L. Weiland, and W. Utschick. Low-complexity computation of LMMSE channel estimates in massive MIMO. *In Proceedings of 19th International ITG WSA*, pages 1–6, Mar. 2015.

[28] 3GPP. Spatial channel model for multiple input multiple output (MIMO) simulations. *3rd Generation Partnership Project (3GPP) Tech. Rep.*, 2015.

[29] F.-W. Sun, Y. Jiang, and J. Baras. On the convergence of the inverses of toeplitz matrices and its applications. *IEEE Transactions on Information Theory*, 49(1):180–190, Jan. 2003.

[30] N. Jindal S. Vishwanath and A. Goldsmith. On the duality of Gaussian multiple-access and broadcast channels. *IEEE Trans. Inform. Theory*, 50(5):768–783, May 2004.

[31] K. S. Gomadam, H. C. Papadopoulos, and C.-E. W. Sundberg. Techniques for Multi-User MIMO with Two-Way Training. *Proc. IEEE International Conference on Communications (ICC'08)*, 24(5):3360–3366, Beijing, China, May. 2008.

[32] D. Neumann, K. Shibli, M. Joham, and W. Utschick. Joint Covariance Matrix Estimation and Pilot Allocation in Massive MIMO systems. *IEEE International Conference on Communications (ICC)*, May 2017.

[33] H. Yin, D. Gesbert, M. Filippou, and Y. Liu. A coordinated approach to channel estimation in large-scale multiple-antenna systems. *IEEE Journal on Selected Areas in Communications*, 31(2):264–273, Feb. 2013.

[34] M. Joham, W. Utschick, and J. A. Nossek. Linear transmit processing in MIMO communications systems. *IEEE Trans. on Signal Processing*, 53(8):2700–2712, Aug. 2005.

[35] Kaare Brandt Petersen and Michael Syskind Pedersen. *The Matrix Cookbook*. Nov. 2012.

[36] S. Vishwanath, N. Jindal, and A. Goldsmith. Duality, achievable rates, and sum-rate capacity of Gaussian MIMO broadcast channels. *IEEE Trans. Inf. Theory*, 49(10), Oct. 2003.

[37] D. Neumann, A. Gründinger, M. Joham, and W. Utschick. Rate-balancing in massive MIMO using statistical precoding. *in Int. Workshop Signal Process. Adv. Wireless Commun.*, pages 226–230, Jun. 2015.

[38] Raphael Hunger. *Analysis and Transceiver Design for the MIMO BC*. Springer Berlin Heidelberg, Aug. 2012.

[39] M. Joham, A. Gründinger, A. Pastore, J. Fonollosa, and W. Utschick. Rate balancing in the vector BC with erroneous CSI at the receivers. *in Conf. Inf. Sci. and Syst.*, pages 1–6, Mar. 2013.

[40] M. Herdin, N. Czink, H. Ozcelil, and E. Bonek. Correlation matrix distance, a meaningful measure for evaluation of non-stationary MIMO channels. *in Proc.2005 IEEE 61st Veh. Technol. Conf.*, pages 136–140, Stockholm, Sweden, Jun.2005.

[41] Michael Joham. *Numerical Linear Algebra for Signal Processing*. Technische Universität München, 2017.

[42] ITU. Guidelines for evaluation of radio interface technologies for IMT-Advanced. *International Telecommunication Union (ITU), Tech. Rep*, ITU-R(M.2135-1), 2009.